STABILITY OF UNCERTAIN PIECEWISE AFFINE TIME-DELAY SYSTEMS WITH APPLICATION TO ALL WHEEL DRIVE CLUTCH CONTROL

by

Shiming Duan

A dissertation submitted in partial fulfillment
of the requirements for the degree of
Doctor of Philosophy
(Mechanical Engineering)
in The University of Michigan
2011

Doctoral Committee:

Professor Jun Ni, Co-Chair
Professor A. Galip Ulsoy, Co-Chair
Professor Huei Peng
Professor Jessy W. Grizzle

To my parents

ACKNOWLEDGMENTS

I would like to express my deepest gratitude to my two advisors, Professor Jun Ni and Professor A. Galip Ulsoy, for their guidance, advice and encouragement throughout my research and dissertation. Without their continuous support, this dissertation would not have been accomplished.

I would like to thank my friends and co-workers in the Wu Manufacturing Research Center for their help and support, especially Hao Yu, Xiaoning Jin, Cindy Kuo, Li Jiang, Adam Brzezinski, Weng Xin, Almad Almuhtady, Xinran Liang, Kuenren Chen, Yong Wang, Shenshen Zhou, Yani Chen, Jae Wook Oh, Chaoye Pan, George Qiao, Dr. Yi Liao, Dr. Jie Zhu, Dr. Seungchul Lee, Dr. Saumil Ambani, Dr. Lijung Tai, Dr. Jia Tao, Dr. Yongqing Li, Dr. Yong Lei, Dr. Yang Liu, Dr. Masa Fujiki, Dr. Min Zhang, Dr. Jianbo Liu, Professor Lin Li and Professor Dragan Djurdjanovic. I would also like to thank Professor Sun Yi, Professor Patrick Nelson, Professor Jessy Grizzle, Professor Huei Peng and Professor Epureanu Bogdan for their help on my research and teaching.

Much appreciation to my dear friends, Rong Fan, Sibo Hu, Jingjing Li, Liang Zhou, Jin Yuan, Yunjiao Cai, Jin Yan and Sifang Li. I really enjoy the time spent with you guys.

Finally, I dedicate this work to my parents for the support that they have never ceased to give me. I also want to give special thanks to Uncle Shuyun Wu, Aunt Ronghua Zhang and my two lovely cousins, Lily Wu and Grace Wu.

TABLE OF CONTENTS

LIST OF FIGURES

LIST OF TABLES

LIST OF APPENDICES

ABSTRACT

Piecewise affine (PWA) systems provide good flexibility and traceability for modeling a variety of nonlinear systems. The stability of PWA systems is an important but challenging problem since the stability of the sub-systems does not directly imply the stability of the global system. Meanwhile, time delays and uncertainty exist in many practical systems in engineering and introduce various complex behaviors such as oscillation, instability and poor performance. Accommodating time delay and uncertainty in the PWA framework is essential for applicability of the method to real systems. To ensure the stability of the control systems developed via the PWA system framework, the stability of uncertain PWA time-delay systems is investigated. In addition, a quantitative description of asymptotic behavior for time-delay systems is also studied since it characterizes the transient response of these systems and can be used for the dwell-time control for switched time-delay systems.

First, the stability problem for uncertain piecewise affine time-delay systems is investigated. It is assumed that there exists a constant time delay in the system and the uncertainly is norm-bounded. Sufficient conditions for the stability of nominal systems and the stability of systems subject to uncertainty are derived using the Lyapunov-Krasovskii functional with a triple integration term. This approach handles switching based on the delayed states (in addition to the states) for a PWA time-delay system, considers structured as well as unstructured uncertainty, and reduces the conservativeness of previous approaches. The effectiveness of the proposed approach is demonstrated by

comparison with existing methods through numerical examples.

Second, an application of the PWA system framework to the modeling and control of an automotive all wheel drive clutch system is presented. The open-loop system is modeled as a PWA system, followed by the design of a piecewise linear feedback controller. The stability of the closed-loop system is examined using linear matrix inequalities based on Lyapunov theory. The response of the closed-loop system under step and sine reference signals and temperature disturbances are simulated to illustrate the effectiveness of the design.

Finally, a new Lambert W function based approach for estimation of the decay function for time-delay systems is presented. This new approach is able to provide a closed-form solution for time-delay systems in terms of an infinite series. Using this solution form, a decay function estimate, which is less conservative than existing methods, is obtained. The method is illustrated with several examples, and the results compare favorably to existing methods for decay function estimation.

In summary, this research work is dedicated to developing stability methods that can work effectively and efficiently for a wide range of practical PWA time-delay systems with uncertainty. An approach based on the Lambert W function is also developed to obtain accurate estimates of transient characteristics of time-delay systems, which can be used for the dwell-time control of switched time-delay systems.

CHAPTER 1
INTRODUCTION

1.1 Motivation

As the customer demand for safety, reliability and environmental friendliness increases, modern engineering systems become more complex and integrated. Benefiting from the advances in manufacturing technology, products with sophisticated structures and complex dynamics can be built to provide diversified functionalities. Further, the components of a system, together with embedded sensors, actuators and controllers, usually interact with one another and lead to an integrated system with highly nonlinear dynamics. In addition, in many applications, the dynamics of the system/subsystem changes with the external environment and input conditions. For example, inputs in automotive and aircraft engine systems undergo significant and unpredictable variations, and the system behavior varies significantly with such changing inputs. Because of these factors, many engineered systems exhibit highly nonlinear behavior.

In order to monitor and control these complex engineering systems, obtaining accurate models that represent the system dynamics over a wide range of inputs and environments is necessary and important, but challenging. Many systems show multi-modal behavior in the sense that their dynamics may depend on inputs and environmental factors. Using a single model to represent these systems may be inadequate and ultimately not successful. An alternative for modeling nonlinear dynamic systems is the

"divide and conquer" approach, which is based on the idea of dividing the entire system operating space into small regions and modeling the local dynamics individually within each region. Since the modeling task for a small region of the system behavior becomes easier to address than modeling the system as a whole, this approach can reduce the difficulty of the modeling procedure. A variety of frameworks for multiple model systems have been proposed in the past for modeling general nonlinear dynamic systems. Takagi-Sugeno (TS) Fuzzy Model (1985) provides smoothed connections between regions. Identifying the TS fuzzy model structure (e.g., finding optimal premise variables and their associated fuzzy partitions) is a difficult problem and often tackled with offline or trial-and-error approaches. Johansen and Foss (1993) proposed to use simple local models to describe the system dynamics within each region and then to interpolate among these models to form a global model. Instead of dividing each individual premise, or input variable, into different value ranges, vector quantization techniques, such as Self-Organizing Maps (SOM) (Kohonen, 1995), have been proposed in (Barreto & Araujo, 2004) to directly partition the operating space.

The switching between sub-models can rely solely on inputs, solely on states or be based upon both inputs and states. If the states are included in the partition vector and only one local model is activated at a time, this type of multi-model system is called a Piecewise-Affine (PWA) system. PWA systems are defined by partitioning the state and input space in a finite number of polyhedral regions and associating with each region a local linear differential equation:

$$\begin{aligned} \dot{\mathbf{x}}(t) &= \mathbf{A}_i\mathbf{x}(t) + \mathbf{B}_i\mathbf{u}(t) + \mathbf{a}_i + \boldsymbol{\delta}_i \\ \mathbf{y}(t) &= \mathbf{C}_i\mathbf{x}(t) + \mathbf{D}_i\mathbf{u}(t) + \mathbf{c}_i + \boldsymbol{\rho}_i \end{aligned}, \quad \forall \begin{bmatrix} \mathbf{x}(t) \\ \mathbf{u}(t) \end{bmatrix} \in \chi_i \tag{1.1}$$

where i is the region index, $\mathbf{A}_i \in \Re^{n\times n}$, $\mathbf{B}_i \in \Re^{n\times r}$, $\mathbf{C}_i \in \Re^{p\times n}$ and $\mathbf{D}_i \in \Re^{p\times r}$ are constant coefficient matrices, $\mathbf{a}_i \in \Re^{n\times 1}$ and $\mathbf{c}_i \in \Re^{p\times 1}$ are constant affine terms which offer additional flexibility in the model, and $\boldsymbol{\delta}_i \in \Re^{n\times 1}$ and $\boldsymbol{\rho}_i \in \Re^{n\times 1}$ are model uncertainties. The set $\{\chi_i\}_{i=1}^{s}$ is the polyhedral partition of the input-state space, $span\left\{\begin{bmatrix}\mathbf{x}(t)^T & \mathbf{u}(t)^T\end{bmatrix}^T\right\}$. The partition of the space is defined as:

$$\mathbf{E}_i\mathbf{x}(t)+\mathbf{E}_{ui}\mathbf{u}(t)+\mathbf{e}_i \geq 0,\ \forall\begin{bmatrix}\mathbf{x}(t)\\ \mathbf{u}(t)\end{bmatrix} \in \chi_i \tag{1.2}$$

where $\mathbf{E}_i$, $\mathbf{E}_{\mathbf{u}i}$ and $\mathbf{e}_i$ are constant matrices with compatible dimension. Note that the switching, $i(t)$, of the PWA system is based on the states and the inputs and cannot be arbitrarily changed.

For rigorous analysis, uncertainties, $\boldsymbol{\delta}_i$ and $\boldsymbol{\rho}_i$, are considered in the model and can be either modeled as structured uncertainty or left unstructured. A detailed discussion about modeling of the uncertainly is provided in Chapter 2. A primary source of model uncertainty is the fact that the nonlinear system being considered has been represented as a PWA system. A refinement of the partition can help to reduce the approximation error but may make subsequent analysis and design difficult due to the increase of model complexity. Thus, a reasonable trade-off between approximation error and model complexity should be considered during partitioning. Uncertainty in system parameters, such as calibration error, may also lead to an increase of the overall uncertainty level, but cannot be reduced by partition refinement.

PWA systems provide a flexible framework to represent a rich class of hybrid systems, such as discrete-time hybrid systems in mixed logic dynamical form (Schutter

and Moor, 1999), systems with interconnections of linear systems and finite automata (Sontag, 1996), and systems with saturation or deadzones (Dai et al., 2009a). This approach has been utilized in various applications, such as automotive systems (Baotic et al., 2003), biosystems (Azuma et al., 2003) and network systems (Dumas & Rondepierre, 2003; Drulhe et al., 2006).

Besides the flexibility for modeling, the PWA system framework is also useful in investigating structural properties of switched systems such as observability and reachability (Bemporad et al., 1999; Rodrigues et al.,2003), limit cycles (Branicky, 1998), multiple equilibrium points, chaos (Li et al., 2007), etc. An exact analysis of these systems is difficult. For a nonlinear system, stability analysis is important since having a stable system, or keeping it operating in a safe region, is always the first priority. Furthermore stability analysis can serve as the basis for control system design. For PWA systems, switching among regions may cause instability problems even if all sub-region models are stable (Branicky, 1998). One needs to find a common Lyapunov function (Hu et al., 2002) or a piecewise Lyapunov function (Johansson & Rantze, 1997; Mignone et al., 2000; Rodrigues & Boyd, 2005) to show global stability.

In many real engineering control systems, delays commonly exist and affect the characteristics of these systems (Niculescu, 2001). Such delays may be inherent in the processes of these systems, or arise in the implementation of control (e.g., delays in sensors, controllers or actuators). Delays may introduce various complex behaviors such as oscillation, instability and poor performance. For stability of linear time-delay systems, the problem has been studied over the past several decades for many applications, such as highway transportation systems (Orosz et al., 2010), machine tool chatter problem (Yi et

al., 2007b), teleoperation systems (Anderson & Spong, 1989), networked control systems (Murray, 2003), HIV pathogenesis (Yi et al., 2008a) and automotive engine control systems (Cook & Powell, 1988). Fruitful results for stability criteria for linear time-delay systems have been analytically derived (Gu & Niculescu, 2003; Richard, 2003). Lyapunov-Krasovskii functional based approaches (Nieulescu et al., 1998; Moon et al., 2001; Xu & Lam 2005; He et al. 2005) and Lyapunov-Razumikhin function based approaches (Hou & Qian, 1998, Jankovic, 2001) are the two major ways to construct Lyapunov functions for time delay systems. Infinite cluster approaches (Sipahi & Olgac, 2003), Hopf bifurcation theorem based approaches (Kalmar-Nagy et al., 2001; Forde & Nelson, 2004), pseudospectral approaches (Michiels et. al., 2006) and Lambert W function approaches (Yi et al., 2007b) have also been proposed.

To consider time delays in practical systems, it is valuable to incorporate it in the model of PWA systems.

$$\begin{aligned}\dot{\mathbf{x}}(t) &= \mathbf{A}_i\mathbf{x}(t)+\mathbf{A}_{\mathbf{d}i}\mathbf{x}(t-\tau)+\mathbf{B}_i\mathbf{u}(t)+\mathbf{a}_i+\boldsymbol{\delta}_i \\ \mathbf{y}(t) &= \mathbf{C}_i\mathbf{x}(t)+\mathbf{C}_{\mathbf{d}i}\mathbf{x}(t-\tau)+\mathbf{D}_i\mathbf{u}(t)+\mathbf{c}_i+\boldsymbol{\rho}_i\end{aligned} \quad , \quad \forall \begin{bmatrix}\mathbf{x}(t)\\ \mathbf{x}(t-\tau)\\ \mathbf{u}(t)\end{bmatrix} \in \chi_i \tag{1.3}$$

where $\mathbf{A}_i \in \Re^{n\times n}$, $\mathbf{A}_{\mathbf{d}i} \in \Re^{n\times n}$, $\mathbf{B}_i \in \Re^{n\times r}$, $\mathbf{C}_i \in \Re^{p\times n}$, $\mathbf{C}_{\mathbf{d}i} \in \Re^{p\times n}$ and $\mathbf{D}_i \in \Re^{p\times r}$ are constant coefficient matrices, $\mathbf{a}_i \in \Re^{n\times 1}$ and $\mathbf{c}_i \in \Re^{p\times 1}$ are constant affine terms which offer additional flexibility in the model, $\boldsymbol{\delta}_i \in \Re^{n\times 1}$ and $\boldsymbol{\rho}_i \in \Re^{n\times 1}$ are uncertainties in the model, $\mathbf{x}(t) \in \Re^{n\times 1}$ is the state vector, $\mathbf{x}(t-\tau) \in \Re^{n\times 1}$ is the delayed state, $\mathbf{y}(t) \in \Re^{p\times 1}$ is the output vector, and $\mathbf{u}(t) \in \Re^{r\times 1}$ are the external inputs. The set $\{\chi_i\}_{i=1}^{s}$ is the polyhedral partition

of the input-state space, $span\left\{\left[\mathbf{x}(t)^T \quad \mathbf{x}(t-\tau)^T \quad \mathbf{u}(t)^T\right]^T\right\}$. The partition of the space is defined as:

$$\left[\bar{\mathbf{E}}_i \quad \bar{\mathbf{E}}_{\mathbf{d}i} \quad \mathbf{E}_{\mathbf{u}i}\right]\begin{bmatrix}\bar{\mathbf{x}}(t)\\ \bar{\mathbf{x}}(t-\tau)\\ \mathbf{u}(t)\end{bmatrix} \geq 0,\ \forall \begin{bmatrix}\mathbf{x}(t)\\ \mathbf{x}(t-\tau)\\ \mathbf{u}(t)\end{bmatrix} \in \chi_i \tag{1.4}$$

where $\bar{\mathbf{x}}_i(t)=\left[\mathbf{x}_i^T(t) \quad 1\right]^T$, $\bar{\mathbf{x}}_i(t-\tau)=\left[\mathbf{x}_i^T(t-\tau) \quad 1\right]^T$ and $\bar{\mathbf{E}}_i=\left[\mathbf{E}_i \quad \mathbf{e}_i\right]$, $\bar{\mathbf{E}}_{di}=\left[\mathbf{E}_{di} \quad \mathbf{e}_{di}\right]$. Note that $\mathbf{E}_i$, $\mathbf{E}_{\mathbf{d}i}$, $\mathbf{E}_{\mathbf{u}i}$, $\mathbf{e}_i$ and $\mathbf{e}_{di}$ are constant matrices with compatible dimension.

For PWA time-delay systems, available methods for stability analysis are very limited. The stability problem for PWA time-delay systems has been investigated in (Kulkarni et al. 2004). In (Moezzi et al., 2009), an approach based on the work of (Rodrigues & How, 2003) has been proposed to address the robust stability problem for PWA time-delay systems with unstructured uncertainty. There are several challenges in applying these approaches to practical systems. First, due to the inherent conservativeness of the Lyapunov approaches, these methods can become inconclusive. Although piecewise Lyapunov functions and Lyapunov-Krasovskii functionals are proposed to accommodate the switching mechanism and the infinite spectrum introduced by time delay, the conservativeness of these methods is still significant. Second, the computational complexity of these methods grows dramatically with the increase of system order and number of regions for PWA systems. Such high computational complexity may prevent these approaches from being effective implemented in real systems. Third, the existing methods consider only unstructured uncertainty in the model. When the structure of the uncertainty is identifiable, using structured uncertainty form in the analysis may lead to much less conservative results. Fourth, controller delays commonly exist in many

engineering systems. Such controller delays may retard the switching in the controller and may render the switching of the closed-loop system dependent on delayed states as well as states. This case is not properly considered in the existing work. Furthermore, although a few examples can be found for applying the PWA system framework to model physical systems, such as automotive electric throttle system (Baotic et al., 2003) and highway transportation system (Kulkarni, 2003), applications with subsequent control system design with stability analysis are hard to find. Such an application would be valuable for demonstrating the feasibility of this framework in practical engineering systems.

The switching of PWA time-delay systems depends on the states and/or the delayed states and cannot be arbitrarily changed. For more general switched time-delay systems, the switching signal, $i(t)$, may be directly controllable. Thus, instead of manipulating the input $\mathbf{u}(t)$, one can design a switching supervisory control signal, $i(t)$, such that the switched system has guaranteed stability by following the switching sequence. It is well known that a switched system will be stable if all the sub-systems are stable and the switching is sufficiently slow (Liberzon, 2003). Finding the lower bound for the frequency of the switching signal that stabilizes such systems is referred as dwell-time control. This dwell-time control for switched time-delay systems has been studied in (Chiou, 2005; S. Kim et al., 2006; Yan & Ozbay, 2008) with applications in power systems (Meyer et al., 2004) and networked control systems (Kim et al., 2004; Dai et al., 2009b). This type of control relies on the estimate of the asymptotic behavior of time-delay systems. More specifically, one needs to estimate the dominant decay rate and the

maximum energy rise during switching. Less conservative estimates of the decay function will lead to lower bounds on dwell time for these applications.

1.2 Research Objectives

The objectives of this research are to develop analysis methods that are computationally efficient, capable of tolerating model uncertainty, work for a wide range of practical problems, and produce guaranteed results for the stability analysis of PWA time-delay systems. We also want to develop an effective approach to obtain accurate estimates of transient characteristics of time-delay systems, and use these estimates for the dwell-time control of switched time-delay systems. Therefore, to further investigate the stability problem for PWA time-delay systems and switched time-delay systems, the related problems described in the following paragraphs have been considered in this research.

For the Lyapunov approach to PWA system stability, a major focus is on reducing the inherent conservativeness, but keeping the problem computationally tractable. Less conservativeness implies more accurate description of the system and less chance for the method to be inconclusive. Furthermore, the case of switching based on delayed states will be investigated for extending the results to more practical systems, such as systems with input delay. For robust stability analysis, systems with structured uncertainty will be considered to further reduce conservativeness when the structure of the uncertainty is known.

To demonstrate the effectiveness of the proposed approach, an application to the modeling and control of a nonlinear automotive clutch system will be considered. The

PWA framework will be applied to model the nonlinear clutch system first. Then, a control system will be designed based on the obtained PWA model to achieve reference tracking with consistent performance under different conditions for the closed-loop system. The stability of the control system in the presence of uncertainty and time delay will be verified using the proposed method.

For the estimation of the decay function for time-delay systems, we expect to develop a new approach, based on the closed-form solutions from the Lambert W function approach, to overcome the inherent conservativeness of matrix measure/norm or Lyapunov approaches and obtain a less conservative estimate of the decay function.

1.3 Organization of the Dissertation

In Chapter 1, the mathematical descriptions of uncertain PWA systems, and PWA time-delay systems, have been introduced. The literature on the stability problem for PWA systems and time-delay systems has been briefly reviewed. The challenges and objectives of the research have been stated.

In Chapter 2, a new approach for analyzing the stability of uncertain PWA time-delay systems is introduced. Sufficient conditions for the stability of nominal systems and systems subject to structured or unstructured uncertainty are derived using the Lyapunov-Krasovskii functional. The effectiveness of the approach is demonstrated in various numerical examples. This chapter is based on the work described in (Duan et al., 2011b, 2011c).

In Chapter 3, the application of the PWA system framework to the modeling and control of a nonlinear clutch system is demonstrated. The plant system is approximated

by a PWA model, followed by subsequent control design and stability analysis. Model uncertainty and time delay are included in the model to illustrate the robustness of the design. This chapter is based on the work described in (Duan et al., 2011d, 2011e).

In Chapter 4, the estimation of the decay function for time-delay systems is investigated. A new Lambert W function based approach for estimation of the decay function for time-delay systems is presented. The method is illustrated with several examples, and results are shown to compare favorably with existing methods. This chapter is based on the work described in (Duan et al., 2010, 2011a).

Finally Chapter 5 summarizes the contributions of the work and discusses possible topics for future research work.

CHAPTER 2
AN LMI-BASED APPROACH FOR STABILITY ANALYSIS OF PIECEWISE AFFINE TIME-DELAY SYSTEMS WITH UNCERTAINTY

2.1 Introduction

Piecewise affine (PWA) systems are defined by partitioning the state-space into a finite number of polyhedral regions and associating with each region a local linear differential equation. PWA systems can be used to model a variety of hybrid systems. The equivalence between PWA systems and interconnections of linear systems and finite automata has been demonstrated in (Sontag, 1996). Schutter and Moor (1999) have shown that PWA systems and discrete-time hybrid systems in mixed logic dynamical form can be mutually transformed into each other. PWA systems have been applied to model various systems showing piecewise characteristics such as systems with saturation or deadzones (Dai et al., 2009a) and logic control systems. PWA systems also provide nice traceability and flexibility to model a rich class of nonlinear systems where nonlinearities can be approximated using piecewise affine functions through linearization around different operating points.

Time delays exist in many systems of interest in engineering, biology, chemistry, physics and ecology (Niculescu, 2001). Such delays may be inherent in the components or the process of these systems, or arise from the deliberate introduction of time-delays

for control purposes. Practical systems are usually subject to various kinds of uncertainties, which may come from estimation errors, approximation errors or modeling errors. Delays and uncertainties can cause various problems such as oscillation, instability, inaccuracy, which may lead to poor performance or even system failure. To consider these effects in practical systems, it is valuable to incorporate time delays and uncertainties in the model of PWA systems. An application example of such system can be found in (Kulkarni, 2003), where the combined vehicle-driver behavior is described via a PWA time-delay system. Moezzi (2009) demonstrated some simple numerical examples such as the modelling of a nonlinear water tank control system and a pendulum control system. The nonlinear plants are approximated by PWA systems and the closed-loop systems are modeled as PWA time-delay systems with uncertainty after the input delays and approximation errors are considered. The author has also studied the control of a clutch for an all wheel drive vehicle as a PWA time-delay system with uncertainty (Duan et al., 2011d), as discussed in Chapter 3.

The stability of PWA systems has been a problem of recurring interest over the past several decades. Stability is, of course, critically important and usually implies safety in practice. Efficient schemes for stability analysis benefit control design for PWA systems (Grieder et al. 2004). However, even without time delay, the stability of PWA systems is a challenging problem since the stability of the sub-systems does not directly imply the stability of the global system (Branicky, 1998). Blondel and Tsitsiklis (1999) showed that, in general, this problem is either NP-complete or undecidable. Although there are various tools in the time-domain and frequency-domain for the stability of time-delay systems (Gu & Niculescu, 2003), accommodating the switching between sub-systems for

a PWA system is very difficult. The Lyapunov approach is still the dominant technique for studying PWA system stability. For time-delay systems, the Krasovskii-type approach (Krasovskii, 1963; Nieulescu et al., 1998; Richard, 1998; Park, 1999; Moon et al., 2001; Fridman & Shaked, 2002; Wu, et al., 2004; Xu & Lam 2005; He et al. 2005; Park 2007; Sun et al., 2009) and the Razumikhin-type approach (Razumikin , 1956; Hale, 1993; Li, et al., 1997; Jankovic, 2001) are two of the best known ways to construct these candidate Lyapunov functions. For PWA systems, the first approach to solve this stability problem is to seek a common Lyapunov function (e.g., Hu et al., 2002; Sun et al., 2006) for all of the sub-regions. To provide better flexibility for accommodating the structure of PWA systems, piecewise Lyapunov functions (Johansson & Rantze, 1997; Hassibi & Boyd, 1998; Pettersson, 1999; Mignone et al., 2000; Rodrigues & How, 2003; Prajna & Papachristodoulou, 2003; Rodrigues & Boyd, 2005) have been introduced. Although some conditions for the existence of common Lyapunov function have been derived using Lie algebra (Liberzon & Morse, 1999), the existence of piecewise Lyapunov function is still an open problem. For PWA time-delay systems, available methods for stability analysis are very limited. The stability problem of PWA time-delay systems has first been investigated in (Kulkarni et al. 2004) following the approach of Johansson (2003). In (Moezzi et al., 2009), an approach based on the work of (Rodrigues & How, 2003) has been proposed to address the robust stability problem for PWA time-delay systems with unstructured uncertainty. Although sufficient conditions have been obtained, these results are significantly conservative. Another important problem not considered in these existing work is the switching of the PWA time-delay systems based on not only on the states, but also on the delayed states. This situation commonly arises

for systems with controller delays (including sensor and actuator delays), which leads to the switching in the controller and the switching in the plant not being synchronized.

A major focus of these Lyapunov approaches is reducing the inherent conservativeness, but keeping the problem easily computable. Less conservativeness leads to not only a more accurate description of the system, but also more efficient control schemes (e.g., the cost of H-∞ control of PWA systems can be lower if a less conservative scheme is used). Computational complexity is also an important issue for PWA systems since the cost grows dramatically with the increase of the model complexity. In this work, we derive less conservative conditions for the stability of PWA time-delay systems compared to the existing methods (Kulkarni et al., 2004; Moezzi et al., 2009) without dramatic increase of computational complexity. Inspired by the bilinear matrix inequality (BMI) based approach for time-delay systems in (Sun & Liu, 2009), we introduce a piecewise Lyapunov-Krasovskii functional candidate with an additional triple integration term and formulate linear matrix inequality (LMI) based conditions for the stability of PWA time-delay systems. There are four major improvements over the current method of (Moezzi et al., 2009). First, the conservativeness of the approach is further reduced with the additional relaxations from the triple integration term. Second, the case of switching based on delayed states is considered in our method but not for the method in (Moezzi et al., 2009). Third, the computational complexity of the method in (Moezzi et al., 2009) increases quadratically with the increase in the number of regions, while the complexity of our approach increases only proportionally. Last, our approach also considers the structured uncertainty case, which is not included in (Moezzi et al., 2009).

The organization of this chapter can be summarized as follows. In Section 2.2, the system is defined and the problem is introduced. In Section 2.3, the approach for nominal systems (i.e., PWA time-delay systems without uncertainty) is proposed, followed by the robust stability analysis in Section 2.4 for unstructured uncertainty case, and in Section 2.5 for structured uncertainty case. Numerical examples are provided for a comparison between the proposed approach and existing ones in Section 2.6. A summary and concluding remarks are in Section 2.7.

2.2 Problem Statement

Consider the PWA time-delay system with unstructured norm-bounded uncertainty:

$$\begin{aligned} &\dot{\mathbf{x}}(t) = \mathbf{A}_i\mathbf{x}(t) + \mathbf{A}_{di}\mathbf{x}(t-\tau) + \mathbf{a}_i + \boldsymbol{\delta}_i \\ &\forall \begin{bmatrix} \mathbf{x}(t) \\ \mathbf{x}(t-\tau) \end{bmatrix} \in \chi_i, \quad i \in I \end{aligned} \tag{2.1}$$

where $\mathbf{A}_i$, $\mathbf{A}_{di} \in \Re^{n\times n}$ are the coefficient matrices, $\mathbf{a}_i \in \Re^{n\times 1}$ are the affine terms, $\mathbf{x} \in \Re^{n\times 1}$ is the state vector, t is time and $\tau \in \Re$ is a constant time delay. The set $\{\chi_i\}_{i=1}^{s}$ is the polyhedral partition of the state space and I is the set of region indices. The partition of the state space is defined as:

$$\begin{bmatrix} \bar{\mathbf{E}}_i & \bar{\mathbf{E}}_{di} \end{bmatrix} \begin{bmatrix} \bar{\mathbf{x}}(t) \\ \bar{\mathbf{x}}(t-\tau) \end{bmatrix} \geq 0, \ \forall \begin{bmatrix} \mathbf{x}(t) \\ \mathbf{x}(t-\tau) \end{bmatrix} \in \chi_i, \ i \in I \tag{2.2}$$

where $\bar{\mathbf{x}}_i(t) = \begin{bmatrix} \mathbf{x}_i^T(t) & 1 \end{bmatrix}^T$, $\bar{\mathbf{x}}_i(t-\tau) = \begin{bmatrix} \mathbf{x}_i^T(t-\tau) & 1 \end{bmatrix}^T$ and $\bar{\mathbf{E}}_i = \begin{bmatrix} \mathbf{E}_i & \mathbf{e}_i \end{bmatrix}$, $\bar{\mathbf{E}}_{di} = \begin{bmatrix} \mathbf{E}_{di} & \mathbf{e}_{di} \end{bmatrix}$ are the region bounding matrices. The continuity matrices $\bar{\mathbf{F}}_i = \begin{bmatrix} \mathbf{F}_i & \mathbf{f}_i \end{bmatrix}$ and $\bar{\mathbf{F}}_{\mathbf{d}i} = \begin{bmatrix} \mathbf{F}_{di} & \mathbf{f}_{di} \end{bmatrix}$, satisfying

$$\begin{bmatrix}\bar{\mathbf{F}}_i & \bar{\mathbf{F}}_{di}\end{bmatrix}\begin{bmatrix}\bar{\mathbf{x}}(t)\\ \bar{\mathbf{x}}(t-\tau)\end{bmatrix}=\begin{bmatrix}\bar{\mathbf{F}}_j & \bar{\mathbf{F}}_{dj}\end{bmatrix}\begin{bmatrix}\bar{\mathbf{x}}(t)\\ \bar{\mathbf{x}}(t-\tau)\end{bmatrix},\ \forall\ \begin{bmatrix}\mathbf{x}(t)\\ \mathbf{x}(t-\tau)\end{bmatrix}\in\chi_i\cap\chi_j,\ i,j\in I \qquad (2.3)$$

can be constructed from $\bar{\mathbf{E}}_i$ and $\bar{\mathbf{E}}_{di}$ by following the procedure in (Johansson, 2003). The set of regions that contain the point $\begin{bmatrix}\mathbf{x}(t)\\ \mathbf{x}(t-\tau)\end{bmatrix}=0$ is denoted I_0. The set of regions that contains $\mathbf{x}(t)$=0 but $\mathbf{x}(t-\tau)\neq 0$ anywhere inside is denoted I_1. The set of regions that contains $\mathbf{x}(t-\tau)$=0 but $\mathbf{x}(t)\neq 0$ anywhere inside is denoted I_2. The region with $\mathbf{x}(t)\neq 0$ and $\mathbf{x}(t-\tau)\neq 0$ anywhere inside is denoted I_3. Correspondingly, we will have: $\mathbf{e}_i=\mathbf{e}_{di}=0$, $\mathbf{f}_i=\mathbf{f}_{di}=0$, $\mathbf{a}_i=0,\ \forall i\in I_0$; $\mathbf{e}_i$ =0, $\mathbf{f}_i=0$, $\mathbf{e}_{di}\neq 0$ and $\mathbf{f}_{di}\neq 0,\ \forall i\in I_1$; $\mathbf{e}\neq 0$, $\mathbf{f}_i\neq 0$, $\mathbf{e}_{di}=0$ and $\mathbf{f}_{di}=0,\ \forall i\in I_2$; $\mathbf{e}\neq 0$, $\mathbf{e}_{di}\neq 0$, $\mathbf{f}_i\neq 0$ and $\mathbf{f}_{di}\neq 0,\ \forall i\in I_3$. A detailed discussion on the construction of the region bounding matrices, $\bar{\mathbf{E}}_i$ and $\bar{\mathbf{E}}_{di}$, and the continuity matrices, $\bar{\mathbf{F}}_i$ and $\bar{\mathbf{F}}_{di}$, can be found in (Johansson, 2003). The switching can be based on both $\mathbf{x}(t)$ and $\mathbf{x}(t-\tau)$, or can be solely based on either of them. If the system switches on $\mathbf{x}(t-\tau)$ only, one will have $\mathbf{E}_i=0$, $\mathbf{e}_i=0$, $\mathbf{f}_i=0$ and $\mathbf{F}_i=\begin{bmatrix}\mathbf{I} & \mathbf{0}\end{bmatrix}^T$. Similarly, if the switching is based on $\mathbf{x}(t)$ only, one will have $\mathbf{E}_{di}=0$, $\mathbf{e}_{di}=0$, $\mathbf{f}_{di}=0$ and $\mathbf{F}_{di}=\begin{bmatrix}\mathbf{0} & \mathbf{I}\end{bmatrix}^T$.

For rigorous analysis, the uncertainty, $\boldsymbol{\delta}_i\in\Re^{n\times 1}$, is considered in the model and is assumed to be norm-bounded. The uncertainty can either be modeled as structured uncertainty or left unstructured. For the first case, assume that it is of the form

$$\boldsymbol{\delta}_i=\Delta\mathbf{A}_i\mathbf{x}(t)+\Delta\mathbf{A}_{di}\mathbf{x}(t-\tau)+\Delta\mathbf{a}_i \qquad (2.4)$$

where

$$\begin{bmatrix}\Delta\mathbf{A}_i & \Delta\mathbf{A}_{di} & \Delta\mathbf{a}_i\end{bmatrix} = \mathbf{G}_i\boldsymbol{\Lambda}_i\begin{bmatrix}\mathbf{H}_{1i} & \mathbf{H}_{2i} & \mathbf{H}_{3i}\end{bmatrix}$$
$$\boldsymbol{\Lambda}_i^T\boldsymbol{\Lambda}_i \le \mathbf{I}$$

and $\mathbf{G}_i$, $\boldsymbol{\Lambda}_i$, $\mathbf{H}_{1i}$, $\mathbf{H}_{2i}$, $\mathbf{H}_{3i}$ are constant matrices with compatible dimension describing how the uncertainty enters the parameter matrices. If the uncertainty is admissible, these matrices can be identified. Note that $\boldsymbol{\Delta}\mathbf{a}_i = 0$ and $\mathbf{H}_{3i} = 0$, $\forall i \in I_0$. If the uncertainty is not admissible, one may use the unstructured uncertainty form

$$\|\boldsymbol{\delta}_i\| \le \varepsilon_i \|\mathbf{x}(t)\| + \varepsilon_{di} \|\mathbf{x}(t-\tau)\| + \varepsilon_{ai} \tag{2.5}$$

where $\varepsilon_i, \varepsilon_{di}, \varepsilon_{ai} \in \Re$ are the factors of the bound with $\varepsilon_{ai} = 0$, $\forall i \in I_0$ and $\|\cdot\|$ is the 2-norm.

The switching in (2.1) is based on $\mathbf{x}(t-\tau)$ as well as $\mathbf{x}(t)$. To illustrate the importance of including $\mathbf{x}(t-\tau)$ in the partition, an example is provided here. Consider the PWA with piecewise state feedback control:

$$\dot{\mathbf{x}}(t) = \mathbf{A}_i\mathbf{x}(t) + \mathbf{B}_i\mathbf{u}(t) + \mathbf{a}_i,\ \mathbf{u}(t) = \mathbf{K}_i x(t) + \mathbf{k}_i,\ \forall \mathbf{x}(t) \in \chi_i \tag{2.6}$$

If a delay exists in the controller, or the sensor or actuator, which is a common occurrence in many engineering systems, one has

$$\mathbf{u}(t-\tau) = \mathbf{K}_j\mathbf{x}(t-\tau) + \mathbf{k}_j,\ \forall \mathbf{x}(t-\tau) \in \chi_j \tag{2.7}$$

where j is the delayed switching signal and is determined by the delayed state, $\mathbf{x}(t-\tau)$. Such a controller delay will not only postpone the control input but also retard the switching in the controller. Thus, the closed-loop system becomes a PWA time-delay system where switching depends on both $\mathbf{x}(t)$ and $\mathbf{x}(t-\tau)$:

$$\dot{\mathbf{x}}(t) = \mathbf{A}_i\mathbf{x}(t) + \mathbf{B}_i\mathbf{K}_j\mathbf{x}(t-\tau) + \mathbf{B}_i\mathbf{k}_j + \mathbf{a}_i,\ \forall \begin{bmatrix}\mathbf{x}(t)\\ \mathbf{x}(t-\tau)\end{bmatrix} \in \begin{bmatrix}\chi_i\\ \chi_j\end{bmatrix}$$

This problem has not been correctly considered in any of the existing work for PWA time-delay systems. Thus, its mathematical treatment here represents a major contribution.

The objective of this work is to find sufficient conditions such that the system in (1) is asymptotically stable. First, the stability of the nominal system (i.e., $\boldsymbol{\delta}_i \equiv 0$) is investigated. Then, the results are extended to the systems with structured uncertainty and the systems with unstructured uncertainty for robust stability analysis.

2.3 Analysis of Nominal PWA Time-Delay Systems

Consider the nominal PWA time-delay system, i.e., the system in (1) with $\boldsymbol{\delta}_i \equiv 0$:

$$\begin{aligned} &\dot{\mathbf{x}}(t) = \mathbf{A}_i\mathbf{x}(t) + \mathbf{A}_{di}\mathbf{x}(t-\tau) + \mathbf{a}_i \\ &\forall \mathbf{x} \in \chi_i, \quad i \in I \end{aligned} \tag{2.8}$$

In this section, sufficient conditions for the stability of the nominal system will be derived. To facilitate the analysis, define the following augmented matrices:

$$\bar{\mathbf{A}}_i = \begin{bmatrix} \mathbf{A}_i & \mathbf{a}_i \\ 0 & 0 \end{bmatrix},\ \bar{\mathbf{A}}_{di} = \begin{bmatrix} \mathbf{A}_{di} & 0 \\ 0 & 0 \end{bmatrix},\ \bar{\mathbf{x}}(t) = \begin{bmatrix} \mathbf{x}(t) \\ 1 \end{bmatrix},\ \dot{\bar{\mathbf{x}}}(t) = \begin{bmatrix} \dot{\mathbf{x}}(t) \\ 0 \end{bmatrix} \tag{2.9}$$

Thus, the system in (2.8) can be written as

$$\begin{aligned} &\dot{\mathbf{x}}(t) = \mathbf{A}_i x(t) + \mathbf{A}_{di}\mathbf{x}(t-\tau), \quad \forall i \in I_0 \\ &\dot{\bar{\mathbf{x}}}(t) = \bar{\mathbf{A}}_i \bar{x}(t) + \bar{\mathbf{A}}_{di}\bar{\mathbf{x}}(t-\tau), \quad \forall i \in I_1,\ I_2,\ I_3 \end{aligned} \tag{2.10}$$

Using the formulation in (2.10), the results for $\forall i \in I_1,\ I_2,\ I_3$ will be analogous to the results for $i \in I_0$ by combining $\mathbf{A}_i$ and $\mathbf{a}_i$ into $\bar{\mathbf{A}}_i$.

Theorem 2.1: Consider symmetric matrices $\mathbf{T}$, $\mathbf{J}_i$, $\mathbf{K}_i$ such that $\mathbf{J}_i$, $\mathbf{K}_i$ have non-negative entries while $\begin{bmatrix} \mathbf{P}_{11i} & \mathbf{P}_{12i} \\ \mathbf{P}_{12i}^T & \mathbf{P}_{22i} \end{bmatrix} = \begin{bmatrix} \mathbf{F}_i^T\mathbf{T}\mathbf{F}_i & \mathbf{F}_i^T\mathbf{T}\mathbf{F}_{di} \\ \mathbf{F}_{di}^T\mathbf{T}\mathbf{F}_i & \mathbf{F}_{di}^T\mathbf{T}\mathbf{F}_{di} \end{bmatrix}$, for $i \in I_0$, and $\begin{bmatrix} \bar{\mathbf{P}}_{11i} & \bar{\mathbf{P}}_{12i} \\ \bar{\mathbf{P}}_{12i}^T & \bar{\mathbf{P}}_{22i} \end{bmatrix} =$

$\begin{bmatrix} \bar{\mathbf{F}}_i^T \mathbf{T} \bar{\mathbf{F}}_i & \bar{\mathbf{F}}_i^T \mathbf{T} \bar{\mathbf{F}}_{di} \\ \bar{\mathbf{F}}_{di}^T \mathbf{T} \bar{\mathbf{F}}_i & \bar{\mathbf{F}}_{di}^T \mathbf{T} \bar{\mathbf{F}}_{di} \end{bmatrix}$, for $i \in \{I_1,\ I_2,\ I_3\}$, such that the LMIs in (2.11) , (2.12) and (2.13) are

satisfied for every region:

For $\forall i \in I_0$,

$$\begin{bmatrix} \boldsymbol{\Lambda}_{11} & \boldsymbol{\Lambda}_{12} & -\tau\mathbf{U} & -\tau\mathbf{Y} & \mathbf{P}_{12i} + \mathbf{V}^T & \frac{1}{2}\tau^2\mathbf{U} \\ * & \boldsymbol{\Lambda}_{22} & 0 & -\tau\mathbf{W} & -\mathbf{Q}_{12} + \mathbf{P}_{22i} - \mathbf{V}^T & 0 \\ * & * & -\tau\mathbf{Z}_{11} & -\tau\mathbf{Z}_{12} & 0 & 0 \\ * & * & * & -\tau\mathbf{Z}_{22} & -\tau\mathbf{V}^T & 0 \\ * & * & * & * & -\mathbf{Q}_{22} & 0 \\ * & * & * & * & * & -\frac{1}{2}\tau^2\mathbf{R} \end{bmatrix} < 0;$$

$$\begin{bmatrix} \mathbf{F}_i^T \mathbf{T} \mathbf{F}_i & \mathbf{F}_i^T \mathbf{T} \mathbf{F}_{di} \\ \mathbf{F}_{di}^T \mathbf{T} \mathbf{F}_i & \mathbf{F}_{di}^T \mathbf{T} \mathbf{F}_{di} \end{bmatrix} - \begin{bmatrix} \mathbf{E}_i^T \mathbf{J}_i \mathbf{E}_i & \mathbf{E}_i^T \mathbf{J}_i \mathbf{E}_{di} \\ \mathbf{E}_{di}^T \mathbf{J}_i \mathbf{E}_i & \mathbf{E}_{di}^T \mathbf{J}_i \mathbf{E}_{di} \end{bmatrix} > 0; \quad \mathbf{R} > 0; \tag{2.11}$$

$$\begin{bmatrix} \mathbf{Q}_{11} & \mathbf{Q}_{12} \\ \mathbf{Q}_{12}^T & \mathbf{Q}_{22} \end{bmatrix} > 0; \quad \begin{bmatrix} \mathbf{Z}_{11} & \mathbf{Z}_{12} \\ \mathbf{Z}_{12}^T & \mathbf{Z}_{22} \end{bmatrix} > 0;$$

For $\forall i \in I_1,\ I_2,\ I_3$,

$$\begin{bmatrix} \bar{\boldsymbol{\Lambda}}_{11} & \bar{\boldsymbol{\Lambda}}_{12} & -\tau\mathbf{U}_1 & -\tau\bar{\mathbf{Y}} & \bar{\mathbf{P}}_{12} + \bar{\mathbf{V}}^T & \frac{1}{2}\tau^2\bar{\mathbf{U}} \\ * & \bar{\boldsymbol{\Lambda}}_{22} & 0 & -\tau\bar{\mathbf{W}} & -\bar{\mathbf{Q}}_{12} + \bar{\mathbf{P}}_{22} - \bar{\mathbf{V}}^T & 0 \\ * & * & -\tau\mathbf{Z}_{11} & -\tau\begin{bmatrix}\mathbf{Z}_{12} & \mathbf{Z}_{121}\end{bmatrix} & 0 & 0 \\ * & * & * & -\tau\bar{\mathbf{Z}}_{22} & -\tau\bar{\mathbf{V}}^T & 0 \\ * & * & * & * & -\bar{\mathbf{Q}}_{22} & 0 \\ * & * & * & * & * & -\frac{1}{2}\tau^2\bar{\mathbf{R}} \end{bmatrix} < 0 \tag{2.12}$$

$$\bar{\mathbf{Q}}_{22} > 0; \quad \bar{\mathbf{Z}}_{22} > 0; \quad \bar{\mathbf{R}} > 0;$$

and additionally,

$$\begin{bmatrix} \mathbf{F}_i^T \mathbf{T} \mathbf{F}_i & \mathbf{F}_i^T \mathbf{T} \bar{\mathbf{F}}_{di} \\ \bar{\mathbf{F}}_{di}^T \mathbf{T} \mathbf{F}_i & \bar{\mathbf{F}}_{di}^T \mathbf{T} \bar{\mathbf{F}}_{di} \end{bmatrix} - \begin{bmatrix} \mathbf{E}_i^T \mathbf{J}_i \mathbf{E}_i & \mathbf{E}_i^T \mathbf{J}_i \bar{\mathbf{E}}_{di} \\ \bar{\mathbf{E}}_{di}^T \mathbf{J}_i \mathbf{E}_i & \bar{\mathbf{E}}_{di}^T \mathbf{J}_i \bar{\mathbf{E}}_{di} \end{bmatrix} > 0; \ \forall i \in I_1$$

$$\begin{bmatrix} \bar{\mathbf{F}}_i^T \mathbf{T} \bar{\mathbf{F}}_i & \bar{\mathbf{F}}_i^T \mathbf{T} \mathbf{F}_{di} \\ \mathbf{F}_{di}^T \mathbf{T} \bar{\mathbf{F}}_i & \mathbf{F}_{di}^T \mathbf{T} \mathbf{F}_{di} \end{bmatrix} - \begin{bmatrix} \bar{\mathbf{E}}_i^T \mathbf{J}_i \bar{\mathbf{E}}_i & \bar{\mathbf{E}}_i^T \mathbf{J}_i \mathbf{E}_{di} \\ \mathbf{E}_{di}^T \mathbf{J}_i \bar{\mathbf{E}}_i & \mathbf{E}_{di}^T \mathbf{J}_i \mathbf{E}_{di} \end{bmatrix} > 0; \ \forall i \in I_2$$

$$\begin{bmatrix} \bar{\mathbf{F}}_i^T \mathbf{T} \bar{\mathbf{F}}_i & \bar{\mathbf{F}}_i^T \mathbf{T} \bar{\mathbf{F}}_{di} \\ \bar{\mathbf{F}}_{di}^T \mathbf{T} \bar{\mathbf{F}}_i & \bar{\mathbf{F}}_{di}^T \mathbf{T} \bar{\mathbf{F}}_{di} \end{bmatrix} - \begin{bmatrix} \bar{\mathbf{E}}_i^T \mathbf{J}_i \bar{\mathbf{E}}_i & \bar{\mathbf{E}}_i^T \mathbf{J}_i \bar{\mathbf{E}}_{di} \\ \bar{\mathbf{E}}_{di}^T \mathbf{J}_i \bar{\mathbf{E}}_i & \bar{\mathbf{E}}_{di}^T \mathbf{J}_i \bar{\mathbf{E}}_{di} \end{bmatrix} > 0; \ \forall i \in I_3 \qquad (2.13)$$

where

$\mathbf{Y}$, $\mathbf{W}$, $\mathbf{U}$, $\mathbf{Q}_{11}$, $\mathbf{Q}_{12}$, $\mathbf{Q}_{22}$, $\mathbf{Z}_{11}$, $\mathbf{Z}_{12}$, $\mathbf{Z}_{22}$, $\mathbf{R} \in \Re^{n \times n}$, $\bar{\mathbf{Y}}$, $\bar{\mathbf{W}} \in \Re^{(n+1)\times(n+1)}$, $\mathbf{U}_1 \in \Re^{(n+1)\times n}$,

$\mathbf{Q}_{121}$, $\mathbf{Q}_{221}$, $\mathbf{Z}_{121}$, $\mathbf{Z}_{221}$, $\mathbf{R}_{12} \in \Re^{n\times 1}$, $\mathbf{Q}_{222}$, $\mathbf{Z}_{222}$, $\mathbf{R}_{22} \in \Re$,

$$\begin{aligned}
\mathbf{\Lambda}_{11} &= \mathbf{P}_{11i}\mathbf{A}_i + \mathbf{A}_i^T \mathbf{P}_{11i} + \mathbf{Y} + \mathbf{Y}^T + \mathbf{Q}_{11} + \mathbf{Q}_{12}\mathbf{A}_i + \mathbf{A}_i^T \mathbf{Q}_{12}^T + \mathbf{A}_i^T \mathbf{Q}_{22}^T \mathbf{A}_i + \tau \mathbf{Z}_{11} + \tau \mathbf{Z}_{12}\mathbf{A}_i \\
&\quad + \tau \mathbf{A}_i^T \mathbf{Z}_{12}^T + \tau \mathbf{A}_i^T \mathbf{Z}_{22}\mathbf{A}_i + \tau \mathbf{U} + \tau \mathbf{U}^T + \frac{1}{2}\tau^2 \mathbf{A}_i^T \mathbf{R}\mathbf{A}_i + \mathbf{E}_i^T \mathbf{K}_i \mathbf{E}_i, \\
\bar{\mathbf{\Lambda}}_{11} &= \bar{\mathbf{P}}_{11i}\bar{\mathbf{A}}_i + \bar{\mathbf{A}}_i^T \bar{\mathbf{P}}_{11i} + \bar{\mathbf{Y}} + \bar{\mathbf{Y}}^{\mathbf{T}} + \bar{\mathbf{Q}}_{11} + \bar{\mathbf{Q}}_{12}\mathbf{A}_i + \mathbf{A}_i^T \bar{\mathbf{Q}}_{12}^T + \mathbf{A}_i^T \bar{\mathbf{Q}}_{22}^T \mathbf{A}_i + \tau \bar{\mathbf{Z}}_{11} + \tau \bar{\mathbf{Z}}_{12}\bar{\mathbf{A}}_i \\
&\quad + \tau \bar{\mathbf{A}}_i^T \bar{\mathbf{Z}}_{12}^T + \tau \bar{\mathbf{A}}_i^T \bar{\mathbf{Z}}_{22}\bar{\mathbf{A}}_i + \tau \bar{\mathbf{U}} + \tau \bar{\mathbf{U}}^T + \frac{1}{2}\tau^2 \bar{\mathbf{A}}_i^T \bar{\mathbf{R}}\bar{\mathbf{A}}_i + \bar{\mathbf{E}}_i^T \mathbf{K}_i \bar{\mathbf{E}}_i, \\
\mathbf{\Lambda}_{12} &= \mathbf{P}_{11i}\mathbf{A}_{di} + \mathbf{A}_i^T \mathbf{P}_{12i} - \mathbf{Y} + \mathbf{W}^T + \tau \mathbf{Z}_{12}\mathbf{A}_{di} + \tau \mathbf{A}_i^T \mathbf{Z}_{22}\mathbf{A}_{di} + \mathbf{Q}_{12}\mathbf{A}_{di} \\
&\quad + \mathbf{A}_i^T \mathbf{Q}_{22}\mathbf{A}_{di} + \frac{1}{2}\tau^2 \mathbf{A}_i^T \mathbf{R}\mathbf{A}_{di} + \bar{\mathbf{E}}_i^T \mathbf{K}_i \bar{\mathbf{E}}_{di}, \\
\bar{\mathbf{\Lambda}}_{12} &= \bar{\mathbf{P}}_{11i}\bar{\mathbf{A}}_{di} + \bar{\mathbf{A}}_i^T \bar{\mathbf{P}}_{12i} - \bar{\mathbf{Y}} + \bar{\mathbf{W}}^T + \tau \bar{\mathbf{Z}}_{12}\bar{\mathbf{A}}_{di} + \tau \bar{\mathbf{A}}_i^T \bar{\mathbf{Z}}_{22}\bar{\mathbf{A}}_{di} + \bar{\mathbf{Q}}_{12}\mathbf{A}_{di} \\
&\quad + \mathbf{A}_i^T \bar{\mathbf{Q}}_{22}\mathbf{A}_{di} + \frac{1}{2}\tau^2 \bar{\mathbf{A}}_i^T \bar{\mathbf{R}}\bar{\mathbf{A}}_{di} + \bar{\mathbf{E}}_i^T \mathbf{K}_i \bar{\mathbf{E}}_{di},
\end{aligned}$$

$$\begin{aligned}
\mathbf{\Lambda}_{22} &= -\mathbf{Q}_{11} + \mathbf{P}_{12i}^T \mathbf{A}_{di} + \mathbf{A}_{di}^T \mathbf{P}_{12i} + \mathbf{A}_{di}^T \mathbf{Q}_{22}\mathbf{A}_{di} - \mathbf{W} - \mathbf{W}^{\mathbf{T}} + \tau \mathbf{A}_{di}^T \mathbf{Z}_{22}\mathbf{A}_{di} \\
&\quad + \frac{1}{2}\tau^2 \mathbf{A}_{di}^T \mathbf{R}\mathbf{A}_{di} + \mathbf{E}_{di}^T \mathbf{K}_i \mathbf{E}_{di}, \\
\bar{\mathbf{\Lambda}}_{22} &= -\bar{\mathbf{Q}}_{11} + \bar{\mathbf{P}}_{12i}^T \bar{\mathbf{A}}_{di} + \bar{\mathbf{A}}_{di}^T \bar{\mathbf{P}}_{12i} + \bar{\mathbf{A}}_{di}^T \bar{\mathbf{Q}}_{22}\bar{\mathbf{A}}_{di} - \bar{\mathbf{W}} - \bar{\mathbf{W}}^{\mathbf{T}} + \tau \bar{\mathbf{A}}_{di}^T \bar{\mathbf{Z}}_{22}\bar{\mathbf{A}}_{di} \\
&\quad + \frac{1}{2}\tau^2 \bar{\mathbf{A}}_{di}^T \bar{\mathbf{R}}\bar{\mathbf{A}}_{di} + \bar{\mathbf{E}}_{di}^T \mathbf{K}_i \bar{\mathbf{E}}_{di},
\end{aligned}$$

$$\bar{\mathbf{Q}}_{11} = \begin{bmatrix} \mathbf{Q}_{11} & 0 \\ 0 & 0 \end{bmatrix}, \ \bar{\mathbf{Q}}_{12} = \begin{bmatrix} \mathbf{Q}_{12} & \mathbf{Q}_{121} \\ 0 & 0 \end{bmatrix}, \ \bar{\mathbf{Q}}_{22} = \begin{bmatrix} \mathbf{Q}_{22} & \mathbf{Q}_{221} \\ \mathbf{Q}_{221}^T & \mathbf{Q}_{222} \end{bmatrix}, \ \bar{\mathbf{U}} = \begin{bmatrix} \mathbf{U}_1 & 0 \end{bmatrix},$$

$$\bar{\mathbf{Z}}_{11} = \begin{bmatrix} \mathbf{Z}_{11} & 0 \\ 0 & 0 \end{bmatrix}, \ \bar{\mathbf{Z}}_{12} = \begin{bmatrix} \mathbf{Z}_{12} & \mathbf{Z}_{121} \\ 0 & 0 \end{bmatrix}, \ \bar{\mathbf{Z}}_{22} = \begin{bmatrix} \mathbf{Z}_{22} & \mathbf{Z}_{221} \\ \mathbf{Z}_{221}^T & \mathbf{Z}_{222} \end{bmatrix}, \ \bar{\mathbf{R}} = \begin{bmatrix} \mathbf{R} & \mathbf{R}_{12} \\ \mathbf{R}_{12}^T & \mathbf{R}_{22} \end{bmatrix}$$

Then every piecewise continuous trajectory of the system in (2.8) tends to zero asymptotically in the absence of attractive sliding modes.

Proof: For $i \in I_0$, consider the following Lyapunov-Krasovskii functional candidate:

$$\mathbf{V} = \mathbf{V}_1 + \mathbf{V}_2 + \mathbf{V}_3 + \mathbf{V}_4 \tag{2.14}$$

where

$$\mathbf{V}_1 = \begin{bmatrix} \mathbf{x}(t) \\ \mathbf{x}(t-\tau) \end{bmatrix}^T \begin{bmatrix} \mathbf{P}_{11i} & \mathbf{P}_{12i} \\ \mathbf{P}_{12i}^T & \mathbf{P}_{22i} \end{bmatrix} \begin{bmatrix} \mathbf{x}(t) \\ \mathbf{x}(t-\tau) \end{bmatrix} \tag{2.15}$$

$$\mathbf{V}_2 = \int_{t-\tau}^{t} \begin{bmatrix} \mathbf{x}(s) \\ \dot{\mathbf{x}}(s) \end{bmatrix}^T \begin{bmatrix} \mathbf{Q}_{11} & \mathbf{Q}_{12} \\ \mathbf{Q}_{12}^T & \mathbf{Q}_{22} \end{bmatrix} \begin{bmatrix} \mathbf{x}(s) \\ \dot{\mathbf{x}}(s) \end{bmatrix} ds \tag{2.16}$$

$$\mathbf{V}_3 = \int_{-\tau}^{0} \int_{t+\theta}^{t} \begin{bmatrix} \mathbf{x}(s) \\ \dot{\mathbf{x}}(s) \end{bmatrix}^T \begin{bmatrix} \mathbf{Z}_{11} & \mathbf{Z}_{12} \\ \mathbf{Z}_{12}^T & \mathbf{Z}_{22} \end{bmatrix} \begin{bmatrix} \mathbf{x}(s) \\ \dot{\mathbf{x}}(s) \end{bmatrix} ds d\theta \tag{2.17}$$

$$\mathbf{V}_4 = \int_{-\tau}^{0} \int_{\theta}^{0} \int_{t+\lambda}^{t} \dot{\mathbf{x}}(s)^T \mathbf{R} \dot{\mathbf{x}}(s) ds d\lambda d\theta \tag{2.18}$$

From the Newton- Leibniz formula, we have

$$\mathbf{x}(t-\tau) = \mathbf{x}(t) - \int_{t-\tau}^{t} \dot{\mathbf{x}}(s) ds \tag{2.19}$$

and

$$\int_{-\tau}^{0} \int_{t+\theta}^{t} \dot{\mathbf{x}}(s) ds d\theta = \int_{-\tau}^{0} \left[\mathbf{x}(t) - \mathbf{x}(t+\theta) \right] d\theta = \tau \mathbf{x}(t) - \int_{t-\tau}^{t} \mathbf{x}(s) ds \tag{2.20}$$

Taking the time derivative of (2.15)-(2.18) along the trajectory of (2.8) and considering (2.19)-(2.20) gives

$$
\begin{aligned}
\dot{\mathbf{V}}_1 &= 2\mathbf{x}(t)^T\mathbf{P}_{11i}\left[\mathbf{A}_i\mathbf{x}(t)+\mathbf{A}_{di}\mathbf{x}(t-\tau)\right]+2\mathbf{x}(t-\tau)^T\mathbf{P}_{12i}^T\left[\mathbf{A}_i\mathbf{x}(t)+\mathbf{A}_{di}\mathbf{x}(t-\tau)\right]\\
&\quad+2\mathbf{x}(t)^T\mathbf{P}_{12i}\dot{\mathbf{x}}(t-\tau)+2\mathbf{x}(t-\tau)^{\mathbf{T}}\mathbf{P}_{22i}\dot{\mathbf{x}}(t-\tau)\\
&\quad+2\mathbf{x}(t)^T\mathbf{Y}\left[\mathbf{x}(t)-\mathbf{x}(t-\tau)-\int_{t-t}^{t}\dot{\mathbf{x}}(s)ds\right]\\
&\quad+2\mathbf{x}(t-\tau)^T\mathbf{W}\left[\mathbf{x}(t)-\mathbf{x}(t-\tau)-\int_{t-t}^{t}\dot{\mathbf{x}}(s)ds\right]\\
&\quad+2\dot{\mathbf{x}}(t-\tau)^T\mathbf{V}\left[\mathbf{x}(t)-\mathbf{x}(t-\tau)-\int_{t-t}^{t}\dot{\mathbf{x}}(s)ds\right]\\
&\quad+2\mathbf{x}(t)^T\mathbf{U}\left[\tau\mathbf{x}(t)-\int_{t-t}^{t}\mathbf{x}(s)ds-\int_{-\tau}^{0}\int_{t+\theta}^{t}\dot{\mathbf{x}}(s)dsd\theta\right]
\end{aligned}
\tag{2.21}
$$

$$
\begin{aligned}
\dot{\mathbf{V}}_2 &= \begin{bmatrix}\mathbf{x}(t)\\ \dot{\mathbf{x}}(t)\end{bmatrix}^T\begin{bmatrix}\mathbf{Q}_{11} & \mathbf{Q}_{12}\\ \mathbf{Q}_{12}^T & \mathbf{Q}_{22}\end{bmatrix}\begin{bmatrix}\mathbf{x}(t)\\ \dot{\mathbf{x}}(t)\end{bmatrix}-\begin{bmatrix}\mathbf{x}(t-\tau)\\ \dot{\mathbf{x}}(t-\tau)\end{bmatrix}^T\begin{bmatrix}\mathbf{Q}_{11} & \mathbf{Q}_{12}\\ \mathbf{Q}_{12}^T & \mathbf{Q}_{22}\end{bmatrix}\begin{bmatrix}\mathbf{x}(t-\tau)\\ \dot{\mathbf{x}}(t-\tau)\end{bmatrix}\\
&= \mathbf{x}(t)^T(\mathbf{Q}_{11}+\mathbf{Q}_{12}\mathbf{A}_i+\mathbf{A}_i^T\mathbf{Q}_{12}^T+\mathbf{A}_i^T\mathbf{Q}_{22}\mathbf{A}_i)\mathbf{x}(t)+\mathbf{x}(t-\tau)^T\mathbf{A}_{di}^T\mathbf{Q}_{22}\mathbf{A}_{di}\mathbf{x}(t-\tau)\\
&\quad+2\mathbf{x}(t)^T(\mathbf{Q}_{12}\mathbf{A}_{di}+\mathbf{A}_i^T\mathbf{Q}_{22}\mathbf{A}_{di})\mathbf{x}(t-\tau)-\begin{bmatrix}\mathbf{x}(t-\tau)\\ \dot{\mathbf{x}}(t-\tau)\end{bmatrix}^T\begin{bmatrix}\mathbf{Q}_{11} & \mathbf{Q}_{12}\\ \mathbf{Q}_{12}^T & \mathbf{Q}_{22}\end{bmatrix}\begin{bmatrix}\mathbf{x}(t-\tau)\\ \dot{\mathbf{x}}(t-\tau)\end{bmatrix}
\end{aligned}
\tag{2.22}
$$

$$
\begin{aligned}
\dot{\mathbf{V}}_3 &= \int_{t-\tau}^{t}\begin{bmatrix}\mathbf{x}(t)\\ \dot{\mathbf{x}}(t)\end{bmatrix}^T\begin{bmatrix}\mathbf{Z}_{11} & \mathbf{Z}_{12}\\ \mathbf{Z}_{12}^T & \mathbf{Z}_{22}\end{bmatrix}\begin{bmatrix}\mathbf{x}(t)\\ \dot{\mathbf{x}}(t)\end{bmatrix}-\begin{bmatrix}\mathbf{x}(s)\\ \dot{\mathbf{x}}(s)\end{bmatrix}^T\begin{bmatrix}\mathbf{Z}_{11} & \mathbf{Z}_{12}\\ \mathbf{Z}_{12}^T & \mathbf{Z}_{22}\end{bmatrix}\begin{bmatrix}\mathbf{x}(s)\\ \dot{\mathbf{x}}(s)\end{bmatrix}ds\\
&= \int_{t-\tau}^{t}\Big\{\mathbf{x}(t)^T(\mathbf{Z}_{11}+\mathbf{Z}_{12}\mathbf{A}_i+\mathbf{A}_i^T\mathbf{Z}_{12}^T+\mathbf{A}_i^T\mathbf{Z}_{22}\mathbf{A}_i)\mathbf{x}(t)\\
&\qquad+2\mathbf{x}(t)^T(\mathbf{Z}_{12}\mathbf{A}_{di}+\mathbf{A}_i^T\mathbf{Z}_{22}\mathbf{A}_{di})\mathbf{x}(t-\tau)+\mathbf{x}(t-\tau)^T\mathbf{A}_{di}^T\mathbf{Z}_{22}\mathbf{A}_{di}\mathbf{x}(t-\tau)\\
&\qquad-\begin{bmatrix}\mathbf{x}(s)\\ \dot{\mathbf{x}}(s)\end{bmatrix}^T\begin{bmatrix}\mathbf{Z}_{11} & \mathbf{Z}_{12}\\ \mathbf{Z}_{12}^T & \mathbf{Z}_{22}\end{bmatrix}\begin{bmatrix}\mathbf{x}(s)\\ \dot{\mathbf{x}}(s)\end{bmatrix}\Big\}ds
\end{aligned}
\tag{2.23}
$$

$$
\begin{aligned}
\dot{\mathbf{V}}_4 &= \frac{\tau^2}{2}\dot{\mathbf{x}}(t)^T\mathbf{R}\dot{\mathbf{x}}(t)-\int_{-\tau}^{0}\int_{t+\theta}^{t}\dot{\mathbf{x}}(s)^T\mathbf{R}\dot{\mathbf{x}}(s)dsd\theta\\
&= \frac{\tau^2}{2}\mathbf{x}(t)^T\mathbf{A}_i^T\mathbf{R}\mathbf{A}_i x(t)+\tau^2\mathbf{x}(t)^T\mathbf{A}_i^T\mathbf{R}\mathbf{A}_{di}\mathbf{x}(t-\tau)+\frac{\tau^2}{2}\mathbf{x}(t-\tau)^T\mathbf{A}_{di}^T\mathbf{R}\mathbf{A}_{di}\mathbf{x}(t-\tau)\\
&\quad-\int_{-\tau}^{0}\int_{t+\theta}^{t}\dot{\mathbf{x}}(s)^T\mathbf{R}\dot{\mathbf{x}}(s)dsd\theta
\end{aligned}
\tag{2.24}
$$

Using the lemma in (Wang, 1992), it can be shown that

$$
\begin{aligned}
-2\mathbf{x}(t)^T\mathbf{U}\int_{-\tau}^{0}\int_{t+\theta}^{t}\dot{\mathbf{x}}(s)dsd\theta &\le \int_{-\tau}^{0}\int_{t+\theta}^{t}\left[\mathbf{x}(t)^T\mathbf{U}\mathbf{R}^{-1}\mathbf{U}^T\mathbf{x}(t)+\dot{\mathbf{x}}(s)^T\mathbf{R}\dot{\mathbf{x}}(s)\right]dsd\theta\\
&\le \frac{\tau^2}{2}\mathbf{x}(t)^T\mathbf{U}\mathbf{R}^{-1}\mathbf{U}^T\mathbf{x}(t)+\int_{-\tau}^{0}\int_{t+\theta}^{t}\dot{\mathbf{x}}(s)^T\mathbf{R}\dot{\mathbf{x}}(s)dsd\theta
\end{aligned}
\tag{2.25}
$$

hold for any symmetric matrices $\mathbf{R} > 0$. Combining (2.21)-(2.25) yields

$$\dot{\mathbf{V}} \le \frac{1}{\tau}\int_{t-\tau}^{t} \zeta^T(t,s)\Pi(\tau,i)\zeta(t,s)ds \tag{2.26}$$

where

$$\zeta(t,s) = \begin{bmatrix} \mathbf{x}(t)^T & \mathbf{x}(t-\tau)^T & \mathbf{x}(s)^T & \dot{\mathbf{x}}(s)^T & \dot{\mathbf{x}}(t-\tau)^T \end{bmatrix}^T$$

$$\Pi(\tau,i) = \begin{bmatrix} \boldsymbol{\Lambda}_{11} - \frac{1}{2}\tau^2\mathbf{U}\mathbf{R}^{-1}\mathbf{U}^T & \boldsymbol{\Lambda}_{12} & -\tau\mathbf{U} & -\tau\mathbf{Y} & \mathbf{P}_{12}+\mathbf{V}^T \\ * & \boldsymbol{\Lambda}_{22} & 0 & -\tau\mathbf{W} & -\mathbf{Q}_{12}+\mathbf{P}_{22}-\mathbf{V}^T \\ * & * & -\tau\mathbf{Z}_{11} & -\tau\mathbf{Z}_{12} & 0 \\ * & * & * & -\tau\mathbf{Z}_{22} & -\tau\mathbf{V}^T \\ * & * & * & * & -\mathbf{Q}_{22} \end{bmatrix}$$

Applying the Schur complement completes the proof for $i \in I_0$.

For $\forall i \in I_1$, since $\mathbf{f}_i = 0$ and $\bar{\mathbf{F}}_i\mathbf{x}(t) = \begin{bmatrix}\mathbf{F}_i & 0\end{bmatrix}\bar{\mathbf{x}}(t)$, define

$$\begin{aligned} \bar{\mathbf{V}}_1 &= \begin{bmatrix} \mathbf{x}(t) \\ \bar{\mathbf{x}}(t-\tau) \end{bmatrix}^T \begin{bmatrix} \mathbf{F}_i^T\mathbf{T}\mathbf{F}_i & \mathbf{F}_i^T\mathbf{T}\bar{\mathbf{F}}_{di} \\ \bar{\mathbf{F}}_{di}^T\mathbf{T}\mathbf{F}_i & \bar{\mathbf{F}}_{di}^T\mathbf{T}\bar{\mathbf{F}}_{di} \end{bmatrix} \begin{bmatrix} \mathbf{x}(t) \\ \bar{\mathbf{x}}(t-\tau) \end{bmatrix} \\ &= \begin{bmatrix} \bar{\mathbf{x}}(t) \\ \bar{\mathbf{x}}(t-\tau) \end{bmatrix}^T \begin{bmatrix} \bar{\mathbf{F}}_i^T\mathbf{T}\bar{\mathbf{F}}_i & \bar{\mathbf{F}}_i^T\mathbf{T}\bar{\mathbf{F}}_{di} \\ \bar{\mathbf{F}}_{di}^T\mathbf{T}\mathbf{F}_i & \bar{\mathbf{F}}_{di}^T\mathbf{T}\bar{\mathbf{F}}_{di}^T \end{bmatrix} \begin{bmatrix} \bar{\mathbf{x}}(t) \\ \bar{\mathbf{x}}(t-\tau) \end{bmatrix} \end{aligned} \tag{2.27}$$

$$\begin{aligned} \bar{\mathbf{V}}_2 &= \int_{t-\tau}^{t} \begin{bmatrix} \bar{\mathbf{x}}(s) \\ \dot{\bar{\mathbf{x}}}(s) \end{bmatrix}^T \begin{bmatrix} \bar{\mathbf{Q}}_{11} & \bar{\mathbf{Q}}_{12} \\ \bar{\mathbf{Q}}_{12}^T & \bar{\mathbf{Q}}_{22} \end{bmatrix} \begin{bmatrix} \bar{\mathbf{x}}(s) \\ \dot{\bar{\mathbf{x}}}(s) \end{bmatrix} ds \\ &= \int_{t-\tau}^{t} \begin{bmatrix} \mathbf{x}(s) \\ 1 \\ \dot{\mathbf{x}}(s) \\ 0 \end{bmatrix}^T \begin{bmatrix} \mathbf{Q}_{11} & 0 & \mathbf{Q}_{12} & \mathbf{Q}_{121} \\ 0 & 0 & 0 & 0 \\ \mathbf{Q}_{12}^T & 0 & \mathbf{Q}_{22} & \mathbf{Q}_{221} \\ \mathbf{Q}_{121}^T & 0 & \mathbf{Q}_{221}^T & \mathbf{Q}_{222} \end{bmatrix} \begin{bmatrix} \mathbf{x}(s) \\ 1 \\ \dot{\mathbf{x}}(s) \\ 0 \end{bmatrix} ds \\ &= \int_{t-\tau}^{t} \begin{bmatrix} \mathbf{x}(s) \\ \dot{\mathbf{x}}(s) \end{bmatrix}^T \begin{bmatrix} \mathbf{Q}_{11} & \mathbf{Q}_{12} \\ \mathbf{Q}_{12}^T & \mathbf{Q}_{22} \end{bmatrix} \begin{bmatrix} \mathbf{x}(s) \\ \dot{\mathbf{x}}(s) \end{bmatrix} ds = \mathbf{V}_2(\mathbf{x},t,\tau) \end{aligned} \tag{2.28}$$

$$
\begin{aligned}
\bar{\mathbf{V}}_3 &= \int_{-\tau}^{0}\int_{t+\theta}^{t}\begin{bmatrix}\bar{\mathbf{x}}(s)\\ \dot{\bar{\mathbf{x}}}(s)\end{bmatrix}^T\begin{bmatrix}\bar{\mathbf{Z}}_{11} & \bar{\mathbf{Z}}_{12}\\ \bar{\mathbf{Z}}_{12}^T & \bar{\mathbf{Z}}_{22}\end{bmatrix}\begin{bmatrix}\bar{\mathbf{x}}(s)\\ \dot{\bar{\mathbf{x}}}(s)\end{bmatrix}dsd\theta \\
&= \int_{-\tau}^{0}\int_{t+\theta}^{t}\begin{bmatrix}\mathbf{x}(s)\\ 1\\ \dot{\mathbf{x}}(s)\\ 0\end{bmatrix}^T\begin{bmatrix}\mathbf{Z}_{11} & 0 & \mathbf{Z}_{12} & \mathbf{Z}_{121}\\ 0 & 0 & 0 & 0\\ \mathbf{Z}_{12}^T & 0 & \mathbf{Z}_{22} & \mathbf{Z}_{221}\\ \mathbf{Z}_{121}^T & 0 & \mathbf{Z}_{221}^T & \mathbf{Z}_{222}\end{bmatrix}\begin{bmatrix}\mathbf{x}(s)\\ 1\\ \dot{\mathbf{x}}(s)\\ 0\end{bmatrix}dsd\theta \\
&= \int_{-\tau}^{0}\int_{t+\theta}^{t}\begin{bmatrix}\mathbf{x}(s)\\ \dot{\mathbf{x}}(s)\end{bmatrix}^T\begin{bmatrix}\mathbf{Z}_{11} & \mathbf{Z}_{12}\\ \mathbf{Z}_{12}^T & \mathbf{Z}_{22}\end{bmatrix}\begin{bmatrix}\mathbf{x}(s)\\ \dot{\mathbf{x}}(s)\end{bmatrix}dsd\theta = \mathbf{V}_3(\mathbf{x},t,\tau)
\end{aligned}
\tag{2.29}
$$

$$
\begin{aligned}
\bar{\mathbf{V}}_4 &= \int_{-\tau}^{0}\int_{\theta}^{0}\int_{t+\lambda}^{t}\dot{\bar{\mathbf{x}}}(s)^T\bar{\mathbf{R}}\dot{\bar{\mathbf{x}}}(s)dsd\lambda d\theta \\
&= \int_{-\tau}^{0}\int_{\theta}^{0}\int_{t+\lambda}^{t}\begin{bmatrix}\dot{\mathbf{x}}(s)\\ 0\end{bmatrix}^T\begin{bmatrix}\mathbf{R} & \mathbf{R}_{12}\\ \mathbf{R}_{12}^T & \mathbf{R}_{22}\end{bmatrix}\begin{bmatrix}\dot{\mathbf{x}}(s)\\ 0\end{bmatrix}dsd\lambda d\theta \\
&= \int_{-\tau}^{0}\int_{\theta}^{0}\int_{t+\lambda}^{t}\dot{\mathbf{x}}(s)^T\mathbf{R}\dot{\mathbf{x}}(s)dsd\lambda d\theta = \mathbf{V}_4(\mathbf{x},t,\tau)
\end{aligned}
\tag{2.30}
$$

Note that $\bar{\mathbf{V}}_2(\mathbf{x},t,\tau)=\mathbf{V}_2(\mathbf{x},t,\tau)$, $\bar{\mathbf{V}}_3(\mathbf{x},t,\tau)=\mathbf{V}_3(\mathbf{x},t,\tau)$, $\bar{\mathbf{V}}_4(\mathbf{x},t,\tau)=\mathbf{V}_4(\mathbf{x},t,\tau)$ always hold. The continuity of $\mathbf{V}_1$ and $\bar{\mathbf{V}}_1$ along the boundaries is guaranteed by using the continuity matrices $\bar{\mathbf{F}}_i$ and $\bar{\mathbf{F}}_{di}$ (Johansson, 2003). Thus, the Lyapunov function in (2.14) is continuous over the entire space not matter what $\mathbf{Q}_{121}$, $\mathbf{Q}_{221}$, $\mathbf{Q}_{222}$, $\mathbf{Z}_{121}$, $\mathbf{Z}_{221}$, $\mathbf{Z}_{222}$, $\mathbf{R}_{12}$, $\mathbf{R}_{22}$ are chosen. Meanwhile, $\bar{\mathbf{Q}}_{22}$, $\bar{\mathbf{Z}}_{22}$, $\bar{\mathbf{R}}$ may still have full rank without affecting the feasibility of (2.12). One can follow the same procedure as above for $i\in I_0$ to complete the proof for $i\in I_1$. An analogous procedure can be applied for $i\in I_2$ and $i\in I_3$.

Remark 1: Since the Lyapunov functional candidate in (2.14) is continuous but not continuously differentiable at every point of the state space, Theorem 2.1 is valid when there is no attractive sliding modes along the region boundaries. The well-known sliding mode concepts are due to (Filippov, 1998). For PWA systems, the sliding modes may

occur between two or more regions on the common boundary and can lead to instability even if a piecewise Lyapunov function in (2.14) is found. Thus, it is important to check the existence of the attractive sliding modes on region boundaries for PWA systems. A discussion of detecting such sliding mode based on the Filippov solution is available in (Johansson, 2003).

Remark 2: The conditions in (2.11) and (2.12) are LMI based and are expected to have reduced conservativeness by introduction of an additional triple integration term (2.18) in the Lyapunov-Krasovskii functional candidate compared with other approaches not including this term. LMIs are much preferred over BMIs since LMIs are convex and can be efficiently solved using existing techniques (Boyd, 1999).

Remark 3: Note that when $\mathbf{U} = \mathbf{R} = 0$, Theorem 2.1 reverts to one equivalent to (Xu & Lam, 2005), which is then a special case of Theorem 2.1. Thus, Theorem 2.1 yields better, or at least equivalent, results compared to (Xu & Lam, 2005) when the time-delay system (i.e., single region case) is considered. Although such a comparison is for time-delay systems, which is a special scenario (i.e., one region case) of PWA time-delay systems, the use of the triple integration term is expected to offer similar advantages when the approach is applied to PWA time-delay systems.

Remark 4: In (Xu & Lam, 2007), the authors have proven that the LMI-based approaches in (Fridman et al., 2002; Lee, Wu et al., 2004; Xu & Lam, 2005) are equivalent while the approach from (Xu & Lam, 2005) has the lowest computational cost. Using a similar scheme as (Xu & Lam, 2005), we intend to minimize the conservativeness and complexity of our approach under the current structure.

Remark 5: The continuity problem for $\mathbf{V}_2/\bar{\mathbf{V}}_2$, $\mathbf{V}_3/\bar{\mathbf{V}}_3$ on region boundaries has not been properly addressed in (Kulkarni et al., 2004), where $\mathbf{V}_2 = \int_{t-\tau}^{t} \mathbf{x}(s)^T \mathbf{Q}\mathbf{x}(s)ds$, $\mathbf{Q} > 0$, $\forall i \in I_0$, and $\bar{\mathbf{V}}_2 = \int_{t-\tau}^{t} \bar{\mathbf{x}}(s)^T \bar{\mathbf{Q}}\bar{\mathbf{x}}(s)ds$, $\bar{\mathbf{Q}} > 0$, $\forall i \in I_1$, are considered. However, $\mathbf{V}_2$ and $\bar{\mathbf{V}}_2$ will not be equal on the region boundaries. In (Moezz et al., 2009), $\bar{\mathbf{V}}_2 = \int_{t-\tau}^{t} \bar{\mathbf{x}}(s)^T \bar{\mathbf{Q}}\bar{\mathbf{x}}(s)ds$ is defined for $\forall i \in I_0$ but it renders $\bar{\mathbf{V}}_2(0) \neq 0$. In our results, following the formulations in (2.28)-(2.30), the continuity are guaranteed.

Remark 6: In (Moezzi et al., 2009), the Newton- Leibniz formula in (2.19) is further expanded as $\mathbf{x}(t-\tau) = \mathbf{x}(t) - \int_{t-\tau}^{t} \dot{\mathbf{x}}(s)ds = \mathbf{x}(t) - \int_{t-\tau}^{t} \mathbf{A}_j\mathbf{x}(s) + \mathbf{A}_{dj}\mathbf{x}(t-\tau)ds$, where j is the region index at time s and can be different from the current region index i. The method in (Moezzi et al., 2009) needs to check for any possible combination of i and j. Thus, the computational complexity increases quadratically with the growth of the number of regions. In our approach, the expansion of $\dot{\mathbf{x}}(s)$ is avoided by keeping it as a state of the LMI in (2.26), whose computational complexity is only proportional to the number of regions.

Remark 7: To accommodate the switching based on $\mathbf{x}(t-\tau)$, first the boundary matrices $\mathbf{E}_{di}$, $\mathbf{e}_{di}$ and the corresponding continuity matrices $\mathbf{F}_{di}$, $\mathbf{f}_{di}$ are introduced to include $\mathbf{x}(t-\tau)$ in the partitioning vector. Then, the Lyapunov function $\bar{\mathbf{V}}_1$ is expanded to include $2\mathbf{x}(t)^T\mathbf{F}_i^T\mathbf{T}\mathbf{F}_{di}\mathbf{x}(t-\tau)$ and $\mathbf{x}(t-\tau)^T\mathbf{F}_{di}^T\mathbf{T}\mathbf{F}_{di}\mathbf{x}(t-\tau)$, which represents the energy change with $\mathbf{x}(t-\tau)$ and increases the flexibility of the Lyapunov function. Finally, additional relaxation matrices, $2\mathbf{x}(t)^T\mathbf{E}_i^T\mathbf{J}_i\mathbf{E}_{di}\mathbf{x}(t-\tau)$, $\mathbf{x}(t-\tau)^T\mathbf{E}_{di}^T\mathbf{J}_i\mathbf{E}_{di}\mathbf{x}(t-\tau)$,

$2\mathbf{x}(t)^T\mathbf{E}_i^T\mathbf{K}_i\mathbf{E}_{di}\mathbf{x}(t-\tau)$ and $\mathbf{x}(t-\tau)^T\mathbf{E}_{di}^T\mathbf{K}_i\mathbf{E}_{di}\mathbf{x}(t-\tau)$, are added to further relax the constraints for each region.

Remark 8: Note that, for $i \in I_1$, the last row and last column of $\bar{\mathbf{P}}_{11i}$ and $\bar{\mathbf{E}}_i^T\mathbf{K}_i\bar{\mathbf{E}}_i$ in $\bar{\mathbf{\Lambda}}_{11}$ will be all zeros and result in reduced freedom. This will be accommodated by matrices $\bar{\mathbf{Y}}$, $\bar{\mathbf{W}}$ and $\bar{\mathbf{E}}_{\mathbf{d}i}^T\mathbf{K}_i\bar{\mathbf{E}}_{\mathbf{d}i}$ in $\begin{bmatrix} \bar{\mathbf{\Lambda}}_{11} & \bar{\mathbf{\Lambda}}_{12} \\ \bar{\mathbf{\Lambda}}_{12}^T & \bar{\mathbf{\Lambda}}_{22} \end{bmatrix}$, which ensures that (2.12) will still be feasible. This is analogous for $i \in I_2$.

2.4 Analysis of PWA Time-Delay Systems with Unstructured Uncertainty

Now consider the PWA time-delay system with the unstructured norm-bounded uncertainty in (2.5). One can show that the system in (2.1) with the uncertainty in (2.5) is equivalent to the system in (2.31)

$$\begin{aligned} &\dot{\mathbf{x}}(t) = \mathbf{A}_i\mathbf{x}(t) + \mathbf{A}_{di}\mathbf{x}(t-\tau) + \boldsymbol{\delta}_i \\ &\|\boldsymbol{\delta}_i\| \le \varepsilon_i\|\mathbf{x}(t)\| + \varepsilon_{di}\|\mathbf{x}(t-\tau)\|, \quad i \in I_0 \\ &\dot{\bar{\mathbf{x}}}(t) = \bar{\mathbf{A}}_i\bar{\mathbf{x}}(t) + \bar{\mathbf{A}}_{di}\bar{\mathbf{x}}(t-\tau) + \bar{\boldsymbol{\delta}}_i \\ &\|\bar{\boldsymbol{\delta}}_i\| \le \bar{\varepsilon}_i\|\bar{\mathbf{x}}(t)\| + \bar{\varepsilon}_{di}\|\bar{\mathbf{x}}(t-\tau)\|, \quad i \in \{I_1,\ I_2,\ I_3\} \end{aligned} \tag{2.31}$$

by defining

$$\bar{\delta}_i = \begin{bmatrix} \delta_i \\ 0 \end{bmatrix}, \quad \bar{\varepsilon}_i = \left\| \begin{bmatrix} \varepsilon_i & \varepsilon_{ai} \end{bmatrix} \right\|, \quad \bar{\varepsilon}_{di} = \varepsilon_{di} \tag{2.32}$$

and considering

$$\left\|\bar{\delta}_i\right\| \le \left\|\begin{bmatrix}\delta_i \\ 0\end{bmatrix}\right\| \le \begin{bmatrix}\varepsilon_i & \varepsilon_{ai}\end{bmatrix}\begin{bmatrix}\|x(t)\| \\ 1\end{bmatrix} + \begin{bmatrix}\varepsilon_{di} & 0\end{bmatrix}\begin{bmatrix}\|x(t-\tau)\| \\ 1\end{bmatrix}$$

$$\le \left\|\begin{bmatrix}\varepsilon_i & \varepsilon_{ai}\end{bmatrix}\right\|\left\|\begin{bmatrix}x(t) \\ 1\end{bmatrix}\right\| + \left\|\begin{bmatrix}\varepsilon_{di} & 0\end{bmatrix}\right\|\left\|\begin{bmatrix}x(t-\tau) \\ 1\end{bmatrix}\right\| \le \bar{\varepsilon}_i\left\|\bar{x}(t)\right\| + \bar{\varepsilon}_{di}\left\|\bar{x}(t-\tau)\right\|,\ \forall\ i \in \{I_1,\ I_2,\ I_3\}$$

(2.33)

Theorem 2.2: Consider symmetric matrices $\mathbf{T}$, $\mathbf{J}_i$, $\mathbf{K}_i$ such that $\mathbf{J}_i$, $\mathbf{K}_i$ have non-negative entries while $\begin{bmatrix}\mathbf{P}_{11i} & \mathbf{P}_{12i} \\ \mathbf{P}_{12i}^T & \mathbf{P}_{22i}\end{bmatrix} = \begin{bmatrix}\mathbf{F}_i^T\mathbf{T}\mathbf{F}_i & \mathbf{F}_i^T\mathbf{T}\mathbf{F}_{di} \\ \mathbf{F}_{di}^T\mathbf{T}\mathbf{F}_i & \mathbf{F}_{di}^T\mathbf{T}\mathbf{F}_{di}\end{bmatrix}$, for $i \in I_0$, and $\begin{bmatrix}\bar{\mathbf{P}}_{11i} & \bar{\mathbf{P}}_{12i} \\ \bar{\mathbf{P}}_{12i}^T & \bar{\mathbf{P}}_{22i}\end{bmatrix} = \begin{bmatrix}\bar{\mathbf{F}}_i^T\mathbf{T}\bar{\mathbf{F}}_i & \bar{\mathbf{F}}_i^T\mathbf{T}\bar{\mathbf{F}}_{di} \\ \bar{\mathbf{F}}_{di}^T\mathbf{T}\bar{\mathbf{F}}_i & \bar{\mathbf{F}}_{di}^T\mathbf{T}\bar{\mathbf{F}}_{di}\end{bmatrix}$, for $i \in \{I_1,\ I_2,\ I_3\}$, and scalars m_{1i}, m_{2i}, m_{3i}, $\bar{m}_{1i}, \bar{m}_{2i}, \bar{m}_{3i}$, l_{1i}, l_{2i}, l_{3i} such that the LMIs in (2.34), (2.35) and (2.36) are satisfied for every region.

For $\forall i \in I_0$,

$$\begin{bmatrix}
\mathbf{\Lambda}_{11}' & \mathbf{\Lambda}_{12}' & -\tau\mathbf{U} & -\tau\mathbf{Y} & \mathbf{P}_{12}+\mathbf{V}^T & \frac{\tau^2\mathbf{U}}{2} & m_{1i}\varepsilon_{di}\mathbf{I} & m_{2i}\varepsilon_i\mathbf{I} & m_{3i}\varepsilon_i\,\varepsilon_{di}\mathbf{I} \\
* & \mathbf{\Lambda}_{22}' & 0 & -\tau\mathbf{W} & -\mathbf{Q}_{12}+\mathbf{P}_{22}-\mathbf{V}^T & 0 & 0 & 0 & 0 \\
* & * & -\tau\mathbf{Z}_{11} & -\tau\mathbf{Z}_{12} & 0 & 0 & 0 & 0 & 0 \\
* & * & * & -\tau\mathbf{Z}_{22} & -\tau\mathbf{V}^T & 0 & 0 & 0 & 0 \\
* & * & * & * & \frac{\tau^2}{2}\mathbf{R}-\mathbf{Q}_{22} & 0 & 0 & 0 & 0 \\
* & * & * & * & * & -\frac{\tau^2\mathbf{R}}{2} & 0 & 0 & 0 \\
* & * & * & * & * & * & -l_{1i}\mathbf{I} & 0 & 0 \\
* & * & * & * & * & * & * & -l_{2i}\mathbf{I} & 0 \\
* & * & * & * & * & * & * & * & -l_{3i}\mathbf{I}
\end{bmatrix}$$

< 0;

$$
\begin{bmatrix} \mathbf{F}_i^T\mathbf{T}\mathbf{F}_i & \mathbf{F}_i^T\mathbf{T}\mathbf{F}_{di} \\ \mathbf{F}_{di}^T\mathbf{T}\mathbf{F}_i & \mathbf{F}_{di}^T\mathbf{T}\mathbf{F}_{di} \end{bmatrix} - \begin{bmatrix} \mathbf{E}_i^T\mathbf{J}_i\mathbf{E}_i & \mathbf{E}_i^T\mathbf{J}_i\mathbf{E}_{di} \\ \mathbf{E}_{di}^T\mathbf{J}_i\mathbf{E}_i & \mathbf{E}_{di}^T\mathbf{J}_i\mathbf{E}_{di} \end{bmatrix} > 0;
$$

$$
\begin{bmatrix} \mathbf{Q}_{11} & \mathbf{Q}_{12} \\ \mathbf{Q}_{12}^T & \mathbf{Q}_{22} \end{bmatrix} > 0; \ \begin{bmatrix} \mathbf{Z}_{11} & \mathbf{Z}_{12} \\ \mathbf{Z}_{12}^T & \mathbf{Z}_{22} \end{bmatrix} > 0; \ \mathbf{R} > 0; \tag{2.34}
$$

$$
\mathbf{P}_{11i} + \mathbf{Q}_{12} + \mathbf{A}_i^T\mathbf{Q}_{22} + \tau\mathbf{Z}_{12} + \tau\mathbf{A}_i^T\mathbf{Z}_{22} + \frac{\tau^2}{2}\mathbf{A}_i^T\mathbf{R} < m_{1i}\mathbf{I};
$$

$$
\mathbf{P}_{12i}^T + \mathbf{A}_{di}^T\mathbf{Q}_{22} + \tau\mathbf{A}_{di}^T\mathbf{Z}_{22} + \frac{\tau^2}{2}\mathbf{A}_{di}^T\mathbf{R} < m_{2i}\mathbf{I}; \ \mathbf{Q}_{22} + \tau\mathbf{Z}_{22} + \frac{\tau^2}{2}\mathbf{R} < m_{3i}\mathbf{I};
$$

For $\forall i \in I_1,\ I_2,\ I_3$,

$$
\begin{bmatrix}
\bar{\mathbf{\Lambda}}_{11}{}' & \bar{\mathbf{\Lambda}}_{12}{}' & -\tau\mathbf{U}_1 & -\tau\bar{\mathbf{Y}} & \bar{\mathbf{P}}_{12} + \bar{\mathbf{V}}^T & \frac{\tau^2\bar{\mathbf{U}}}{2} & \bar{m}_{1i}\bar{\varepsilon}_{di}\mathbf{I} & \bar{m}_{2i}\bar{\varepsilon}_i\,\mathbf{I} & \bar{m}_{3i}\bar{\varepsilon}_i\,\bar{\varepsilon}_{di}\mathbf{I} \\
* & \bar{\mathbf{\Lambda}}_{22}{}' & 0 & -\tau\bar{\mathbf{W}} & -\bar{\mathbf{Q}}_{12} + \bar{\mathbf{P}}_{22} - \bar{\mathbf{V}}^T & 0 & 0 & 0 & 0 \\
* & * & -\tau\mathbf{Z}_{11} & -\tau\hat{\mathbf{Z}}_{12} & 0 & 0 & 0 & 0 & 0 \\
* & * & * & -\tau\bar{\mathbf{Z}}_{22} & -\tau\bar{\mathbf{V}}^T & 0 & 0 & 0 & 0 \\
* & * & * & * & -\bar{\mathbf{Q}}_{22} & 0 & 0 & 0 & 0 \\
* & * & * & * & * & -\frac{\tau^2\bar{\mathbf{R}}}{2} & 0 & 0 & 0 \\
* & * & * & * & * & * & -\bar{l}_{1i}\mathbf{I} & 0 & 0 \\
* & * & * & * & * & * & * & -\bar{l}_{2i}\mathbf{I} & 0 \\
* & * & * & * & * & * & * & * & -\bar{l}_{3i}\mathbf{I}
\end{bmatrix}
< 0;
$$

$$
\bar{\mathbf{Q}}_{22} > 0; \ \ \bar{\mathbf{Z}}_{22} > 0; \ \ \ \bar{\mathbf{R}} > 0;
$$

$$
\bar{\mathbf{P}}_{11i} + \bar{\mathbf{Q}}_{12} + \bar{\mathbf{A}}_i^T\bar{\mathbf{Q}}_{22} + \tau\bar{\mathbf{Z}}_{12} + \tau\bar{\mathbf{A}}_i^T\bar{\mathbf{Z}}_{22} + \frac{\tau^2}{2}\bar{\mathbf{A}}_i^T\bar{\mathbf{R}} < \bar{m}_{1i}\mathbf{I}; \tag{2.35}
$$

$$
\bar{\mathbf{P}}_{12i}^T + \bar{\mathbf{A}}_{di}^T\bar{\mathbf{Q}}_{22} + \tau\bar{\mathbf{A}}_{di}^T\bar{\mathbf{Z}}_{22} + \frac{\tau^2}{2}\bar{\mathbf{A}}_{di}^T\bar{\mathbf{R}} < \bar{m}_{2i}\mathbf{I}; \ \bar{\mathbf{Q}}_{22} + \tau\bar{\mathbf{Z}}_{22} + \frac{\tau^2}{2}\bar{\mathbf{R}} < \bar{m}_{3i}\mathbf{I};
$$

and additionally,

$$
\begin{bmatrix} \mathbf{F}_i^T\mathbf{T}\mathbf{F}_i & \mathbf{F}_i^T\mathbf{T}\bar{\mathbf{F}}_{di} \\ \bar{\mathbf{F}}_{di}^T\mathbf{T}\mathbf{F}_i & \bar{\mathbf{F}}_{di}^T\mathbf{T}\bar{\mathbf{F}}_{di} \end{bmatrix} - \begin{bmatrix} \mathbf{E}_i^T\mathbf{J}_i\mathbf{E}_i & \mathbf{E}_i^T\mathbf{J}_i\bar{\mathbf{E}}_{di} \\ \bar{\mathbf{E}}_{di}^T\mathbf{J}_i\mathbf{E}_i & \bar{\mathbf{E}}_{di}^T\mathbf{J}_i\bar{\mathbf{E}}_{di} \end{bmatrix} \geq 0; \ \forall i \in I_1
$$

$$
\begin{bmatrix} \bar{\mathbf{F}}_i^T\mathbf{T}\bar{\mathbf{F}}_i & \bar{\mathbf{F}}_i^T\mathbf{T}\mathbf{F}_{di} \\ \mathbf{F}_{di}^T\mathbf{T}\bar{\mathbf{F}}_i & \mathbf{F}_{di}^T\mathbf{T}\mathbf{F}_{di} \end{bmatrix} - \begin{bmatrix} \bar{\mathbf{E}}_i^T\mathbf{J}_i\bar{\mathbf{E}}_i & \bar{\mathbf{E}}_i^T\mathbf{J}_i\mathbf{E}_{di} \\ \mathbf{E}_{di}^T\mathbf{J}_i\bar{\mathbf{E}}_i & \mathbf{E}_{di}^T\mathbf{J}_i\mathbf{E}_{di} \end{bmatrix} \geq 0; \ \forall i \in I_2
$$

$$\begin{bmatrix} \bar{\mathbf{F}}_i^T \mathbf{T} \bar{\mathbf{F}}_i & \bar{\mathbf{F}}_i^T \mathbf{T} \bar{\mathbf{F}}_{di} \\ \bar{\mathbf{F}}_{di}^T \mathbf{T} \bar{\mathbf{F}}_i & \bar{\mathbf{F}}_{di}^T \mathbf{T} \bar{\mathbf{F}}_{di} \end{bmatrix} - \begin{bmatrix} \bar{\mathbf{E}}_i^T \mathbf{J}_i \bar{\mathbf{E}}_i & \bar{\mathbf{E}}_i^T \mathbf{J}_i \bar{\mathbf{E}}_{di} \\ \bar{\mathbf{E}}_{di}^T \mathbf{J}_i \bar{\mathbf{E}}_i & \bar{\mathbf{E}}_{di}^T \mathbf{J}_i \bar{\mathbf{E}}_{di} \end{bmatrix} \geq 0; \ \forall i \in I_3 \tag{2.36}$$

where

$$\begin{aligned} &\mathbf{I} \text{ is the Identity Matrix,} \\ &\boldsymbol{\Lambda}_{11}{}' = \boldsymbol{\Lambda}_{11} + 2m_{1i}\varepsilon_i \mathbf{I} + m_{3i}\varepsilon_i^2 \mathbf{I}, \\ &\bar{\boldsymbol{\Lambda}}_{11}{}' = \bar{\boldsymbol{\Lambda}}_{11} + 2\bar{m}_{1i}\bar{\varepsilon}_i \mathbf{I} + \bar{m}_{3i}\bar{\varepsilon}_i^2 \mathbf{I}, \\ &\boldsymbol{\Lambda}_{12}{}' = \boldsymbol{\Lambda}_{12}, \ \bar{\boldsymbol{\Lambda}}_{12}{}' = \bar{\boldsymbol{\Lambda}}_{12}, \\ &\boldsymbol{\Lambda}_{22}{}' = \boldsymbol{\Lambda}_{22} + l_{1i}\mathbf{I} + l_{2i}\mathbf{I} + l_{3i}\mathbf{I} + 2m_{2i}\varepsilon_{di}\mathbf{I} + m_{3i}\varepsilon_{di}^2 \mathbf{I}, \\ &\bar{\boldsymbol{\Lambda}}_{22}{}' = \bar{\boldsymbol{\Lambda}}_{22} + \bar{l}_{1i}\mathbf{I} + \bar{l}_{2i}\mathbf{I} + \bar{l}_{3i}\mathbf{I} + 2\bar{m}_{2i}\bar{\varepsilon}_{di}\mathbf{I} + \bar{m}_{3i}\bar{\varepsilon}_{di}^2 \mathbf{I}, \\ &\hat{\mathbf{Z}}_{12} = \begin{bmatrix} \mathbf{Z}_{12} & \mathbf{Z}_{121} \end{bmatrix} \end{aligned} \tag{2.37}$$

Then every piecewise continuous trajectory of the system in (2.31) tends to zero asymptotically in the absence of attractive sliding modes.

Proof: Consider the same Lyapunov-Krasovskii functional candidate defined in (2.14) :

$$\mathbf{V}' = \mathbf{V}_1{}' + \mathbf{V}_2{}' + \mathbf{V}_3{}' + \mathbf{V}_4{}' = \mathbf{V}_1 + \mathbf{V}_2 + \mathbf{V}_3 + \mathbf{V}_4 \tag{2.38}$$

The time derivative of the Lyapunov function along the trajectory of (2.1) becomes

$$\dot{\mathbf{V}}_1{}' = \dot{\mathbf{V}}_1 + 2\mathbf{x}(t)^T \mathbf{P}_{11i} \boldsymbol{\delta}_i + 2\mathbf{x}(t-\tau)^{\mathbf{T}} \mathbf{P}_{12i}^T \boldsymbol{\delta}_i \tag{2.39}$$

$$\dot{\mathbf{V}}_2{}' = \dot{\mathbf{V}}_2 + 2\mathbf{x}(t)^T \mathbf{Q}_{12} \boldsymbol{\delta}_i + 2\mathbf{x}(t)^T \mathbf{A}_i^T \mathbf{Q}_{22} \boldsymbol{\delta}_i + 2\mathbf{x}(t-\tau)^T \mathbf{A}_{di}^T \mathbf{Q}_{22} \boldsymbol{\delta}_i + \boldsymbol{\delta}_i{}^T \mathbf{Q}_{22} \boldsymbol{\delta}_i \tag{2.40}$$

$$\dot{\mathbf{V}}_3{}' = \dot{\mathbf{V}}_3 + 2\tau\mathbf{x}(t)^T \mathbf{Z}_{12} \boldsymbol{\delta}_i + 2\tau\mathbf{x}(t)^T \mathbf{A}_i^T \mathbf{Z}_{22} \boldsymbol{\delta}_i + 2\tau\mathbf{x}(t-\tau)^T \mathbf{A}_{di}^T \mathbf{Z}_{22} \boldsymbol{\delta}_i + \tau\boldsymbol{\delta}_i{}^T \mathbf{Z}_{22} \boldsymbol{\delta}_i \tag{2.41}$$

$$\dot{\mathbf{V}}_4{}' = \dot{\mathbf{V}}_4 + \frac{\tau^2}{2}\left[2\mathbf{x}(t)^T \mathbf{A}_i^T \mathbf{R} \boldsymbol{\delta}_i + 2\mathbf{x}(t-\tau)^T \mathbf{A}_{di}^T \mathbf{R} \boldsymbol{\delta}_i + \boldsymbol{\delta}_i{}^T \mathbf{R} \boldsymbol{\delta}_i \right] \tag{2.42}$$

Note that

$$
\begin{aligned}
&2\mathbf{x}(t)^T(\mathbf{P}_{11i}+\mathbf{Q}_{12}+\mathbf{A}_i^T\mathbf{Q}_{22}+\tau\mathbf{Z}_{12}+\tau\mathbf{A}_i^T\mathbf{Z}_{22}+\frac{\tau^2}{2}\mathbf{A}_i^T\mathbf{R})\boldsymbol{\delta}_i \\
&\quad\le 2\|\mathbf{x}(t)\|\cdot\left\|\mathbf{P}_{11i}+\mathbf{Q}_{12}+\mathbf{A}_i^T\mathbf{Q}_{22}+\tau\mathbf{Z}_{12}+\tau\mathbf{A}_i^T\mathbf{Z}_{22}+\frac{\tau^2}{2}\mathbf{A}_i^T\mathbf{R}\right\|\cdot\|\boldsymbol{\delta}_i\| \\
&\quad\le 2m_{1i}\varepsilon_i\|\mathbf{x}(t)\|^2+2m_{1i}\varepsilon_{di}\|\mathbf{x}(t)\|\|\mathbf{x}(t-\tau)\| \\
&\quad\le 2m_{1i}\varepsilon_i\mathbf{x}(t)^T\mathbf{x}(t)+\varepsilon_{di}^2m_{1i}^2l_{1i}^{-1}\mathbf{x}(t)^T\mathbf{x}(t)+l_{1i}\mathbf{x}(t-\tau)^T\mathbf{x}(t-\tau)
\end{aligned}
\tag{2.43}
$$

$$
\begin{aligned}
&2\mathbf{x}(t-\tau)^T(\mathbf{P}_{12i}^T+\mathbf{A}_{di}^T\mathbf{Q}_{22}+\tau\mathbf{A}_{di}^T\mathbf{Z}_{22}+\frac{\tau^2}{2}\mathbf{A}_{di}^T\mathbf{R})\boldsymbol{\delta}_i \\
&\quad\le 2\|\mathbf{x}(t-\tau)\|\cdot\left\|\mathbf{P}_{12i}^T+\mathbf{A}_{di}^T\mathbf{Q}_{22}+\tau\mathbf{A}_{di}^T\mathbf{Z}_{22}+\frac{\tau^2}{2}\mathbf{A}_{di}^T\mathbf{R}\right\|\cdot\|\boldsymbol{\delta}_i\| \\
&\quad\le 2m_{2i}\varepsilon_i\|\mathbf{x}(t)\|\cdot\|\mathbf{x}(t-\tau)\|+2m_{2i}\varepsilon_{di}\|\mathbf{x}(t-\tau)\|^2 \\
&\quad\le m_{2i}^2\varepsilon_i^2l_{2i}^{-1}\mathbf{x}(t)^T\mathbf{x}(t)+l_{2i}\mathbf{x}(t-\tau)^T\mathbf{x}(t-\tau)+2m_{2i}\varepsilon_{di}\mathbf{x}(t-\tau)^T\mathbf{x}(t-\tau)
\end{aligned}
\tag{2.44}
$$

$$
\begin{aligned}
&\boldsymbol{\delta}_i^T(\mathbf{Q}_{22}+\tau\mathbf{Z}_{22}+\frac{\tau^2}{2}\mathbf{R})\boldsymbol{\delta}_i\le\left\|\mathbf{Q}_{22}+\tau\mathbf{Z}_{22}+\frac{\tau^2}{2}\mathbf{R}\right\|\|\boldsymbol{\delta}_i\|^2 \\
&\quad\le m_{3i}\varepsilon_i^2\|\mathbf{x}(t)\|^2+2m_{3i}\varepsilon_i\varepsilon_{di}\|\mathbf{x}(t)\|\|\mathbf{x}(t-\tau)\|+m_{3i}\varepsilon_{di}^2\|\mathbf{x}(t-\tau)\|^2 \\
&\quad\le m_{3i}\varepsilon_i^2\mathbf{x}(t)^T\mathbf{x}(t)+l_{3i}^{-1}m_{3i}^2\varepsilon_i^2\varepsilon_{di}^2\mathbf{x}(t)^T\mathbf{x}(t) \\
&\qquad+l_{3i}\mathbf{x}(t-\tau)^T\mathbf{x}(t-\tau)+m_{3i}\varepsilon_{di}^2\mathbf{x}(t-\tau)^T\mathbf{x}(t-\tau)
\end{aligned}
\tag{2.45}
$$

Substituting (2.39) - (2.45) into (2.38) yields

$$
\begin{aligned}
\dot{\mathbf{V}}'\le\dot{\mathbf{V}}&+\mathbf{x}(t)^T(2m_{1i}\varepsilon_i\mathbf{I}+m_{3i}\varepsilon_i^2\mathbf{I})\mathbf{x}(t) \\
&+l_{1i}\mathbf{x}(t-\tau)^T(l_{1i}\mathbf{I}+l_{2i}\mathbf{I}+l_{3i}\mathbf{I}+2m_{2i}\varepsilon_{di}\mathbf{I}+m_{3i}\varepsilon_{di}^2\mathbf{I})\mathbf{x}(t-\tau) \\
&+\mathbf{x}(t)^T(\varepsilon_{di}^2m_{1i}^2l_{1i}^{-1}\mathbf{I}+m_{2i}^2\varepsilon_i^2l_{2i}^{-1}\mathbf{I}+l_{3i}^{-1}m_{3i}^2\varepsilon_i^2\varepsilon_{di}^2\mathbf{I})\mathbf{x}(t)
\end{aligned}
\tag{2.46}
$$

Applying the Schur complement completes the proof of Theorem 2.2.

2.5 Analysis of PWA Time-Delay Systems with Structured Uncertainty

In this section, we will consider the PWA time-delay system with the structured norm-bounded uncertainty in (2.4):

$$\begin{aligned}\dot{\mathbf{x}}(t) &= (\mathbf{A}_i + \Delta\mathbf{A}_i)\mathbf{x}(t) + (\mathbf{A}_{di} + \Delta\mathbf{A}_{di})\mathbf{x}(t-\tau), \quad \forall i \in I_0 \\ \dot{\bar{\mathbf{x}}}(t) &= (\bar{\mathbf{A}}_i + \Delta\bar{\mathbf{A}}_i)\bar{\mathbf{x}}(t) + (\bar{\mathbf{A}}_{di} + \Delta\bar{\mathbf{A}}_{di})\bar{\mathbf{x}}(t-\tau), \quad \forall i \in \{I_1, I_2, I_3\}\end{aligned} \tag{2.47}$$

where

$$\begin{aligned}\begin{bmatrix}\Delta\mathbf{A}_i & \Delta\mathbf{A}_{di}\end{bmatrix} &= \mathbf{G}_i\Delta_i\begin{bmatrix}\mathbf{H}_{1i} & \mathbf{H}_{2i}\end{bmatrix}, \ \Delta_i^T\Delta_i \le \mathbf{I}, \ \forall i \in I_0 \\ \begin{bmatrix}\Delta\bar{\mathbf{A}}_i & \Delta\bar{\mathbf{A}}_{di}\end{bmatrix} &= \bar{\mathbf{G}}_i\Delta_i\begin{bmatrix}\bar{\mathbf{H}}_{1i} & \bar{\mathbf{H}}_{2i}\end{bmatrix}, \ \Delta_i^T\Delta_i \le \mathbf{I}, \ \forall i \in \{I_1, I_2, I_3\}\end{aligned} \tag{2.48}$$

with $\Delta\bar{\mathbf{A}}_i = \begin{bmatrix}\Delta\mathbf{A}_i & \Delta\mathbf{a}_i \\ 0 & 0\end{bmatrix}$, $\Delta\bar{\mathbf{A}}_{di} = \begin{bmatrix}\Delta\mathbf{A}_{di} & 0 \\ 0 & 0\end{bmatrix}$, $\bar{\mathbf{G}}_i = \begin{bmatrix}\mathbf{G}_i \\ 0\end{bmatrix}$, $\bar{\mathbf{H}}_{1i} = \begin{bmatrix}\mathbf{H}_{1i} & \mathbf{H}_{3i}\end{bmatrix}$, and $\bar{\mathbf{H}}_{2i} = \begin{bmatrix}\mathbf{H}_{2i} & 0\end{bmatrix}$ for $i \in \{I_1, I_2, I_3\}$. Note that $\mathbf{a}_i = 0$ and $\Delta\mathbf{a}_i = 0$ for $i \in I_0$.

Theorem 2.3: Consider symmetric matrices $\mathbf{T}$, $\mathbf{J}_i$, $\mathbf{K}_i$ such that $\mathbf{J}_i$, $\mathbf{K}_i$ have non-negative entries while $\begin{bmatrix}\mathbf{P}_{11i} & \mathbf{P}_{12i} \\ \mathbf{P}_{12i}^T & \mathbf{P}_{22i}\end{bmatrix} = \begin{bmatrix}\mathbf{F}_i^T\mathbf{T}\mathbf{F}_i & \mathbf{F}_i^T\mathbf{T}\mathbf{F}_{di} \\ \mathbf{F}_{di}^T\mathbf{T}\mathbf{F}_i & \mathbf{F}_{di}^T\mathbf{T}\mathbf{F}_{di}\end{bmatrix}$, for $i \in I_0$, and $\begin{bmatrix}\bar{\mathbf{P}}_{11i} & \bar{\mathbf{P}}_{12i} \\ \bar{\mathbf{P}}_{12i}^T & \bar{\mathbf{P}}_{22i}\end{bmatrix} = \begin{bmatrix}\bar{\mathbf{F}}_i^T\mathbf{T}\bar{\mathbf{F}}_i & \bar{\mathbf{F}}_i^T\mathbf{T}\bar{\mathbf{F}}_{di} \\ \bar{\mathbf{F}}_{di}^T\mathbf{T}\bar{\mathbf{F}}_i & \bar{\mathbf{F}}_{di}^T\mathbf{T}\bar{\mathbf{F}}_{di}\end{bmatrix}$, for $i \in \{I_1, I_2, I_3\}$, and scalars e_i, $\bar{e}_i$ >0, such that the LMIs in (2.49), (2.50) and (2.51) are satisfied for every region:

For $\forall i \in I_0$,

$$\begin{aligned}&\begin{bmatrix}\mathbf{\Phi}_{11i} & \mathbf{\Phi}_{12i} & \mathbf{\Phi}_{13i} \\ * & \mathbf{\Phi}_{22i} & \mathbf{\Phi}_{23i} \\ * & * & -e_i\mathbf{I}\end{bmatrix} + e_i\mathbf{H}_i^{*T}\mathbf{H}_i^* < 0; \ \begin{bmatrix}\mathbf{Q}_{11} & \mathbf{Q}_{12} \\ \mathbf{Q}_{12}^T & \mathbf{Q}_{22}\end{bmatrix} > 0; \ \begin{bmatrix}\mathbf{Z}_{11} & \mathbf{Z}_{12} \\ \mathbf{Z}_{12}^T & \mathbf{Z}_{22}\end{bmatrix} > 0; \ \mathbf{R} > 0; \\ &\begin{bmatrix}\mathbf{F}_i^T\mathbf{T}\mathbf{F}_i & \mathbf{F}_i^T\mathbf{T}\mathbf{F}_{di} \\ \mathbf{F}_{di}^T\mathbf{T}\mathbf{F}_i & \mathbf{F}_{di}^T\mathbf{T}\mathbf{F}_{di}\end{bmatrix} - \begin{bmatrix}\mathbf{E}_i^T\mathbf{J}_i\mathbf{E}_i & \mathbf{E}_i^T\mathbf{J}_i\mathbf{E}_{di} \\ \mathbf{E}_{di}^T\mathbf{J}_i\mathbf{E}_i & \mathbf{E}_{di}^T\mathbf{J}_i\mathbf{E}_{di}\end{bmatrix} > 0;\end{aligned} \tag{2.49}$$

For $\forall i \in I_1, I_2, I_3$,

$$\begin{bmatrix}\bar{\mathbf{\Phi}}_{11i} & \bar{\mathbf{\Phi}}_{12i} & \bar{\mathbf{\Phi}}_{13i} \\ * & \bar{\mathbf{\Phi}}_{22i} & \bar{\mathbf{\Phi}}_{23i} \\ * & * & -\bar{e}_i\mathbf{I}\end{bmatrix} + \bar{e}_i\bar{\mathbf{H}}_i^{*T}\bar{\mathbf{H}}_i^* < 0; \ \bar{\mathbf{Q}}_{22} > 0; \ \bar{\mathbf{Z}}_{22} > 0; \ \bar{\mathbf{R}} > 0; \tag{2.50}$$

and additionally,

$$\begin{bmatrix} \mathbf{F}_i^T\mathbf{T}\mathbf{F}_i & \mathbf{F}_i^T\mathbf{T}\bar{\mathbf{F}}_{di} \\ \bar{\mathbf{F}}_{di}^T\mathbf{T}\mathbf{F}_i & \bar{\mathbf{F}}_{di}^T\mathbf{T}\bar{\mathbf{F}}_{di} \end{bmatrix} - \begin{bmatrix} \mathbf{E}_i^T\mathbf{J}_i\mathbf{E}_i & \mathbf{E}_i^T\mathbf{J}_i\bar{\mathbf{E}}_{di} \\ \bar{\mathbf{E}}_{di}^T\mathbf{J}_i\mathbf{E}_i & \bar{\mathbf{E}}_{di}^T\mathbf{J}_i\bar{\mathbf{E}}_{di} \end{bmatrix} \geq 0;\ \forall i \in I_1$$

$$\begin{bmatrix} \bar{\mathbf{F}}_i^T\mathbf{T}\bar{\mathbf{F}}_i & \bar{\mathbf{F}}_i^T\mathbf{T}\mathbf{F}_{di} \\ \mathbf{F}_{di}^T\mathbf{T}\bar{\mathbf{F}}_i & \mathbf{F}_{di}^T\mathbf{T}\mathbf{F}_{di} \end{bmatrix} - \begin{bmatrix} \bar{\mathbf{E}}_i^T\mathbf{J}_i\bar{\mathbf{E}}_i & \bar{\mathbf{E}}_i^T\mathbf{J}_i\mathbf{E}_{di} \\ \mathbf{E}_{di}^T\mathbf{J}_i\bar{\mathbf{E}}_i & \mathbf{E}_{di}^T\mathbf{J}_i\mathbf{E}_{di} \end{bmatrix} \geq 0;\ \forall i \in I_2$$

$$\begin{bmatrix} \bar{\mathbf{F}}_i^T\mathbf{T}\bar{\mathbf{F}}_i & \bar{\mathbf{F}}_i^T\mathbf{T}\bar{\mathbf{F}}_{di} \\ \bar{\mathbf{F}}_{di}^T\mathbf{T}\bar{\mathbf{F}}_i & \bar{\mathbf{F}}_{di}^T\mathbf{T}\bar{\mathbf{F}}_{di} \end{bmatrix} - \begin{bmatrix} \bar{\mathbf{E}}_i^T\mathbf{J}_i\bar{\mathbf{E}}_i & \bar{\mathbf{E}}_i^T\mathbf{J}_i\bar{\mathbf{E}}_{di} \\ \bar{\mathbf{E}}_{di}^T\mathbf{J}_i\bar{\mathbf{E}}_i & \bar{\mathbf{E}}_{di}^T\mathbf{J}_i\bar{\mathbf{E}}_{di} \end{bmatrix} \geq 0;\ \forall i \in I_3 \qquad (2.51)$$

where

$$\mathbf{\Phi}_{11} = \begin{bmatrix} \mathbf{\Lambda}_{11}^* & \mathbf{\Lambda}_{12}^* & -\tau\mathbf{U} & -\tau\mathbf{Y} & \mathbf{P}_{12i} + \mathbf{V}^T & \frac{1}{2}\tau^2\mathbf{U} \\ * & \mathbf{\Lambda}_{22}^* & 0 & -\tau\mathbf{W} & -\mathbf{Q}_{12} + \mathbf{P}_{22i} - \mathbf{V}^T & 0 \\ * & * & -\tau\mathbf{Z}_{11} & -\tau\mathbf{Z}_{12} & 0 & 0 \\ * & * & * & -\tau\mathbf{Z}_{22} & -\tau\mathbf{V}^T & 0 \\ * & * & * & * & -\mathbf{Q}_{22} & 0 \\ * & * & * & * & * & -\frac{1}{2}\tau^2\mathbf{R} \end{bmatrix},$$

$$\bar{\mathbf{\Phi}}_{11} = \begin{bmatrix} \bar{\mathbf{\Lambda}}_{11}^* & \bar{\mathbf{\Lambda}}_{11}^* & -\tau\mathbf{U}_1 & -\tau\bar{\mathbf{Y}} & \bar{\mathbf{P}}_{12} + \bar{\mathbf{V}}^T & \frac{1}{2}\tau^2\bar{\mathbf{U}} \\ * & \bar{\mathbf{\Lambda}}_{11}^* & 0 & -\tau\bar{\mathbf{W}} & -\bar{\mathbf{Q}}_{12} + \bar{\mathbf{P}}_{22} - \bar{\mathbf{V}}^T & 0 \\ * & * & -\tau\mathbf{Z}_{11} & -\tau\begin{bmatrix}\mathbf{Z}_{12} & \mathbf{Z}_{121}\end{bmatrix} & 0 & 0 \\ * & * & * & -\tau\bar{\mathbf{Z}}_{22} & -\tau\bar{\mathbf{V}}^T & 0 \\ * & * & * & * & -\bar{\mathbf{Q}}_{22} & 0 \\ * & * & * & * & * & -\frac{1}{2}\tau^2\bar{\mathbf{R}} \end{bmatrix},$$

$$\mathbf{\Phi}_{12} = \begin{bmatrix} \mathbf{A}_i^T\mathbf{Q}_{22} + \tau\mathbf{A}_i^T\mathbf{Z}_{22} + \frac{\tau^2}{2}\mathbf{A}_i^T\mathbf{R} \\ \mathbf{A}_{di}^T\mathbf{Q}_{22} + \tau\mathbf{A}_{di}^T\mathbf{Z}_{22} + \frac{\tau^2}{2}\mathbf{A}_{di}^T\mathbf{R} \\ 0 \\ 0 \\ 0 \\ 0 \end{bmatrix},\ \mathbf{\Phi}_{13} = \begin{bmatrix} (\mathbf{P}_{11i} + \mathbf{Q}_{12} + \tau\mathbf{Z}_{12})\mathbf{G}_i \\ \mathbf{P}_{12i}^T\mathbf{G}_i \\ 0 \\ 0 \\ 0 \\ 0 \end{bmatrix},$$

$$\bar{\mathbf{\Phi}}_{12}=\begin{bmatrix}\bar{\mathbf{A}}_i^T\bar{\mathbf{Q}}_{22}+\tau\bar{\mathbf{A}}_i^T\bar{\mathbf{Z}}_{22}+\frac{\tau^2}{2}\bar{\mathbf{A}}_i^T\bar{\mathbf{R}}\\ \bar{\mathbf{A}}_{di}^T\bar{\mathbf{Q}}_{22}+\tau\bar{\mathbf{A}}_{di}^T\bar{\mathbf{Z}}_{22}+\frac{\tau^2}{2}\bar{\mathbf{A}}_{di}^T\bar{\mathbf{R}}\\ 0\\ 0\\ 0\\ 0\end{bmatrix},\ \bar{\mathbf{\Phi}}_{13}=\begin{bmatrix}(\bar{\mathbf{P}}_{11i}+\bar{\mathbf{Q}}_{12}+\tau\bar{\mathbf{Z}}_{12})\bar{\mathbf{G}}_i\\ \bar{\mathbf{P}}_{12i}^T\bar{\mathbf{G}}_i\\ 0\\ 0\\ 0\\ 0\end{bmatrix},$$

$$\mathbf{\Phi}_{22}=-\mathbf{Q}_{22}-\tau\mathbf{Z}_{22}-\frac{\tau^2}{2}\mathbf{R},\ \bar{\mathbf{\Phi}}_{22}=-\bar{\mathbf{Q}}_{22}-\tau\bar{\mathbf{Z}}_{22}-\frac{\tau^2}{2}\bar{\mathbf{R}},$$

$$\mathbf{\Phi}_{23}=\mathbf{Q}_{22}\mathbf{G}_i+\tau\mathbf{Z}_{22}\mathbf{G}_i+\frac{\tau^2}{2}\mathbf{R}\mathbf{G}_i,\ \bar{\mathbf{\Phi}}_{23}=\bar{\mathbf{Q}}_{22}\bar{\mathbf{G}}_i+\tau\bar{\mathbf{Z}}_{22}\bar{\mathbf{G}}_i+\frac{\tau^2}{2}\bar{\mathbf{R}}\bar{\mathbf{G}}_i,$$

$$\mathbf{\Lambda}_{11}^*=\mathbf{\Lambda}_{11}-\mathbf{A}_i^T\mathbf{Q}_{22}^T\mathbf{A}_i-\tau\mathbf{A}_i^T\mathbf{Z}_{22}\mathbf{A}_i-\frac{1}{2}\tau^2\mathbf{A}_i^T\mathbf{R}\mathbf{A}_i,$$

$$\bar{\mathbf{\Lambda}}_{11}^*=\bar{\mathbf{\Lambda}}_{11}-\bar{\mathbf{A}}_i^T\bar{\mathbf{Q}}_{22}^T\bar{\mathbf{A}}-\tau\bar{\mathbf{A}}_i^T\bar{\mathbf{Z}}_{22}\bar{\mathbf{A}}_i-\frac{1}{2}\tau^2\bar{\mathbf{A}}_i^T\bar{\mathbf{R}}\bar{\mathbf{A}}_i,$$

$$\mathbf{\Lambda}_{12}^*=\mathbf{\Lambda}_{12}-\mathbf{A}_i^T\mathbf{Q}_{22}\mathbf{A}_{di}-\tau\mathbf{A}_i^T\mathbf{Z}_{22}\mathbf{A}_{di}-\frac{1}{2}\tau^2\mathbf{A}_i^T\mathbf{R}\mathbf{A}_{di},$$

$$\bar{\mathbf{\Lambda}}_{12}^*=\bar{\mathbf{\Lambda}}_{12}-\bar{\mathbf{A}}_i^T\bar{\mathbf{Q}}_{22}\bar{\mathbf{A}}_{di}-\tau\bar{\mathbf{A}}_i^T\bar{\mathbf{Z}}_{22}\bar{\mathbf{A}}_{di}-\frac{1}{2}\tau^2\bar{\mathbf{A}}_i^T\bar{\mathbf{R}}\bar{\mathbf{A}}_{di},$$

$$\mathbf{\Lambda}_{22}^*=\mathbf{\Lambda}_{22}-\mathbf{A}_{di}^T\mathbf{Q}_{22}\mathbf{A}_{di}-\tau\mathbf{A}_{di}^T\mathbf{Z}_{22}\mathbf{A}_{di}-\frac{1}{2}\tau^2\mathbf{A}_{di}^T\mathbf{R}\mathbf{A}_{di},$$

$$\bar{\mathbf{\Lambda}}_{22}^*=\bar{\mathbf{\Lambda}}_{22}-\bar{\mathbf{A}}_{di}^T\bar{\mathbf{Q}}_{22}\bar{\mathbf{A}}_{di}-\tau\bar{\mathbf{A}}_{di}^T\bar{\mathbf{Z}}_{22}\bar{\mathbf{A}}_{di}-\frac{1}{2}\tau^2\bar{\mathbf{A}}_{di}^T\bar{\mathbf{R}}\bar{\mathbf{A}}_{di},$$

$$\mathbf{H}_i^*=\begin{bmatrix}\mathbf{H}_{1i} & \mathbf{H}_{2i} & 0 & 0 & 0 & 0 & 0 & 0 & 0\end{bmatrix},$$

$$\bar{\mathbf{H}}_i^*=\begin{bmatrix}\bar{\mathbf{H}}_{1i} & \bar{\mathbf{H}}_{2i} & 0 & 0 & 0 & 0 & 0 & 0 & 0\end{bmatrix}.$$

Then every piecewise continuous trajectory of the system in (2.47) tends to zero asymptotically in the absence of attractive sliding modes.

Proof: First, one can show that the first set of the LMIs in (2.11) is equivalent to

$$\mathbf{\Phi}_{11}-\mathbf{\Phi}_{12}\mathbf{\Phi}_{22}^{-1}\mathbf{\Phi}_{12}^T<0 \tag{2.52}$$

which is further equivalent to:

$$\begin{bmatrix} \mathbf{\Phi}_{11} & \mathbf{\Phi}_{12} \\ \mathbf{\Phi}_{12}^T & \mathbf{\Phi}_{22} \end{bmatrix} > 0 \tag{2.53}$$

Replacing $\mathbf{A}_i$ and $\mathbf{A}_{di}$ in (2.53) with $\mathbf{A}_i + \mathbf{H}_i\mathbf{\Delta}_i\mathbf{G}_{1i}$ and $\mathbf{A}_{di} + \mathbf{H}_i\mathbf{\Delta}_i\mathbf{G}_{2i}$ respectively, the condition in (2.53) is equivalent to the following condition

$$\begin{bmatrix} \mathbf{\Phi}_{11} & \mathbf{\Phi}_{12} \\ \mathbf{\Phi}_{12}^T & \mathbf{\Phi}_{22} \end{bmatrix} + \mathbf{G}_i^* \Delta_i \mathbf{H}_i^* + \mathbf{H}_i^{*T} \Delta_i^T \mathbf{G}_i^{*T} < 0 \tag{2.54}$$

where

$$\mathbf{G}_i^* = \left[\mathbf{G}_i^T (\mathbf{P}_{11i} + \mathbf{Q}_{12} + \tau \mathbf{Z}_{12})^T \quad \mathbf{G}_i^T \mathbf{P}_{12i} \quad 0 \quad 0 \quad 0 \quad 0 \quad \mathbf{G}_i^T (\tau \mathbf{Z}_{22} + \mathbf{Q}_{22} + \frac{\tau^2}{2} \mathbf{R}) \right]^T$$

Using the Lemma in (Xie, 1996), one can obtain a sufficient condition for (2.54):

$$\lambda \begin{bmatrix} \mathbf{\Phi}_{11} & \mathbf{\Phi}_{12} \\ \mathbf{\Phi}_{12}^T & \mathbf{\Phi}_{22} \end{bmatrix} + \lambda^2 \mathbf{G}_i^* \mathbf{G}_i^{*T} + \mathbf{H}_i^{*T} \mathbf{H}_i^* < 0 \tag{2.55}$$

Applying the Schur complement completes the proof of Theorem 2.3.

Remark 9: The existing work of (Kulkarni et al., 2004; Moezzi et al., 2009) is not applicable to the structured uncertainty case in (2.47). Our work considers not only the structure of the uncertainty, but also the switching based on $\mathbf{x}(t-\tau)$ as well as $\mathbf{x}(t)$, which has not been previously considered.

2.6 Numerical Examples

In this section the proposed approach will be compared with existing ones, where applicable, for several examples to demonstrate the performance improvement.

Example 2.1: Consider the time-delay system in (Fridman, 2001)

$$\dot{\mathbf{x}}(t) = \mathbf{A}\mathbf{x}(t) + \mathbf{A}_d\mathbf{x}(t-\tau)$$
$$\mathbf{A} = \begin{bmatrix} -1 & 0.5 \\ -0.5 & -1 \end{bmatrix},\ \mathbf{A}_d = \begin{bmatrix} -2 & 2 \\ -2 & -2 \end{bmatrix} \tag{2.56}$$

This example is for a single region, and is a special case of the PWA systems in (2.1). The upper bound on the delay (UBD), a commonly used indicator for conservativeness, is obtained by increasing the time delay value until the approach fails to prove stability. The UBDs obtained from different methods are compared in Table 2.1 for Example 2.1.

Table 2.1 Comparison of UBDs for Example 2.1

Methods	UBD
Li & Souza (1997)	0.268
Kulkarni et al. (2004) *	0.268
Moezzi et al. (2009) *	0.268
Fridman (2001)	0.271
Wu et al. (2004)	0.344
Xu and Lam (2005)	0.344
He et al. (2005)	0.344
Theorem 2.1*	0.349
Sun & Liu (2009)	0.353

* Methods applicable to PWA time-delay systems

Note that the method proposed in (Sun & Liu, 2009) is a BMI based approach and its performance depends on the selection of a preset coefficient matrix. The improvement using our approach (Theorem 2.1) over the other LMI-based approaches is incremental, but still remarkable, toward the theoretical UBD value of 0.364, which can be verified via simulation. Although Example 2.1 is for a time-delay system, which is a special one region case of PWA time-delay systems, it provides a comparison between our proposed approach with (Kulkarni et al., 2004; Moezzi et al., 2009) in the special one region case.

Also note that the result from our approach (i.e., Theorem 2.1) is better than the results of the other LMI-based approaches for time-delay systems, since Theorem 2.1 is an extension of (Xu & Lam, 2005).

Example 2.2: Consider the uncertain time-delay system in (Wu et. al, 2004)

$$\begin{aligned} \dot{\mathbf{x}}(t) &= (\mathbf{A} + \Delta\mathbf{A})\mathbf{x}(t) + (\mathbf{A}_d + \Delta\mathbf{A}_d)\mathbf{x}(t-\tau) \\ \begin{bmatrix}\Delta\mathbf{A} & \Delta\mathbf{A}_d\end{bmatrix} &= \mathbf{G}\Delta\begin{bmatrix}\mathbf{H}_1 & \mathbf{H}_2\end{bmatrix},\ \Delta^T\Delta \le \mathbf{I} \end{aligned} \tag{2.57}$$

with coefficients

$$\mathbf{A} = \begin{bmatrix} -0.5 & -2 \\ 1 & -1 \end{bmatrix},\ \mathbf{A}_d = \begin{bmatrix} -0.5 & -1 \\ 0 & 0.6 \end{bmatrix},\ \mathbf{G} = \mathbf{I},\ \mathbf{H}_1 = \begin{bmatrix} 0.2 & 0 \\ 0 & 0.2 \end{bmatrix},\ \mathbf{H}_2 = \begin{bmatrix} 0.2 & 0 \\ 0 & 0.2 \end{bmatrix}$$

Table 2.2 Comparison of UBDs for Example 2.2

Methods	UBD
Fridman and Shake (2002)	0.6812
Wu et al. (2004)	0.8435
Theorem 2.3	0.92

The upper bounds on time delay obtained from Theorem 2.3 is compared with other approaches in Table 2.2 showing noticeable improvement.

Example 2.3: Consider the piecewise time-delay system in (Kulkarni et al., 2004)

$$\dot{\mathbf{x}}(t) = \mathbf{A}_i x(t) + \mathbf{A}_{di} x(t-\tau) \tag{2.58}$$

with coefficients

$$\mathbf{A}_1 = \mathbf{A}_3 = \begin{bmatrix} -0.1 & 0 \\ 0 & -0.1 \end{bmatrix},\ \mathbf{A}_2 = \mathbf{A}_4 = \begin{bmatrix} -0.1 & 0 \\ 0 & -0.1 \end{bmatrix}$$

$$\mathbf{A}_{d1} = \mathbf{A}_{d3} = \begin{bmatrix} 0 & 5 \\ -1 & 0 \end{bmatrix},\ \mathbf{A}_{d2} = \mathbf{A}_{d4} = \begin{bmatrix} 0 & 1 \\ -5 & 0 \end{bmatrix}$$

and partition

$$\mathbf{E}_1 = -\mathbf{E}_3 = \begin{bmatrix} -1 & 1 \\ -1 & -1 \end{bmatrix}, \ \mathbf{E}_2 = -\mathbf{E}_4 = \begin{bmatrix} -1 & 1 \\ 1 & 1 \end{bmatrix}$$

Table 2.3 Comparison of UBDs for Example 2.3

Methods	UBD
Kulkarni et al. (2004)	0.0142
Moezzi et al. (2009)	0.0142
Theorem 2.1	0.0168

It has been verified in (Kulkarni et al., 2004) that the PWA system becomes unstable with time delay between 0.020 and 0.021. It can been seen from Table 2.3 that the proposed approach yields less conservative results compared to current existing ones (Kulkarni, 2004; Moezzi, 2009) for this example.

Example 2.4: Consider the piecewise time-delay system in (Moezzi, 2009)

$$\begin{aligned} \dot{\mathbf{x}}(t) &= \mathbf{A}_i x(t) + \mathbf{A}_{di} x(t-\tau) + \delta_i \\ \|\boldsymbol{\delta}_i\| &\le \boldsymbol{\varepsilon}_i \|x(t)\| + \boldsymbol{\varepsilon}_{di} \|x(t-\tau)\| \end{aligned} \tag{2.59}$$

with coefficients

$$\mathbf{A}_1 = \mathbf{A}_3 = \begin{bmatrix} -1 & 0 \\ 0 & -1 \end{bmatrix}, \ \mathbf{A}_2 = \mathbf{A}_4 = \begin{bmatrix} -0.9 & 0 \\ 0 & -0.9 \end{bmatrix}$$
$$\mathbf{A}_{d1} = \mathbf{A}_{d3} = \begin{bmatrix} 0.1 & 5 \\ -5 & 0.1 \end{bmatrix}, \ \mathbf{A}_{d2} = \mathbf{A}_{d4} = \begin{bmatrix} 1 & 5 \\ -5 & -1 \end{bmatrix}$$

and partition

$$\mathbf{E}_1 = -\mathbf{E}_3 = \begin{bmatrix} -1 & 1 \\ -1 & -1 \end{bmatrix}, \ \mathbf{E}_2 = -\mathbf{E}_4 = \begin{bmatrix} -1 & 1 \\ 1 & 1 \end{bmatrix}$$

and bounds on uncertainty

$$\varepsilon_i = \varepsilon_{di} = 0.1, \ i = 1, ..., 4$$

Table 2.4 Comparison of UBDs for Example 2.4

Methods	UBD for Nominal System	UBD for System with Uncertainty
Kulkarni et al. (2004)	0.0299	n/a
Moezzi et al. (2009)	0.0264 (0.0299*)	0.024 (0.026*)
Theorems 2.1&2.2	0.0367	0.0323

* The value inside the bracket is what we obtained when we tried to confirm their results, while the value outside is reported in (Moezzi, 2009).

For the nominal system (i.e., $\varepsilon_i = \varepsilon_{di} = 0,\ i = 1,...,4$), the UBDs obtained from the proposed approach, from (Kulkarni et al., 2004) and from (Moezzi et al., 2009) are compared. For the system with uncertainty (i.e., $\varepsilon_i = \varepsilon_{di} = 0.1,\ i = 1,...,4$), since the method in (Kulkarni et al., 2004) cannot tolerate uncertainty, only the results from the proposed approach and from (Moezzi et al., 2009) are provided.

The simulation results using the Matlab function *dde23* are given in Fig.2.1 and show that the nominal system is stable with $\tau = 0.052$ but becomes unstable when $\tau = 0.053$, which implies that the theoretical UBD is between 0.052 and 0.053. As shown in Table 2.4, our proposed approach is able to achieve less conservative estimates of the UBDs for both the nominal system and the system subject to uncertainty compared to existing ones (Kulkarni et al., 2004; Moezzi et al., 2009) for this example.

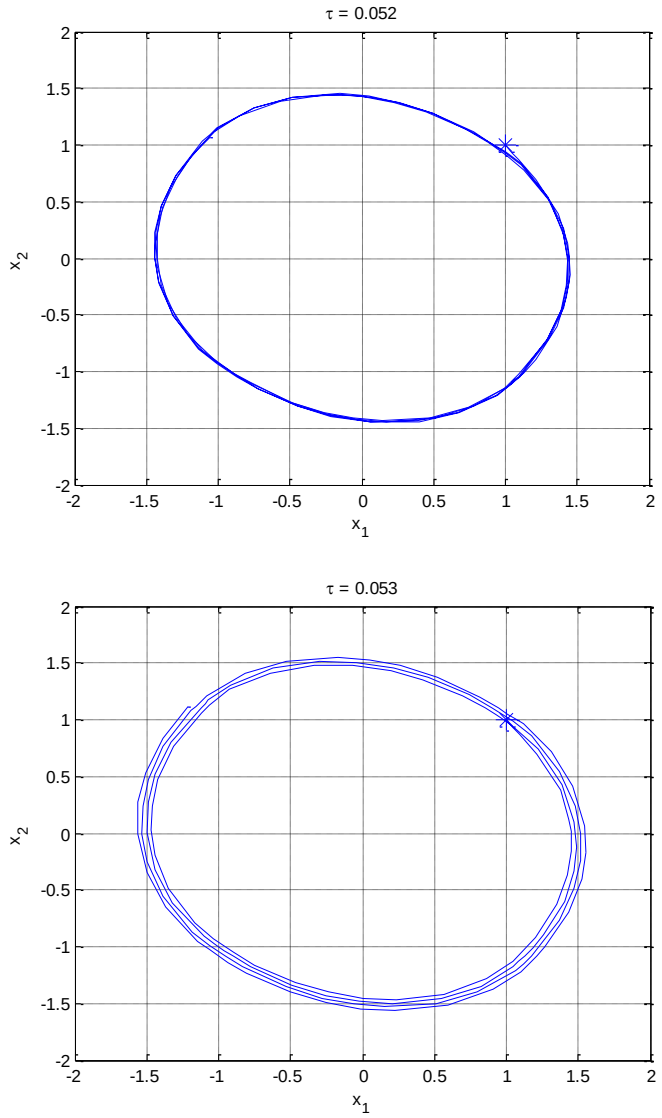

Fig. 2.1 The trajectory of the nominal piecewise affine time-delay system in Example 2.4 with $\tau = 0.052$ and $\tau = 0.053$

Example 2.5: Consider the equation of motion of a simple pendulum as follows (Franklin, et al, 2002):

$$T(t-h) - mgl\sin(\theta(t)) = ml^2\ddot{\theta}(t) \tag{2.60}$$

where l=9.8m is the length of the pendulum, g is gravitational acceleration, m=1kg is the pendulum mass and T is the input torque. A constant delay, h, between the sensor and the

controller is considered in the model. It is desired to keep the pendulum at $\theta = 45^{\circ}\,(0.7854\ rad)$.

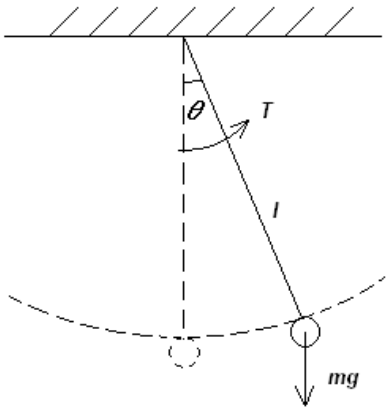

Fig. 2.2 Pendulum system

The feedback control is designed to be $T = T_e + \delta T$, where $T_e = mgl\sin(\theta_e)$. The closed-loop system becomes

$$ml^2\delta\ddot{\theta}(t) = -mgl\sin(\delta\theta(t) + \theta_e) + mgl\sin\theta_e + \delta T(t-h) \tag{2.61}$$

where $\delta\theta(t) = \theta(t) - \theta_e$. The nonlinear model in (2.61) is approximated via a piecewise affine system:

$$\begin{bmatrix}\delta\dot{\theta}(t)\\ \delta\ddot{\theta}(t)\end{bmatrix} = \begin{bmatrix}0 & 1\\ -\dfrac{0.825g}{l} + \Delta_1 & 0\end{bmatrix}\begin{bmatrix}\delta\theta(t)\\ \delta\dot{\theta}(t)\end{bmatrix} + \begin{bmatrix}0\\ \dfrac{1}{ml^2}\end{bmatrix}\delta T(t-h), \tag{2.62}$$
$$\forall -0.7854 \le \delta\theta(t) \le 0$$

$$\begin{bmatrix}\delta\dot{\theta}(t)\\ \delta\ddot{\theta}(t)\end{bmatrix} = \begin{bmatrix}0 & 1\\ -\dfrac{0.4875g}{l} + \Delta_2 & 0\end{bmatrix}\begin{bmatrix}\delta\theta(t)\\ \delta\dot{\theta}(t)\end{bmatrix} + \begin{bmatrix}0\\ \dfrac{1}{ml^2}\end{bmatrix}\delta T(t-h) \tag{2.63}$$
$$\forall\ 0 \le \delta\theta(t) \le 0.7854$$

with uncertainty $|\Delta_1| \le 0.175$ and $|\Delta_2| \le 0.3$, which is illustrated in Fig.2.3. Assume a state feedback control retarded by delay

$$\delta T(t-\tau) = -ml^2\delta\theta(t-\tau) - ml^2\delta\dot{\theta}(t-\tau),\ \forall -0.7854 \le \delta\theta(t-\tau) \le 0 \qquad (2.64)$$

$$\delta T(t-\tau) = -5ml^2\delta\theta(t-\tau) - 5ml^2\delta\dot{\theta}(t-\tau),\ \forall 0 \le \delta\theta(t-\tau) \le 0.7854 \qquad (2.65)$$

Note that the switching in the controller is also delayed and depends on $\delta\theta(t-\tau)$, while the plant model in (2.62) and (2.63) switches on $\delta\theta(t)$. Thus, the closed-loop system with input delay becomes a PWA time-delay system switching on both $\delta\theta(t)$ and $\delta\theta(t-\tau)$

$$\begin{bmatrix}\delta\dot{\theta}(t)\\ \delta\ddot{\theta}(t)\end{bmatrix} = \begin{bmatrix}0 & 1\\ -0.825+\Delta_1 & 0\end{bmatrix}\begin{bmatrix}\delta\theta(t)\\ \delta\dot{\theta}(t)\end{bmatrix} + \begin{bmatrix}0 & 0\\ -1 & -1\end{bmatrix}\begin{bmatrix}\delta\theta(t-h)\\ \delta\dot{\theta}(t-h)\end{bmatrix},\ \forall\begin{bmatrix}\delta\theta(t)\\ \delta\theta(t-h)\end{bmatrix} \in \chi_1,$$

$$\begin{bmatrix}\delta\dot{\theta}(t)\\ \delta\ddot{\theta}(t)\end{bmatrix} = \begin{bmatrix}0 & 1\\ -0.825+\Delta_1 & 0\end{bmatrix}\begin{bmatrix}\delta\theta(t)\\ \delta\dot{\theta}(t)\end{bmatrix} + \begin{bmatrix}0 & 0\\ -5 & -5\end{bmatrix}\begin{bmatrix}\delta\theta(t-h)\\ \delta\dot{\theta}(t-h)\end{bmatrix},\ \forall\begin{bmatrix}\delta\theta(t)\\ \delta\theta(t-h)\end{bmatrix} \in \chi_2,$$

$$\begin{bmatrix}\delta\dot{\theta}(t)\\ \delta\ddot{\theta}(t)\end{bmatrix} = \begin{bmatrix}0 & 1\\ -0.4875+\Delta_2 & 0\end{bmatrix}\begin{bmatrix}\delta\theta(t)\\ \delta\dot{\theta}(t)\end{bmatrix} + \begin{bmatrix}0 & 0\\ -5 & -5\end{bmatrix}\begin{bmatrix}\delta\theta(t-h)\\ \delta\dot{\theta}(t-h)\end{bmatrix},\ \forall\begin{bmatrix}\delta\theta(t)\\ \delta\theta(t-h)\end{bmatrix} \in \chi_3,$$

$$\begin{bmatrix}\delta\dot{\theta}(t)\\ \delta\ddot{\theta}(t)\end{bmatrix} = \begin{bmatrix}0 & 1\\ -0.4875+\Delta_2 & 0\end{bmatrix}\begin{bmatrix}\delta\theta(t)\\ \delta\dot{\theta}(t)\end{bmatrix} + \begin{bmatrix}0 & 0\\ -5 & -5\end{bmatrix}\begin{bmatrix}\delta\theta(t-h)\\ \delta\dot{\theta}(t-h)\end{bmatrix},\ \forall\begin{bmatrix}\delta\theta(t)\\ \delta\theta(t-h)\end{bmatrix} \in \chi_4, \qquad (2.66)$$

with partition

$$\chi_1 = \{[\delta\theta(t)\quad \delta\theta(t-h)]^T \mid -0.7854 \le \delta\theta(t) \le 0 \text{ and } -0.7854 \le \delta\theta(t-\tau) \le 0\};$$
$$\chi_2 = \{[\delta\theta(t)\quad \delta\theta(t-h)]^T \mid -0.7854 \le \delta\theta(t) \le 0 \text{ and } 0 \le \delta\theta(t-\tau) \le 0.7854\};$$
$$\chi_3 = \{[\delta\theta(t)\quad \delta\theta(t-h)]^T \mid 0 \le \delta\theta(t) \le 0.7854 \text{ and } -0.7854 \le \delta\theta(t-\tau) \le 0\};$$
$$\chi_4 = \{[\delta\theta(t)\quad \delta\theta(t-h)]^T \mid 0 \le \delta\theta(t) \le 0.7854 \text{ and } 0 \le \delta\theta(t-\tau) \le 0.7854\};$$

and $|\Delta_1| \le 0.175$ and $|\Delta_2| \le 0.3$. Using Theorem 2.1 and Theorem 2.3, one can obtain that UBD = 0.161s for the nominal system (i.e., $\Delta_1 = \Delta_2 = 0$) and UBD = 0.15s for the

uncertain system. The method in (Moezzi et al, 2009) cannot deal with the system in this example since the switching depends on the delayed states as well as the states.

Remark 10: For systems with uncertainty, the theoretical UBD value cannot be obtained via simulation because of the infinite number of possible conditions. Thus, the theoretical values of UBD are not provided in those examples.

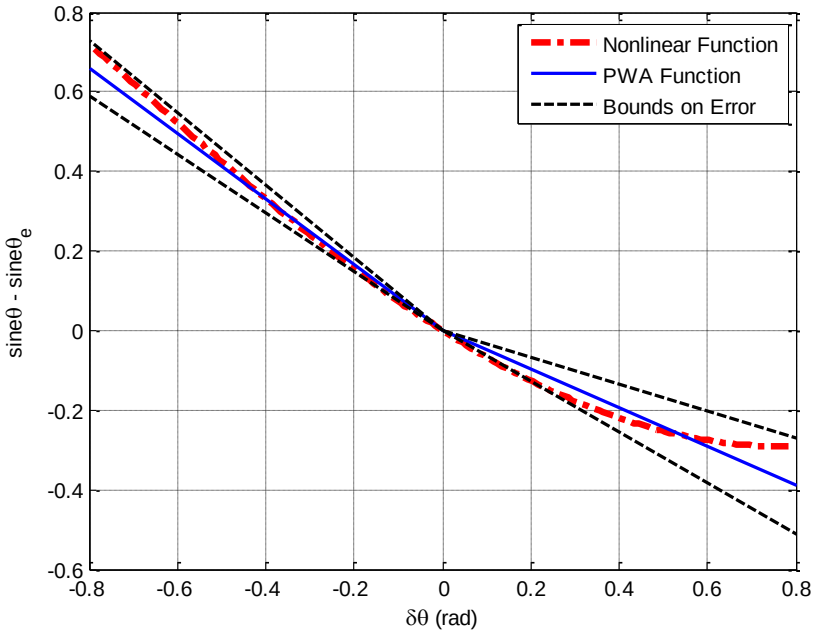

Fig. 2.3 PWA approximation with norm-bounded error

2.7 Concluding Remarks

In this chapter, sufficient conditions for the stability of PWA time-delay systems with and without norm-bounded uncertainty, which can be either structured or unstructured, are derived in the form of LMIs. With the addition of a triple integration term in the Lyapunov-Krasovskii functional, the proposed approach yields less conservative results, at least for the examples considered, over existing methods. Furthermore, compared with existing methods for uncertain PWA time-delay systems, the proposed approach requires

much less computational power especially for PWA systems with many regions. More significantly, this work addresses for the first time the problem of switching based on delayed states as well as states. Such situation exists in many cases of practical engineering interest such as systems with controller, sensor or actuator delay.

CHAPTER 3
MODELING AND CONTROL OF AN AUTOMOTIVE ALL WHEEL DRIVE CLUTCH AS A PIECEWISE AFFINE SYSTEM

3.1 Introduction

Piecewise affine (PWA) systems are defined by dividing the state-space into a finite number of polyhedral regions where the dynamics within the region is described via a local linear model. The switching between these local models may depend upon both inputs and states or may depend upon states only. This structure provides a flexible and traceable framework to model a large class of nonlinear systems as well as a suitable platform for rigorous analysis and design. PWA systems coincide with many other types of hybrid systems such as interconnections of linear systems, finite automata (Sontag, 1996) and mixed logic dynamical systems (Schutter and Moor, 1999).

The PWA system framework has been demonstrated for several simple engineering applications. An application of the PWA system framework to the modeling of combined vehicle-driver behaviour on highways can be found in (Kulkarni, 2003). The modelling of systems with saturation or deadzone as PWA systems is discussed in (Dai et al., 2009a). Problems of casting linear hybrid dynamic systems and T-S fuzzy systems into the PWA system framework are discussed in (Johansson, 2003). In (Moezzi, 2009), the modeling and control of a nonlinear pendulum system and a nonlinear water tank system are illustrated using the PWA system framework.

Besides the flexibilities for modeling, the PWA system framework also provides a nice platform for analysis and design. For example, the observability and reachability of PWA systems can be examined using the methods in (Bemporad et al., 2000; Rodrigues et al.,2003; Habets et al, 2006). A critically important but challenging problem for PWA systems is stability. Switching among regions may cause instability even if all sub-region models are stable (Branicky, 1998). One needs to find a common Lyapunov function, or a piecewise Lyapunov function (Johansson, 2003), to show global stability. Although one can apply the extensive theory for linear systems to design controllers region by region to achieve optimized local performance, the global stability of closed-loop systems must still be guaranteed (Rodrigues, 2005). Further, time delays exist in many practical systems, where delays can be inherent in the process or can arise due to control (e.g., delays in sensing, control or actuation). Excessive delays in control systems can deteriorate and destabilize the closed-loop system. Thus, accommodating potential time delays in the analysis is important for guaranteed closed-loop performance.

In this work, the application of the PWA system framework to the modeling and control of a nonlinear automotive all wheel drive (AWD) clutch system is presented. The nonlinear clutch system is formulated into the PWA system framework first, subsequently a switched control system is designed to ensure the closed-loop stability in the presence of uncertainties and delays through Lyapunov stability analysis. The results show significant improvements in performance over current designs, as well as demonstrating the trade-off among performance, robustness to modeling uncertainty, and time delays.

The organization of this chapter can be summarized as follows. In Section 3.2, the PWA system framework is introduced. In Section 3.3, an application of this framework to control design for an automatic AWD clutch system is demonstrated. The dynamics of the clutch system is first modeled as a PWA system, followed by the design of a piecewise controller and then the stability analysis of the closed-loop system. Simulation results and discussion are provided in Section 3.4 to demonstrate the effectiveness of the design. A summary and concluding remarks are given in Section 3.5.

3.2 PWA System Framework

3.2.1 PWA Systems

Consider a nonlinear time-invariant dynamic time-delay system described as

$$\begin{aligned} \dot{\mathbf{x}}(t) &= \mathbf{f}(\mathbf{x}(t), \mathbf{x}(t-\tau), \mathbf{u}(t)) \\ \mathbf{y}(t) &= \mathbf{g}(\mathbf{x}(t), \mathbf{x}(t-\tau), \mathbf{u}(t)) \end{aligned}, \quad \forall \begin{bmatrix} \mathbf{x}(t) \\ \mathbf{x}(t-\tau) \\ \mathbf{u}(t) \end{bmatrix} \in \chi_i \tag{3.1}$$

where t is time, τ is a constant time delay, $\mathbf{f}(\cdot) \in \Re^{n\times 1}$ and $\mathbf{g}(\cdot) \in \Re^{p\times 1}$ are nonlinear functions, $\mathbf{x}(t) \in \Re^{n\times 1}$ is the state vector, $\mathbf{x}(t-\tau) \in \Re^{n\times 1}$ is the delayed state, $\mathbf{y}(t) \in \Re^{p\times 1}$ is the output vector, and $\mathbf{u}(t) \in \Re^{r\times 1}$ are the external inputs. Assume that $\mathbf{f}(\cdot)$ and $\mathbf{g}(\cdot)$ are piecewise differentiable, the linearization of the system in (3.1) about selected fixed operating points will result in a series of interconnected linear affine models, which together form a PWA time-delay system:

$$\begin{aligned} \dot{\mathbf{x}}(t) &= \mathbf{A}_i\mathbf{x}(t) + \mathbf{A}_{\mathbf{d}i}\mathbf{x}(t-\tau) + \mathbf{B}_i\mathbf{u}(t) + \mathbf{a}_i \\ \mathbf{y}(t) &= \mathbf{C}_i\mathbf{x}(t) + \mathbf{C}_{\mathbf{d}i}\mathbf{x}(t-\tau) + \mathbf{D}_i\mathbf{u}(t) + \mathbf{c}_i \end{aligned}, \quad \forall \begin{bmatrix} \mathbf{x}(t) \\ \mathbf{x}(t-\tau) \\ \mathbf{u}(t) \end{bmatrix} \in \chi_i \tag{3.2}$$

where $\mathbf{A}_i \in \Re^{n\times n}$, $\mathbf{A}_{\mathbf{d}i} \in \Re^{n\times n}$, $\mathbf{B}_i \in \Re^{n\times r}$, $\mathbf{C}_i \in \Re^{p\times n}$, $\mathbf{C}_{\mathbf{d}i} \in \Re^{p\times n}$ and $\mathbf{D}_i \in \Re^{p\times r}$ are constant coefficient matrices, and $\mathbf{a}_i \in \Re^{n\times 1}$ and $\mathbf{c}_i \in \Re^{p\times 1}$ are constant affine terms which offer additional flexibility in the model. The set $\{\chi_i\}_{i=1}^{s}$ is the polyhedral partition of the input-state space, $span\left\{\begin{bmatrix}\mathbf{x}(t)^T & \mathbf{x}(t-\tau)^T & \mathbf{u}(t)^T\end{bmatrix}^T\right\}$. The partition of the space is defined as:

$$\begin{bmatrix}\bar{\mathbf{E}}_i & \bar{\mathbf{E}}_{\mathbf{d}i} & \mathbf{E}_{\mathbf{u}i}\end{bmatrix}\begin{bmatrix}\bar{\mathbf{x}}(t)\\ \bar{\mathbf{x}}(t-\tau)\\ \mathbf{u}(t)\end{bmatrix} \geq 0,\ \forall \begin{bmatrix}\mathbf{x}(t)\\ \mathbf{x}(t-\tau)\\ \mathbf{u}(t)\end{bmatrix} \in \chi_i \tag{3.3}$$

where $\bar{\mathbf{x}}_i(t)=\begin{bmatrix}\mathbf{x}_i^T(t) & 1\end{bmatrix}^T$, $\bar{\mathbf{x}}_i(t-\tau)=\begin{bmatrix}\mathbf{x}_i^T(t-\tau) & 1\end{bmatrix}^T$ and $\bar{\mathbf{E}}_i = \begin{bmatrix}\mathbf{E}_i & \mathbf{e}_i\end{bmatrix}$, $\bar{\mathbf{E}}_{di} = \begin{bmatrix}\mathbf{E}_{di} & \mathbf{e}_{di}\end{bmatrix}$. Note that $\mathbf{E}_i$, $\mathbf{E}_{\mathbf{d}i}$, $\mathbf{E}_{\mathbf{u}i}$, $\mathbf{e}_i$ and $\mathbf{e}_{di}$ are constant matrices with compatible dimension. With a sufficiently fine partition, the PWA time-delay system in (3.2) is able to provide a good approximation of the original nonlinear system in (3.1) over the entire space. Although introducing more regions in the space can help to lower the approximation errors, the increase of model complexity may make subsequent analysis and design difficult. A good choice of the partition size should achieve a reasonable trade-off between approximation error and model complexity. Clearly, the partitioning of the input-state space influences the level of modeling uncertainty.

3.2.2 Stability Analysis

Since the stability of the sub-systems does not directly imply the stability of the global system for PWA systems, an examination of the global stability for PWA systems is necessary and important. One needs to construct a Lyapunov function to show that the energy of the system approaches zero over time, in spite of switching, to prove global

stability. Note that $\mathbf{u} = 0$ when Lyapunov stability is considered and the system in (3.2) simplifies to:

$$\dot{\mathbf{x}}(t) = \mathbf{A}_i\mathbf{x}(t) + \mathbf{A}_{\mathbf{d}i}\mathbf{x}(t-\tau) + \mathbf{a}_i + \boldsymbol{\delta}_i, \ \forall \begin{bmatrix} \mathbf{x}(t) \\ \mathbf{x}(t-\tau) \end{bmatrix} \in \tilde{\chi}_i \tag{3.4}$$

with the partition

$$\begin{bmatrix} \bar{\mathbf{E}}_i & \bar{\mathbf{E}}_{\mathbf{d}i} \end{bmatrix} \begin{bmatrix} \bar{\mathbf{x}}(t) \\ \bar{\mathbf{x}}(t-\tau) \end{bmatrix} \geq 0, \ \forall \begin{bmatrix} \mathbf{x}(t) \\ \mathbf{x}(t-\tau) \end{bmatrix} \in \tilde{\chi}_i \tag{3.5}$$

The set $\{\tilde{\chi}_i\}_{i=1}^{s}$ is the polyhedral partition of the space, $span\left\{\begin{bmatrix} \mathbf{x}(t)^T & \mathbf{x}(t-\tau)^T \end{bmatrix}^T\right\}$. For rigorous analysis, the uncertainty, $\boldsymbol{\delta}_i \in \Re^{n\times 1}$, is considered in the model and is assumed to be norm-bounded. A primary source of model uncertainty is the fact that the nonlinear system being considered has been represented as a PWA system. The uncertainty can either be modeled as structured uncertainty or left unstructured. For the first case, assume that it is of the form

$$\boldsymbol{\delta}_i = \Delta\mathbf{A}_i\mathbf{x}(t) + \Delta\mathbf{A}_{di}\mathbf{x}(t-\tau) + \Delta\mathbf{a}_i \tag{3.6}$$

where

$$\begin{bmatrix} \Delta\mathbf{A}_i & \Delta\mathbf{A}_{di} & \Delta\mathbf{a}_i \end{bmatrix} = \mathbf{G}_i\boldsymbol{\Lambda}_i \begin{bmatrix} \mathbf{H}_{1i} & \mathbf{H}_{2i} & \mathbf{H}_{3i} \end{bmatrix}$$
$$\boldsymbol{\Lambda}_i^T\boldsymbol{\Lambda}_i \leq \mathbf{I}$$

and $\mathbf{G}_i$, $\mathbf{H}_{1i}$, $\mathbf{H}_{2i}$, $\mathbf{H}_{3i}$ are constant matrices with compatible dimension describing how the uncertainty enters the parameter matrices. If the uncertainty is admissible, the coefficient matrices $\mathbf{G}_i$, $\mathbf{H}_{1i}$, $\mathbf{H}_{2i}$ and $\mathbf{H}_{3i}$ can be identified. If the uncertainty is not admissible, one may use the unstructured uncertainty form

$$\left\|\boldsymbol{\delta}_i\right\| \leq \varepsilon_i \left\|\mathbf{x}(t)\right\| + \varepsilon_{di} \left\|\mathbf{x}(t-\tau)\right\| + \varepsilon_{ai} \tag{3.7}$$

where $\varepsilon_i, \varepsilon_{di}, \varepsilon_{ai} \in \Re$ are the factors of the bound and $\|\cdot\|$ is the 2-norm.

For stability analysis of the system in (3.4), some methods based on the Lyapunov method have been developed. The stability problem of nominal PWA time-delay systems (i.e., the system in (3.4) with $\boldsymbol{\delta}_i = 0$) has been studied in (Kulkarni et al. 2004), which follows the work of Johansson (2003). An extension of the work in (Rodrigues & How, 2003) has been proposed in (Moezzi et al., 2009) to address the robust stability problem for PWA time-delay systems with unstructured uncertainty. To address the problem of switching based on delayed state as well as state, an approach based on the work of (Johansson, 2003) and (Xu & Lam, 2005) is proposed in (Duan et al., 2011). This work also further reduces the conservativeness and computational complexity of the approach and considers both the structured and unstructured uncertainty case. In the chapter, this method will be applied to an AWD clutch control system.

3.3 Application to an Automotive Clutch Control System

3.3.1 Introduction

A clutch works like a valve, controlling the energy flow from the engine to the transmission. By engaging and disengaging the clutch, it transmits power from the engine to the output shaft. The conventional clutch is known as a compressed clutch and consists of two basic components, the clutch cover and disc. The clutch cover is an outer shell that contains the friction plate and drive block. The friction plate is a cast piece that provides the pivot point for the diaphragm as well as a friction surface for the steel plate and mounting surface for the drive block. The drive block, driven by a hydraulic system or a magnetic coil system, translates and provides pressure between the steel plate and friction

plate. The clutch housing protects the clutch components and also works as a heat sink for the coolant which helps heat dissipation during operation.

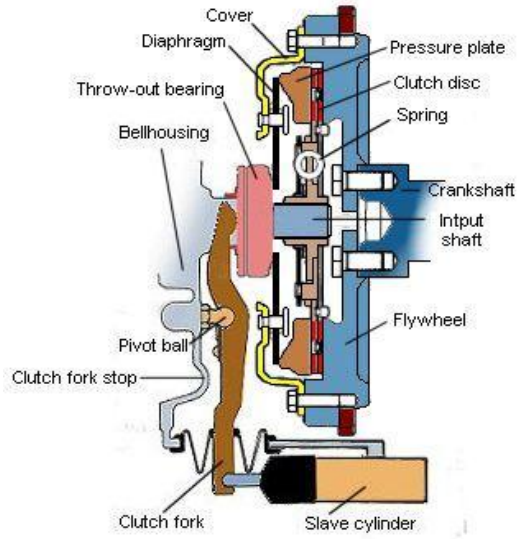

Fig. 3.1 Structure of a clutch system
http://img528.imageshack.us/img528/575/25838775lk1.jpg

Clutch systems for various vehicles are different in functionality and capacity. In this chapter, a clutch system for an automatic all wheel drive (AWD) vehicle is studied. Automatic AWD (Hallowell, 2005), which is also called “active AWD” or “smart AWD”, is essentially a complex 2WD system. The torque from the engine is not transferred to all four wheels all the time, but on demand. The primary shaft (can be front or rear shaft) is always engaged with the engine shaft while the secondary shaft is engaged through an AWD clutch system when necessary, thus switching the power train system from 2WD mode to 4WD mode. For example, when slippage occurs on the primary wheels, the clutch system will engage and power the secondary shaft to enable the car to move smoothly. Some other situations such as turning, climbing or accelerating also require traction on the secondary wheels for improved vehicle dynamics. The

automatic AWD has been widely implemented in many types of vehicles (e.g., Honda CRV, Toyota RAV4, LandRover Freelander, Isuze Trooper, Jeep Grand Cherokee).

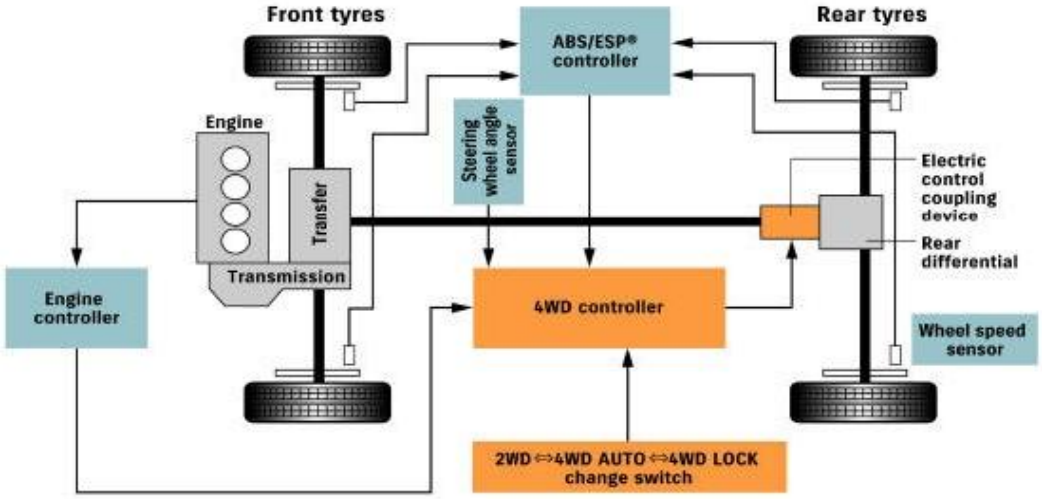

Fig. 3.2 An automatic AWD system
(http://www.autopressnews.com/2006/m03/suzuki/sx4_iawd_system.jpg)

The clutch in automatic AWD systems provides more sophisticated functionalities compared with the ones in 2WD systems (see Fig.3.2). The control of the clutch takes into consideration not only the impact and friction mechanism during engagement, but also the delivery of a certain amount of torque to the secondary shaft to achieve a proper torque distribution all the time. The clutch control system in automatic AWD systems can be further divided into two parts. The first part calculates the desired torque distribution and the desired output torque on the secondary shaft based on vehicle dynamics and current vehicle status (e.g., longitudinal velocity, yaw rate, lateral acceleration). The second part calculates the control effort for the actuator to compress the plate and transfer the requested torque under the current state of the clutch. In this work, we focus on the design of the second part of the control for a particular type of AWD clutch (see Fig.3.3). This wet-friction type of clutch does not have an active pump system for cooling. Instead,

two thirds of the clutch plate is immersed in the oil, where the heat from the plate is dissipated. A coil system is used as an actuator and generates electro-magnetic forces to provide a compressive force between plates.

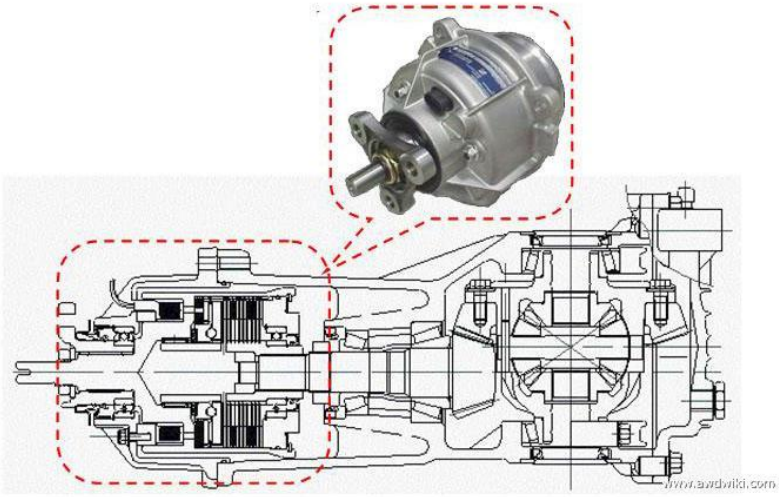

Fig. 3.3 An AWD clutch system
(http://www.awdwiki.com/images/hyundai-tuscon-electromagnetic-clutch.jpg)

The objective of the control is to achieve fast and accurate tracking of the reference torque signal under different operating conditions and to protect clutch components from overheating and failure. However, there are several challenges for designing an effective control for the clutch system. The dynamics of the system changes with different input and operating conditions, especially the temperature states of the components and exhibits a highly nonlinear behavior. During engagement, the friction between the steel plate and friction plate generates a large amount of heat and may raise the temperature of the components up to 180 ℃ under typical operations. Such a large temperature change can significantly change many mechanical properties of the components, such as the friction coefficient between plate and the coil resistance of actuator, and result in a noticeable fluctuation in the output torque. Furthermore, even without temperature

variation, the mapping between the input (coil voltage) and the output torque is nonlinear. Thus, designing a control that can achieve consistent performance under different conditions is challenging for such a nonlinear system.

The existing design for the clutch control system is an open-loop feed forward proportional control with an open-loop observer (see Fig.3.4). The controller estimates the error between the reference torque and the output torque using an open-loop observer and computes the control for driving the plant to yield the desired output. There are several major drawbacks of the current design. First, due to the lack of feedback, it is hard to achieve satisfactory performance with an open-loop observer since uncertainty in the system will lead to poor state estimates. Second, the setting of improper initial conditions affects the system performance for a long period because of the slow dynamics of the thermal system. Third, the proportional control is not able to achieve zero steady-state error. Fourth, a single controller will not be able to offer consistent performance for different operating conditions. Fifth, there is no analytical basis for selecting the gain of the controller, which is tuned by trial and error. Last, the stability of the system, the effects of model uncertainty, and the effects of the potential time delay in the controller have not been investigated.

In this chapter, we will design a more effective control for the clutch system via the PWA system framework. Based on that framework, a piecewise control is proposed to achieve consistent performance under different operating conditions. The gains of the controller are analytically selected and the stability of the closed-loop system with the presence of uncertainty and controller delay is guaranteed by analyzing the global stability of the system.

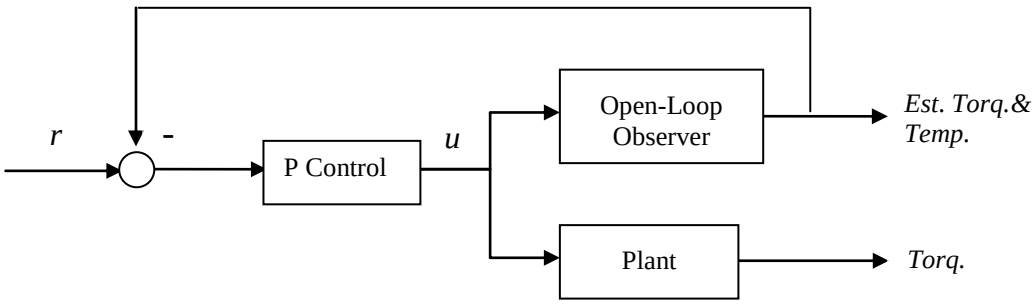

Fig. 3.4 Current control design (open-loop observer + feed forward P control)

3.3.2 Model Development

Since temperature fluctuation introduces significant disturbances to the clutch system and may lead to premature degradation of the components, the estimation of the temperature states is necessary for temperature compensation and failure prevention. A model is developed to estimate the temperature states of the clutch components. Three first order differential equations are obtained for the thermal system:

$$\begin{aligned} \dot{\mathbf{x}}_{\mathbf{T}}(t) &= \mathbf{A}_{\mathbf{T}}\mathbf{x}_{\mathbf{T}}(t) + \mathbf{B}_{\mathbf{T}}\mathbf{u}_{\mathbf{w}}(t) \\ y_T(t) &= \mathbf{C}_{\mathbf{T}}\mathbf{x}_{\mathbf{T}}(t) \end{aligned} \tag{3.8}$$

where

$$\mathbf{A}_{\mathbf{T}} = \begin{bmatrix} -\dfrac{R_{po}+R_{pa}+R_{pc}}{C_p} & \dfrac{R_{po}}{C_p} & \dfrac{R_{pc}}{C_p} \\ \dfrac{R_{po}}{C_o} & -\dfrac{R_{po}+R_{oa}+R_{oc}}{C_o} & \dfrac{R_{oc}}{C_o} \\ \dfrac{R_{pc}}{C_c} & \dfrac{R_{oc}}{C_c} & -\dfrac{R_{oc}+R_{pc}+R_{ca}}{C_c} \end{bmatrix}, \quad \mathbf{B}_{\mathbf{T}} = \begin{bmatrix} \dfrac{1}{C_p} & \dfrac{R_{pa}}{C_p} \\ 0 & \dfrac{R_{oa}}{C_s} \\ 0 & \dfrac{R_{ca}}{C_c} \end{bmatrix},$$

$\mathbf{C}_{\mathbf{T}} = \begin{bmatrix} 0 & 0 & 1 \end{bmatrix}$, $\mathbf{x}_{\mathbf{T}}(t) = \begin{bmatrix} T_p(t) \\ T_o(t) \\ T_c(t) \end{bmatrix}$ is the temperature state vector, $\mathbf{u}_{\mathbf{w}}(t) = \begin{bmatrix} P_{mech}(t) \\ T_a(t) \end{bmatrix}$

$= \begin{bmatrix} y_o(t) | \omega_o(t) - \omega_i(t) | \\ T_a(t) \end{bmatrix}$ is the disturbance input vector, $y_T(t) = T_c(t)$ is the temperature system output. Also, T_a is the ambient temperature, y_o is the output torque, ω_i is the input shaft speed, $\omega_o \in \Re^1$ is the output shaft speed, and T_p, T_o, T_c are the temperature states of the clutch plate, oil and coil, respectively, C_p, C_o, C_c are the constant scalars representing corresponding thermal capacities, R_{po}, R_{pa}, R_{pc}, R_{oa}, R_{oc}, R_{ca} are the constant thermal resistances between the three components. The mechanical power, P_{mech}, generated by friction, is estimated as the product between absolute slip speed and output torque. The inputs, T_a, ω_i and ω_o, are measured in the current design. The coefficients for thermal capacitance and thermal resistance will be identified using experimental data. This temperature model will be used in the design of a temperature disturbance observer and for feed forward control.

The resistor-inductor circuit system generates magnetic compressive force to engage the clutch. To identify the mapping between the control input (coil voltage) and the output torque, first, a first-order differential equation is used to describe the relationship between the coil voltage and the coil current

$$\frac{d}{dt} i_c(t) = A_{qc}(T_c) i_c(t) + B_q u(t) \tag{3.9}$$

where

$$A_{qc}(T_c) = A_q + \Delta A_q(T_c) = -\frac{\Omega_{c0}}{L_c} - \frac{\Omega_{c0} \alpha (T_c(t) - T_{c0})}{L_c} \tag{3.10}$$

$B_q = \frac{1}{L_c}$, $u(t) = V_c(t)$ is the coil voltage input, $i_c(t)$ is the coil current, L_c is the coil

inductance, α is the temperature coefficient of the coil resistance, Ω_{c0} is the nominal coil resistance and T_{c0} is the nominal coil temperature.

Then, a model is developed to estimate the output torque, which is determined by both the coil current and the plate temperature:

$$y_o(t) = \mu(T_p)C_q(i_c) \tag{3.11}$$

where $y_o(t)$ is the output torque, $\mu(T_p)$ is a scalar function and represents the effects of plate temperature, T_p, on the μ factor (i.e., plate friction coefficient) and $C_q(i_c)$ is the nominal output torque under nominal plate temperature T_{p0}. Assuming $\mu(T_p)$ and $C_q(i_c)$ are independent and can be approximated by the polynomial functions in (3.12) and (3.13), respectively :

$$\mu(T_p) = 1 + \sum_{j=1}^{m} l_j (T_p(t) - T_{p0})^j \tag{3.12}$$

$$C_q(i_c) = \begin{cases} \sum_{k=1}^{n} p_k i_c(t)^k, & if \ i_c > 0 \\ 0, & if \ i_c \le 0 \end{cases} \tag{3.13}$$

where T_{p0} is the nominal plate temperature and l_j, p_k are the coefficients which will be identified later empirically. Note that when a negative current is applied, the clutch will be disengaged and no output torque will be transferred (i.e., $C_q(i_c)$ saturates at zero when $i_c \le 0$). The temperature effects introduce nonlinearities in (3.10) and (3.12).

3.3.3 Control Design and Stability Analysis

The proposed controller, as shown in Fig.3.5, contains three parts: an observer that estimates the unmeasured temperature states, a feed forward control that compensates for

the disturbances (temperature variation) and a piecewise proportional plus integral (PI) control that realizes torque feedback control :

$$u(t) = u_{ff}(t) + u_{fb}(t) + r(t) \tag{3.14}$$

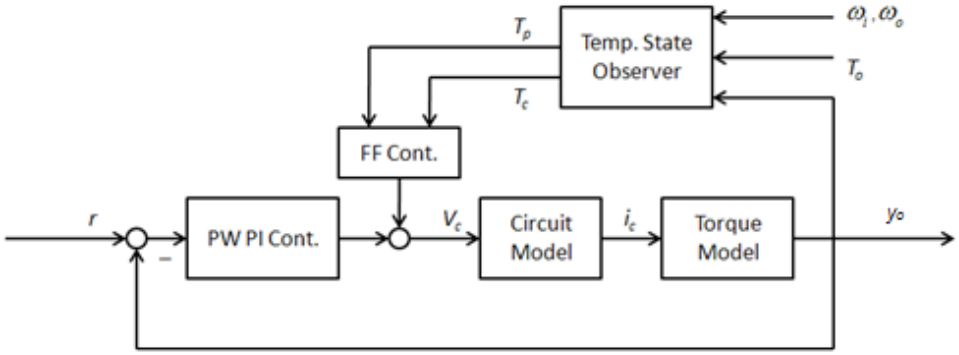

Fig. 3.5 Proposed feedback control design (disturbance observer + feed forward control + piecewise PI feedback control)

Several steps are required to develop the controller. First, an observer is designed based on the temperature model in (3.8) to estimate the temperature disturbance. Then, a feed forward controller is designed to remove the temperature effects in (3.10) and (3.12), making the dynamics of the nominal plant system (i.e., the plant plus feed forward system) independent of temperature states. Last, approximating the nonlinearity in (3.13) via a piecewise linear function leads to a PWA model for the nominal plant system. Based on the PWA model, a piecewise PI feedback control is developed. Compared to the original controller in Fig.3.4, three additional sensors, i.e., coil current sensor, output torque sensor and coil temperature sensor, are proposed to be implemented to realize this new design. The coil temperature sensor provides temperature measurements and helps the temperature estimates of the observer converge to the actual states. The torque sensor and current sensor provide feedback signals to realize the piecewise PI feedback control.

A Luenberger type observer is designed to estimate the plate temperature and oil temperature, which are not directly measured:

$$\begin{aligned}\dot{\hat{\mathbf{x}}}_{\mathbf{T}} &= \mathbf{A}_{\mathbf{T}}\hat{\mathbf{x}}_{\mathbf{T}} + \mathbf{B}_{\mathbf{T}}\mathbf{u}_{\mathbf{w}}(t) + \mathbf{L}_{\mathbf{T}}(y_T - \mathbf{C}_{\mathbf{T}}\hat{\mathbf{x}}_{\mathbf{T}}) \\ \mathbf{y}_{\mathbf{b}} &= \mathbf{C}_{\mathbf{b}}\hat{\mathbf{x}}_{\mathbf{T}}\end{aligned} \tag{3.15}$$

where $\hat{\mathbf{x}}_{\mathbf{T}}(t) = \begin{bmatrix}\hat{T}_p(t) & \hat{T}_o(t) & \hat{T}_c(t)\end{bmatrix}^T$ is the estimated state, $\mathbf{C}_{\mathbf{b}} = \begin{bmatrix}1 & 0 & 0 \\ 0 & 1 & 0\end{bmatrix}$, and $\mathbf{y}_{\mathbf{b}} = \begin{bmatrix}\hat{T}_p & \hat{T}_o\end{bmatrix}^T$ is the output of the observer. The temperature estimates will be used as inputs to the feed forward controller and the failure prevention system, which shuts down the clutch system when the temperature states exceed preset thresholds.

A feed forward compensator, $u_{ff}(t) = u_{ffc}(t) + u_{ffp}(t)$, is designed to approximately cancel the nonlinear terms arising due to the temperature effects in (3.10) and (3.12) :

$$u_{ffc}(t) = \alpha i_c(t)(T_c(t) - T_{c0}) \tag{3.16}$$

$$u_{ffp}(t) = \frac{1-\mu(\hat{T}_p(t))}{\mu(\hat{T}_p(t))}\left[r(t) + u_{fb}(t)\right] \tag{3.17}$$

After the feed forward controller is implemented, the system becomes

$$\begin{aligned}\dot{x}_o(t) &= A_q x_o(t) + B_q u_o(t) + \delta_1(t) \\ y_o(t) &= C_q(x_o) + \delta_2(t)\end{aligned} \tag{3.18}$$

where

$$u_o(t) = r(t) + u_{fb}(t),\ x_o(t) = \tilde{i}_c(t) = \mu(\hat{T}_p) i_c(t) \tag{3.19}$$

and δ_1, δ_2 are the model uncertainties

$$\begin{aligned}\delta_1(t) &= \frac{\tilde{i}_c(t)}{\mu(\Delta\hat{T}_p)} \cdot \frac{d\,\mu(\hat{T}_p(t))}{dt} \\ \delta_2(t) &= \mu(T_p) C_q(i_c) - C_q(\mu(\hat{T}_p) i_c)\end{aligned} \tag{3.20}$$

Note that in (3.18), the equivalent coil current, $\tilde{i}_c(t)$, is used as the state variable after the feed forward controller is implemented. Since the estimated plate temperature $\hat{T}_p(t)$ is used in the feed forward controller, the plate temperature error will introduce uncertainty in the model. Further, the design of the feed forward control in (3.17) is based on the dc-gain of the system, the neglect of the system dynamics will also introduce error. These errors are included as the uncertainties in (3.20). Since the plate temperature usually changes very slowly (typically less than $10^{\circ}C/\sec$), $\delta_1(t)$ is usually very small (less than $0.01\tilde{i}_c(t)$). Therefore, it is neglected from this point forward.

Based on the nonlinearity of $C_q(x_o)$, the space of x_o can be divided into multiple regions, where a linear affine model is used to approximate $C_q(x_o)$ locally.

$$C_q(x_o) = C_{oi}x_o(t) + c_{oi} + \delta_3,\ \forall x_o \in \chi_i \tag{3.21}$$

where δ_3 represents the approximation error, C_{oi}, c_{oi} are the coefficient for each region and χ_i is the partition of the space and will be determined based on the nonlinearity of (3.13).

As a result, a PWA system is obtained for the compensated plant system

$$\begin{aligned} \dot{x}_o(t) &= A_{oi}x_o(t) + B_{oi}u_o(t) + \delta_1(t) \\ y_o(t) &= C_{oi}x_o(t) + c_{oi} + \delta_2(t) + \delta_3(t) \end{aligned},\quad \forall x_o(t) \in \chi_i \tag{3.22}$$

where $A_{oi} \equiv A_q$, $B_{oi} \equiv B_q$. Assume δ_2 and δ_3 are norm-bounded, i.e., there exist $\varepsilon \in \Re$ such that

$$\delta_2(t) + \delta_3(t) = \sigma\tilde{i}_c(t),\ \|\sigma\| \le \varepsilon \tag{3.23}$$

Based on the PWA model in (3.22) of the nominal plant system, a feedback piecewise

generalized proportional plus integral (PI) controller is proposed, as it provides flexibility in each region to achieve consistent performance under different operating conditions. Note that the output of the system saturates when $x_o \le 0$, thus, the integral term of the PI control will accumulate a significant error when the system stays in the saturation zone, drifting the state to very large value. Thus, to avoid integrator windup, an anti-windup control is designed for the saturation region. The piecewise PI feedback plus anti-windup control is:

$$\begin{aligned} u_{fb}(t) &= K_{Ii} z(t) - K_{Pi} y_o(t) \\ \dot{z}(t) &= r(t) - y_o(t) \end{aligned}, \; i \notin I_s \tag{3.24}$$

$$\begin{aligned} u_{fb}(t) &= K_{Pi}(r(t) - y_o(t)) \\ \dot{z}(t) &= -K_Z z(t) \end{aligned}, \; i \in I_s \tag{3.25}$$

where K_{Ii}, K_{Pi}, K_Z are the gains for the i^{th} region, $r(t)$ is the reference torque and I_s denotes the set of regions in the saturation zone. When the system enters the saturation zone, the integral control will be disconnected and its state will be brought back to zero. The region ID, *i*, is determined by the plant state $\tilde{i}_c(t)$ for the controller.

Finally, the entire closed-loop system can be described as a PWA system:

$$\begin{aligned} \dot{\mathbf{x}}(t) &= \mathbf{A}_i \mathbf{x}(t) + \mathbf{B}_i r(t) + \mathbf{a}_i + \Delta\mathbf{A}_i \mathbf{x}(t) \\ y_o(t) &= \mathbf{C}_i \mathbf{x}(t) + \mathbf{c}_i + \Delta\mathbf{C}_i \mathbf{x}(t) \end{aligned}, \; \forall \mathbf{x}(t) \in \chi_i \tag{3.26}$$

where

$$\mathbf{A}_i = \begin{bmatrix} -\frac{\Omega_0}{L_c} - \frac{K_{Pi} q_1^i}{L_c} & \frac{K_S K_{Ii}}{L_c} \\ -K_S q_1^i & (K_S - 1) K_Z \end{bmatrix}, \; \mathbf{B}_i = \begin{bmatrix} \frac{(1 - K_S)}{L_c} \\ K_S \end{bmatrix}, \; \mathbf{a}_i = \begin{bmatrix} -\frac{K_{Pi} q_2^i}{L_c} \\ -K_S q_2^i \end{bmatrix}, \; \mathbf{C}_i = \begin{bmatrix} q_1^i & 0 \end{bmatrix},$$

$$\mathbf{c}_i = \begin{bmatrix} q_2^i \\ 0 \end{bmatrix}, \; \Delta\mathbf{A}_i = \mathbf{G}_i \Delta_i \mathbf{H}_{1i} = \begin{bmatrix} -\frac{K_{Pi}}{L_c} \\ -1 \end{bmatrix} \Delta_i \begin{bmatrix} \varepsilon & 0 \end{bmatrix}, \; \Delta\mathbf{C}_i = \Delta_i \mathbf{H}_{1i} = \Delta_i \begin{bmatrix} \varepsilon & 0 \end{bmatrix}, \; K_S \begin{cases} = 0, & i \in I_s \\ = 1, & i \notin I_s \end{cases}.$$

Further, if a time delay exists in the output torque measurements, i.e,

$$y_o(t-\tau) = \mathbf{C}_j \mathbf{x}(t-\tau) + \mathbf{c}_j + \Delta\mathbf{C}_j \mathbf{x}(t-\tau), \quad \forall \mathbf{x}(t-\tau) \in \chi_j \tag{3.27}$$

the torque feedback signal will be delayed. For the controller, choose to delay the switching of the feedback gains K_{Pi} and K_{Ii} to synchronize with the switching in (3.27). To do this, one can use a look-up table to estimate $i_c(t-\tau)$ from $y_o(t-\tau)$. Then use $i_c(t-\tau)$ to estimate the delayed switching signal $j(t)$. The closed-loop system will become a PWA time-delay system:

$$\begin{aligned} \dot{\mathbf{x}}(t) &= \hat{\mathbf{A}}_j \mathbf{x}(t) + \hat{\mathbf{A}}_{\mathbf{d}j} \mathbf{x}(t-\tau) + \hat{\mathbf{B}}_j r(t) + \hat{\mathbf{a}}_j + \Delta\hat{\mathbf{A}}_{\mathbf{d}j} \mathbf{x}(t-\tau) \\ y(t-\tau) &= \hat{\mathbf{C}}_j \mathbf{x}(t-\tau) + \hat{\mathbf{c}}_j + \Delta\hat{\mathbf{C}}_j \mathbf{x}(t-\tau) \\ &\forall \mathbf{x}(t-\tau) \in \chi_j \end{aligned} \tag{3.28}$$

where

$$\hat{\mathbf{A}}_j = \begin{bmatrix} -\dfrac{\Omega_0}{L_c} & \dfrac{K_S K_{Ij}}{L_c} \\ 0 & (K_S - 1)K_Z \end{bmatrix}, \ \hat{\mathbf{A}}_{\mathbf{d}j} = \begin{bmatrix} -\dfrac{K_{Pj} q_1^j}{L_c} & 0 \\ -K_S q_1^j & 0 \end{bmatrix}, \ \hat{\mathbf{B}}_j = \begin{bmatrix} \dfrac{(1-K_S)}{L_c} \\ K_S \end{bmatrix}, \ \hat{\mathbf{a}}_j = \begin{bmatrix} -\dfrac{K_{Pj} q_2^j}{L_c} \\ -K_S q_2^j \end{bmatrix},$$

$$\hat{\mathbf{C}}_k = \begin{bmatrix} q_1^j & 0 \end{bmatrix}, \ \hat{\mathbf{c}}_j = \begin{bmatrix} q_2^j \\ 0 \end{bmatrix}, \ \Delta\hat{\mathbf{A}}_{\mathbf{d}j} = \mathbf{G}_j \Delta_j \mathbf{H}_{2j} = \begin{bmatrix} -\dfrac{K_{Pi}}{L_c} \\ -1 \end{bmatrix} \Delta_j \begin{bmatrix} \varepsilon & 0 \end{bmatrix},$$

$$\Delta\hat{\mathbf{C}}_j = \Delta_j \mathbf{H}_{2j} = \Delta_j \begin{bmatrix} \varepsilon & 0 \end{bmatrix}, \ K_S = \begin{cases} 0, \ j \in I_S \\ 1, \ j \notin I_S \end{cases}.$$

Note that due to the delay, the switching of the closed-loop system now depends on $\mathbf{x}(t-\tau)$. One may also choose not to delay the switching of the feedback gains and the resulting system will switch based on both $\mathbf{x}(t)$ and $\mathbf{x}(t-\tau)$. Here we choose to delay the switching in the feedback control to reduce model complexity.

The Lyapunov stability of the closed-loop system in (3.28) will be examined using the LMI criteria in Lemma 1. The upper bounds on delay (UBDs) for the system with uncertainty will be calculated.

3.3.4 Experiments

In order to calibrate the parameters of the clutch model, experimental tests are conducted. The clutch is mounted on a test-bed where different operating conditions are simulated. The outside shell of the clutch is fixed on the body of the test bed while the input shaft and output shaft are connected to two motors, whose speed can be arbitrarily changed. Applying a voltage in the clutch coil generates a magnetic force and engages the clutch. Torque sensors and angular velocity sensors are placed on the motors for monitoring the input/output speed and torque. Several thermistors are placed on the clutch for measuring the temperature of the plate, oil and coil. The measurements in these calibration experiments are T_p, T_o, T_c, T_a, ω_i, ω_o, i_c, V_c and Q.

A test profile shown in Fig.3.6 is used for calibrating the temperature model. It consists of a series of input and slip speeds, with a sequence of constant-power torque steps at each combination. Coil current is periodically applied to generate frictional energy into the system. The temperature of the components increases when there is an energy input and decreases when no energy is supplied. Therefore, the temperature curves take on a zigzag pattern. Input speeds range from 125 rpm to 3500 rpm. At each input speed, the slip speed starts at 150 rpm and is reduced by steps. The sampling rates for all the data are 10 Hz.

The parameters of the circuit model can be obtained from the tests. To calibrate the torque model, two experiments with a similar setup are conducted to identify the

functions $\mu(T_p)$ and $C_q(i_c)$ respectively. A constant current input is used in the first experiment to investigate the relationship between the plate temperature and the μ factor. For the second experiment, different coil currents are applied sequentially with sufficient cooling time in between to characterize the relationship between the coil current and the output torque under nominal plate temperature.

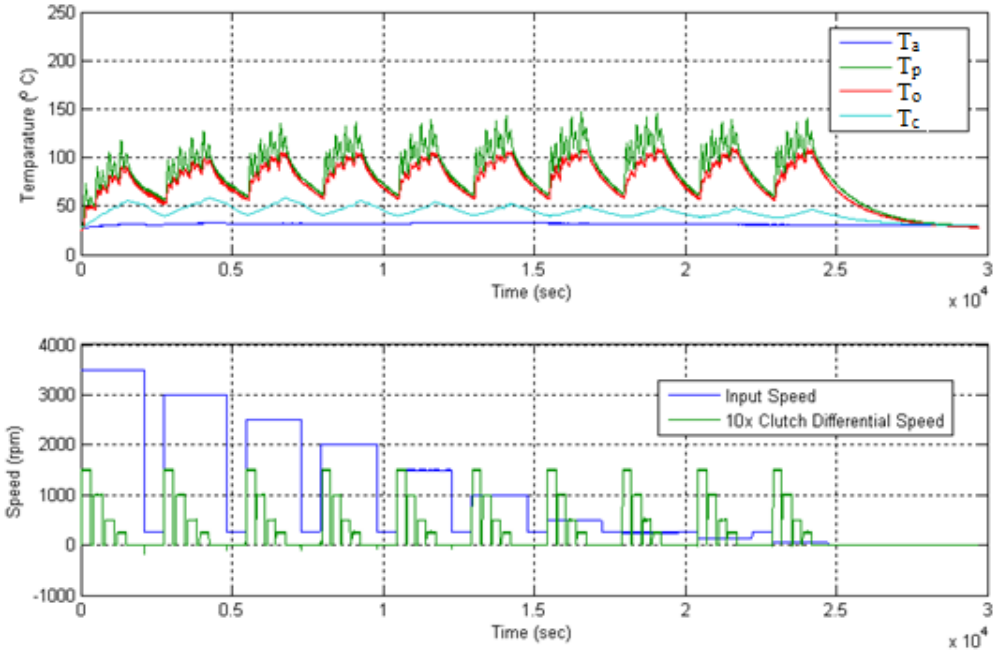

Fig. 3.6 Test profile for clutch thermal system modeling

3.4 Results

3.4.1 Open-Loop System

Using the experimental data collected and the system identification toolbox from Matlab, the model parameters are obtained as:

$$\mathbf{A_T} = \begin{bmatrix} -0.05 & 1.02 & 0.395 \\ 0.004 & -0.026 & 0.096 \\ 0.004 & 0.025 & -0.049 \end{bmatrix}, \mathbf{B_T} = \begin{bmatrix} 0.074 & 0.33 \\ 0 & 0.004 \\ 0 & 0.01 \end{bmatrix}, \mathbf{C_T} = \begin{bmatrix} 0 & 0 & 1 \end{bmatrix}$$

$$\Omega_{c0} = 2.00 \text{ Ohm}, \; L_c = 0.121\text{H}, \; \alpha = 0.004 \; {}^{\circ}c^{-1}.$$

$$\mu(T_p) = 1 - 0.0014(T_p - 40) - 6.8\times10^{-6}(T_p - 40)^2$$

$$y_o(i_c) = \begin{cases} -51.2585 i_c + 218.6445 i_c^{\,2} - 56.9184 i_c^{\,3} + 4.4563 i_c^{\,4}, & if \;\; i_c > 0 \\ 0, \;\; if \;\; i_c \le 0 \end{cases}$$

The polynomial model for Mu factor is calibrated using the experimental data shown in Fig. 3.7. Based on the nonlinearity of y_o, a piecewise affine function with the partition in Table 3.1 is used to approximate y_o as shown in Fig.3.8.

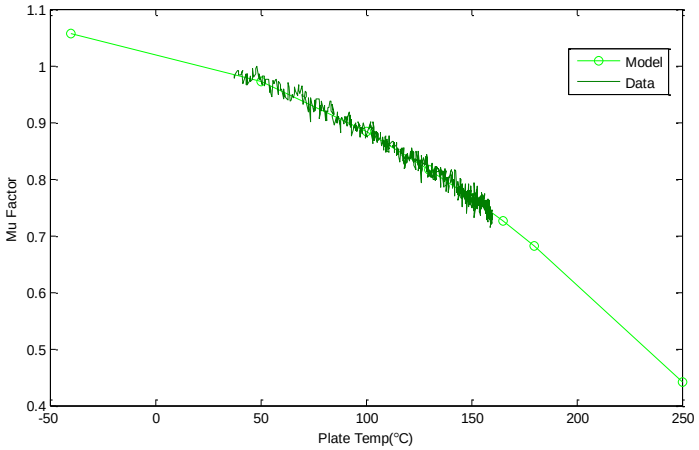

Fig. 3.7 Mu factor vs. plate temperature

Table 3.1 Partition over Space of Coil Current

Region	1	2	3	4
i_c	<0 A	0~0.8 A	0.8~3.3 A	>3.3A
$q_1^i i_c + q_2^i$	0	$103\, i_c$	$250\, i_c$ -117	$101\, i_c$ +372

For these types of clutch systems, the error in the plate temperature estimates are typically within $15\,^{\circ}C$. Thus, the bounds for the uncertainty in the model can be estimated as

$$|\delta_2(t)| \le 15|\tilde{i}_c(t)|,\ |\delta_3(t)| \le 10|\tilde{i}_c(t)|,\ \varepsilon = 15+10 = 25$$

The step response and sine input response of the open-loop system, under the temperature disturbance in Fig.3.9, are shown in Fig.3.10 and Fig.3.11. Note that the variation of the temperature states results in significant fluctuation and drop of the output torque for the open-loop system.

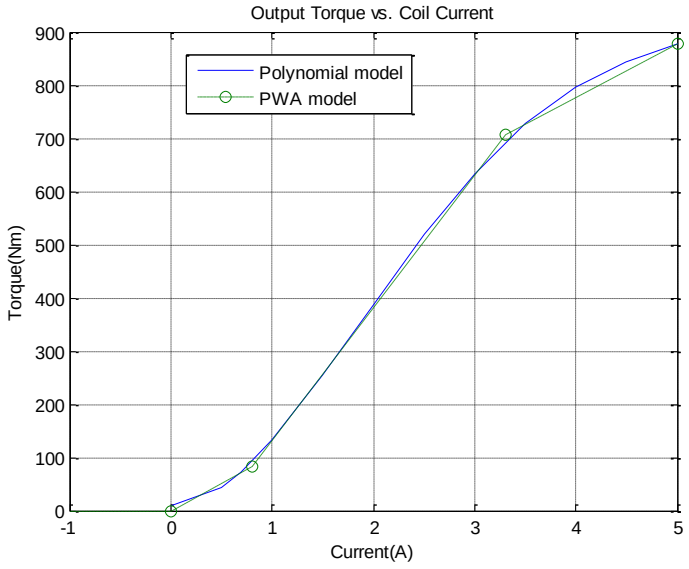

Fig. 3.8 Nonlinear torque model vs. piecewise affine approximation

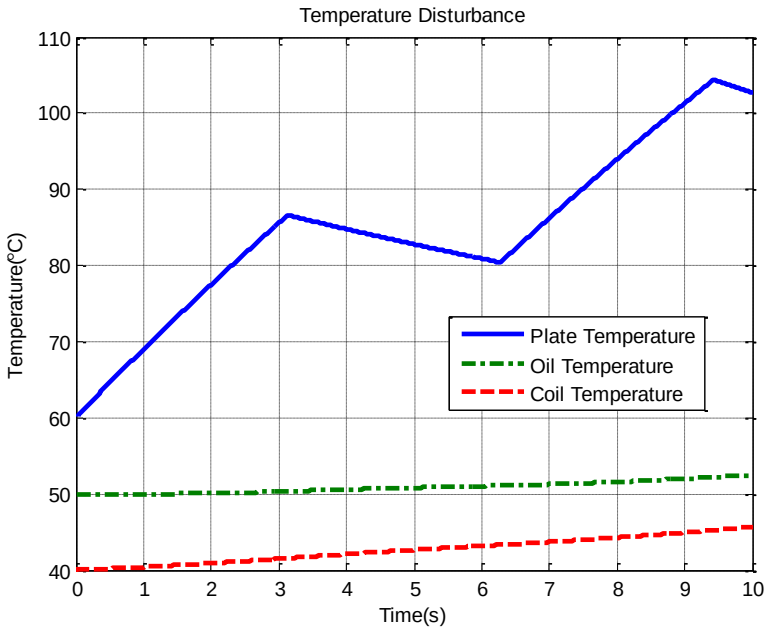

Fig. 3.9 Simulated temperature fluctuation

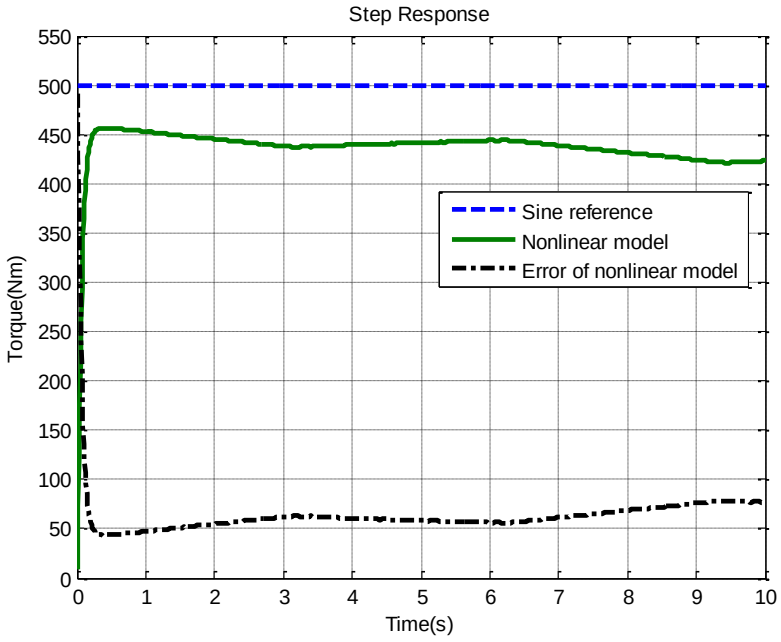

Fig. 3.10 Step response of the open-loop system

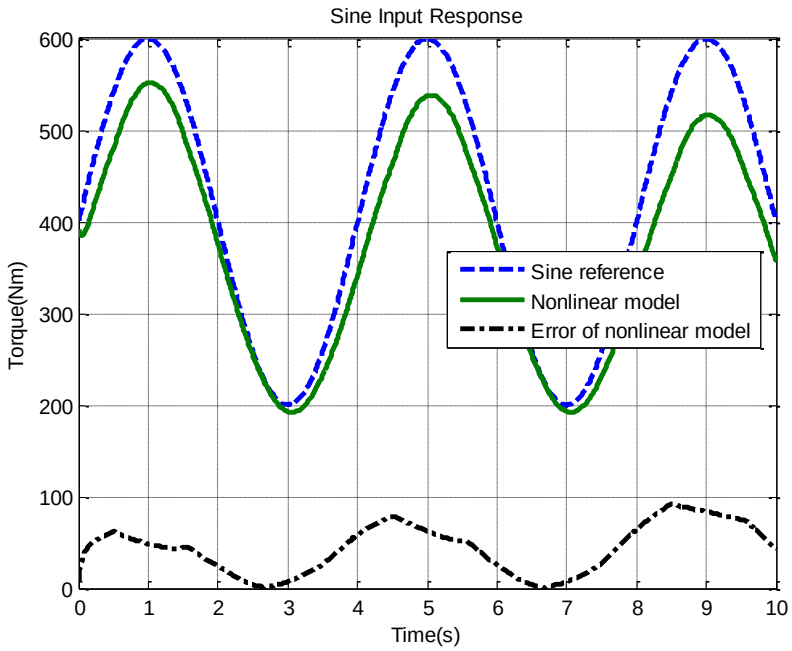

Fig. 3.11 Open-loop system responses under a sine input signal

3.4.2 Closed-Loop System

The feed forward controller is calibrated using the parameters listed in Section 3.4.1. For the feedback controller, the gains K_{Pi} and K_{Ii} are selected to place the eigenvalues of each region of the closed-loop system at $-21.21 \pm 21.21i$ (i.e., $\omega_n = -30$, $\xi = 0.707$) except for region 1 (saturation region), where the anti-windup control is applied and K_{Pi} is designed separately in the absence of K_{Ii}.

Table 3.2 Controller Gains for Each Region

Region	1	2	3	4
K_P^i	0.03	0.0296	0.012	0.0301
K_I^i	0	1.0597	0.426	1.0781
K_Z^i	40	0	0	0

The step response and sine input responses of the closed-loop system, under the same temperature disturbance in Fig.3.9, are provided in Fig.3.12 and Fig.3.13. As shown in these figures, the nonlinear model and the PWA model show good agreement for both cases. The feedback PI control and feed forward control help the system yield desired output and achieve fast tracking of the reference signals. The comparison between the proposed design and the current design is provided in Fig. 3.14, where the current design leads to a significant steady state error even if a large gain is used ($K_P = 0.1$ here).

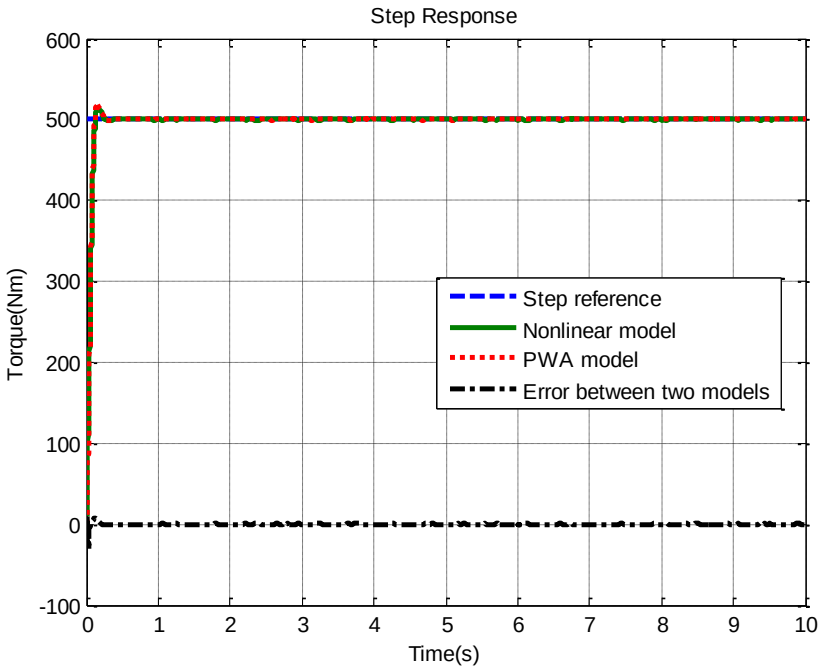

Fig. 3.12 Step response of the closed-loop system

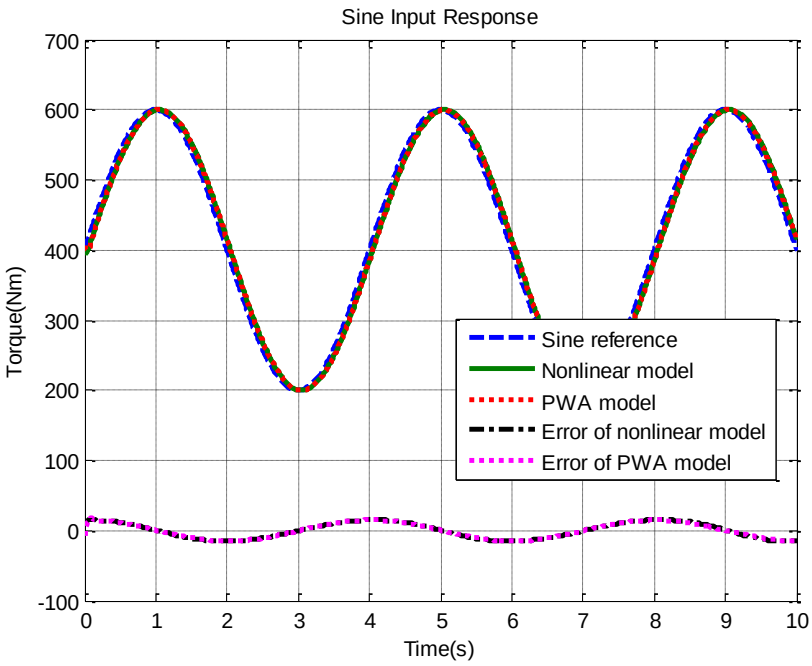

Fig. 3.13 Closed-loop system responses under a sine input signal

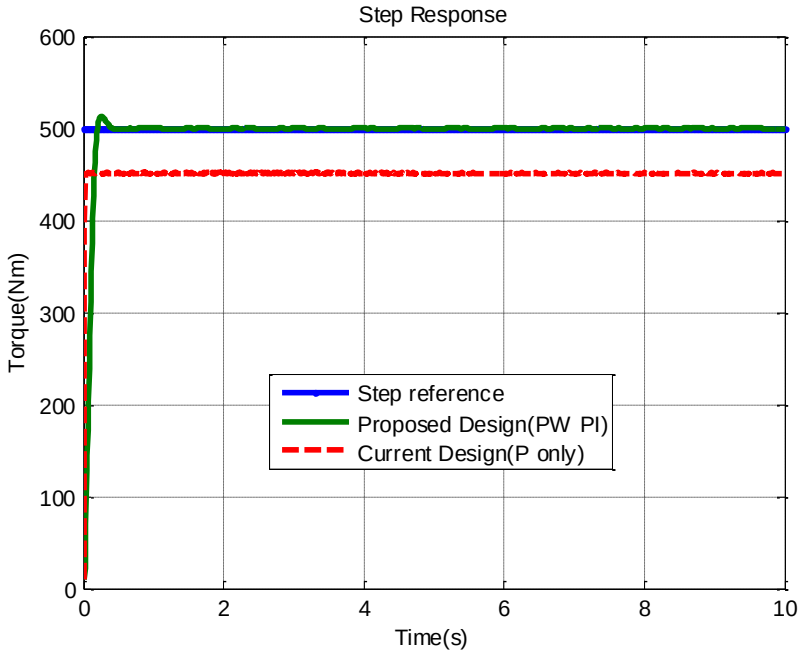

Fig. 3.14 Comparison between current design and proposed design

The feedback system is designed assuming no delays. The responses of the closed-loop system with the proposed design and different level of output delay are shown in Fig.3.15. As shown in the figure, the increase of the delay will lead to more oscillations and worse performance. Because of the delay, the rightmost eigenvalue of the system will no longer be at the original place ($-21.21 \pm 21.21i$). If the change of system dynamics is significant, instead of placing eigenvalues for the nominal ODE system in (3.26), one may directly assign the rightmost eigenvalues for the DDE system in (3.28) using existing methods (e.g., the LambertW function approach in (Yi. et al., 2010a)).

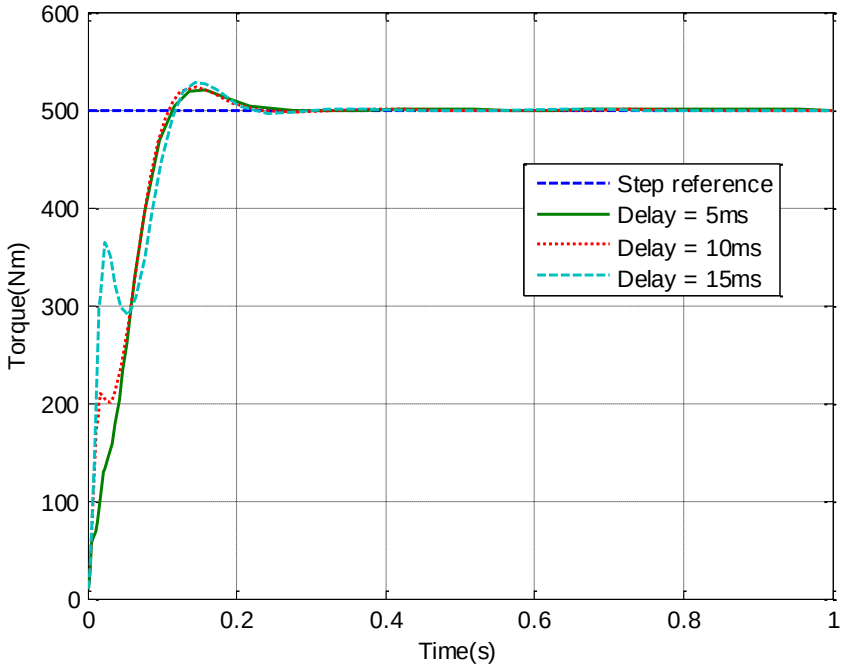

Fig. 3.15 Step responses of closed-loop systems with proposed control design and different level of delays

3.4.3 Stability Analysis

In this section, the stability of the closed-loop system will be examined to ensure system performance. Since the frequency of the reference output torque signal (usually

less than 1Hz) is typically much lower than the dynamics of the clutch system, the reference signal tracking can be treated as the shift in different steady state operating points (equilibrium points). Thus, the stability of the system about different equilibrium points is examined. Here, stability analysis is conducted for the equilibrium points $\tilde{i}_{ce} = \{0,\ 0.5,\ 1.5,\ 3.3\ , 4.2\}$ (see Appendix A), which represents the cases of at rest and in operation with different level torque requests. The final results are the lower bound of the results from these cases as shown in Table 3.3.

The stability of the nominal closed-loop system (i.e., no time delay and uncertainty in the PWA model) is verified using the criterion in Theorem 2.3. A feasible solution is obtained using the LMI toolbox in Matlab showing that the system is stable.

When uncertainty is considered in the model, the upper bound for ε is 93 from Theorem 2.3 and is larger than the actual value of 25 for this system. Thus, the stability of the PWA system with uncertainty is also verified.

When time delay in the output measurements is considered, the upper bound on delay (UBD) is found to be 0.0169s from Theorem 2.3, implying the PWA time-delay system has guaranteed stability with time delay smaller than this UBD. Further, for the system subject to both time delay and uncertainty, the UBD becomes 0.0144s for $\varepsilon = 25$.

The trade-off among delay, uncertainty and performance (location of the closed-loop eigenvalues) is provided in Fig.3.16. The bottom left area is the feasible design region with guaranteed stability. As shown in this figure, the increase in delay will reduce the maximum tolerable uncertainty for a particular control design. A larger control gain will improve the speed of the system but will make the system less robust against uncertainty

and delay. Such a map can help the selection of controller parameters to obtain a sufficiently robust system with satisfactory performance in the presence of delay.

Table 3.3 UBDs for Different Equilibrium Points

$\tilde{i}_{ce}$	0	0.5	1.5	3.3	4.2
$\varepsilon = 0$	16.9ms	16.9ms	16.9ms	17.3ms	18.5ms
$\varepsilon = 25$ (14%)	15.5ms	14.4ms	14.5ms	15.5ms	14.8ms

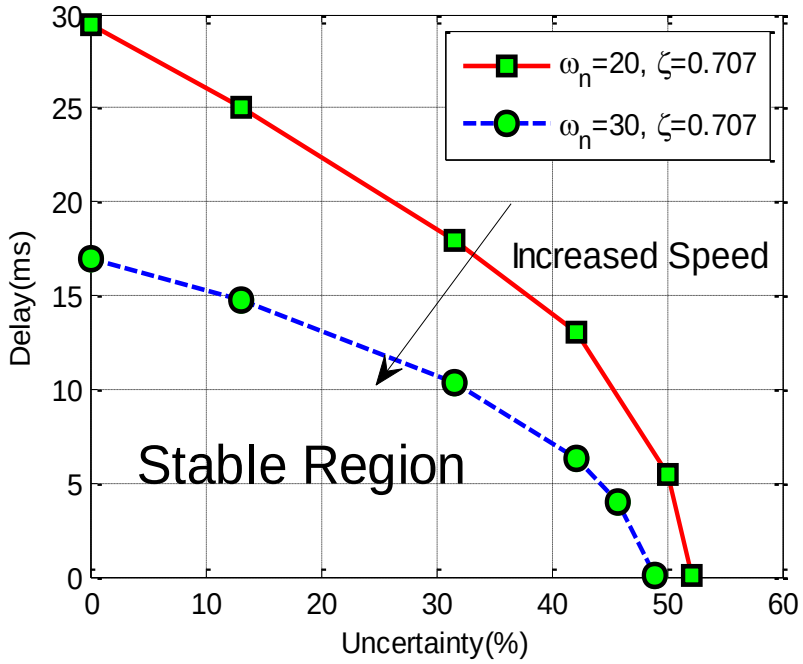

Fig. 3.16 Map of feasible design region showing the trade-off between speed of response, uncertainty and delay

3.5 Summary and Conclusions

In this chapter, a general procedure for modeling and control of nonlinear engineering systems via the PWA system framework is proposed and applied to a nonlinear

automotive clutch system. A feed forward plus piecewise PI control design based on the PWA framework is proposed to realize reference torque tracking and temperature disturbance rejection. The stability of the closed-loop PWA system is examined, with the presence of model uncertainty and time delay. Finally, simulation results for the system are provided to illustrate the effectiveness of the design.

Compared with the existing industrial design, the proposed control not only improves the output torque accuracy during reference torque tracking, but also achieves more consistent performance under different operating conditions and temperature variation. In addition, using the PWA system framework, the stability of the system is analytically studied, with consideration of uncertainty and time delay in the model, to obtain rigorous design guarantees. A feasibility map for design illustrates the trade-off among speed of response, robustness of the system, and time delay. Such a map can provide a useful guideline for practical design of the AWD clutch control system.

3.6 Acknowledgments

We would like to acknowledge the contribution from the Torque Transfer System control group at BorgWarner Inc for making available the data and the test equipment for this project.

CHAPTER 4
DECAY FUNCTION ESTIMATION FOR LINEAR TIME-DELAY SYSTEMS VIA THE LAMBERT W FUNCTION

4.1 Introduction

The stability of time-delay systems has been a problem of recurring interest over the past several decades. Time delays exist in many practical systems in engineering, biology, chemistry, physics and ecology and can lead to effects such as oscillation, instability or inaccuracy. For highway transportation systems (Orosz et al., 2010), delays from human reactions and vehicle systems are critical for analyzing traffic flow stability and designing safe flow control algorithms. In machine tool chatter problem (Nagy et al., 2001; Yi et al., 2007b), inherent delays in the milling process may lead to instability and further deteriorate surface finish. The effects of time-delay systems are also studied for teleoperation systems (Anderson & Spong, 1989), networked control systems (Murray, 2003), HIV pathogenesis (Yi et al., 2008) and automotive engine control systems (Cook & Powell, 1988). Besides these applications, fruitful results for stability criteria for time-delay systems have been analytically derived. Detailed reviews of these techniques can be found in (Gu & Niculescu, 2003; Richard, 2003).

In addition to stability criteria, a quantitative description of asymptotic behavior for time-delay systems is also valuable since it characterizes the transient response of these systems. Considerable work has been done toward deriving exponential bounds of the

form $Ke^{\alpha t}\Phi$ (see Eq. (4.2)) for the solution of time-delay systems for completely characterizing their exponential time response. Examples of such decay functions are shown in Fig.4.1, where the normed state trajectory of a second order time-delay system is bounded by the two exponential envelope functions (dotted and dash-dot line) after the system is excited by the preshape function $[1,0]^{\mathrm{T}}$ over the time interval $-h \le t \le 0$ (delay h=1 in this example). As shown in the figure, decay function 1 with better estimates of α and K yields a closer bound to the actual trajectory than decay function 2, which is more conservative. A less conservative estimate of the decay function gives a more accurate description of the system transient behavior.

Although most existing literature focuses on the estimation of decay rate, α, the estimation of K is also important. With an estimate of K, the exact value of the bound over time can be determined, which could be useful in engineering practice. For example, the decay function can be used for dwell-time control for switched time-delay systems (Chiou, 2005; S. Kim et al., 2006; Zhang et al., 2007; Yan & Ozbay, 2008), where the factor K represents the maximum energy rise during switching and α represents the energy decay rate. An application to a distributed cart pendulum control system with delay is given in (Chen & Zhang, 2010) showing that the system can still be stable if the control loop is opened with low frequency and small time period. Some applications to engineering systems can be found in power systems (Meyer et al., 2004) and networked control systems (Kim et al., 2004; Dai et al., 2009b). Less conservative estimate of the decay function will lead to more effective control design (e.g., lower bound on dwell time) for these applications.

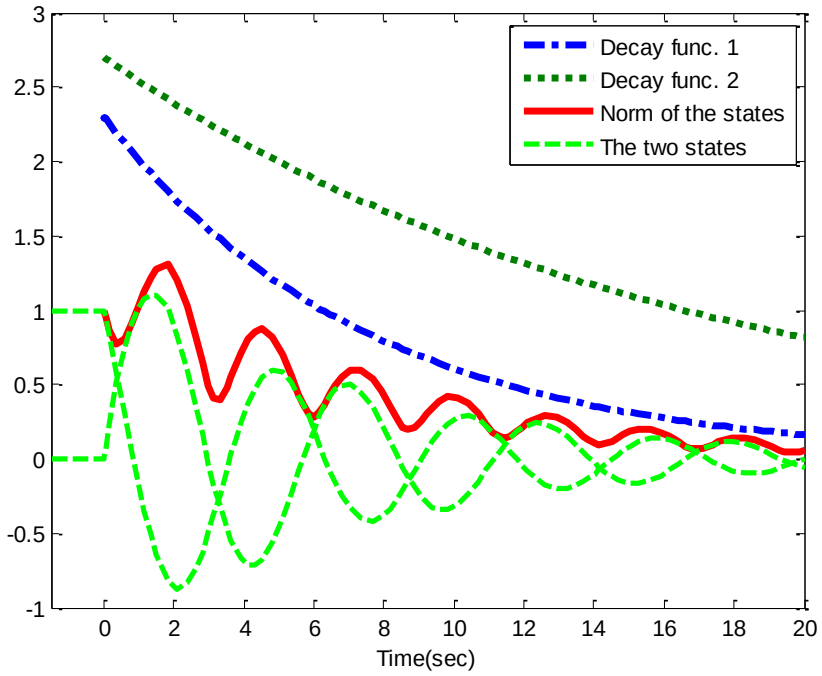

Fig. 4.1 An example of decay functions for a second order time-delay system $\dot{\mathbf{x}}(t)+\mathbf{A}\mathbf{x}(t)+\mathbf{A}_\mathbf{d}\mathbf{x}(t-h)=0$ with $\mathbf{A}$ = [0 1;-1.25 -1], $\mathbf{A}_\mathbf{d}$=[-0.1 0.6;0.2 0], h=1 and $\mathbf{g}(t)$=[0 1]^T for $t\leq 0$

A variety of approaches have been proposed for α-stability, i.e., the dominant (slowest) decay rate of time-delay systems. Methods based on the Bellman-Gronwall Lemma and matrix measure/norm have been proposed in (Mori et al., 1982, 1989a, 1989b; Bourlès, 1987; Lehman & Shujaee, 1994; Niculescu et al., 1998). Methods based on Lypapunov's second method, such as Lyapunov-Krasovskii functional based approaches (Niculescu et al., 1998; Mondié & Kharitonov, 2005; Xu et al., 2006; Kacem et al., 2009), Lyapunov-Razumikhin functional based approaches (Hou & Qian, 1998, Jankovic, 2001) and Riccati equation approaches (Phat & Niamsup, 2006) have also been proposed. Methods using the Hopf Bifurcation Theorem are proposed in (Kalmar-Nagy et al., 2001; Engelborghs et. al., 2001; Fofana, 2003; Forde & Nelson, 2004). In (Sipahi &

Olgac, 2003), a method based on examining one infinite cluster of roots at a time has been developed. Methods using pseudospectral and operator approximation techniques are proposed in (Bred, et al., 2005; Michiels et. al., 2006).

Although fruitful results for α-stability of time-delay systems have been obtained, the methods for a complete estimation of the decay function are limited. The estimation of K requires knowledge of the system trajectory over time, since such an exponential function needs to bound the states for any $t>0$. Although it is feasible to approximate the optimal decay rate, i.e., the optimal α, using some frequency domain approaches (e.g., finite dimensional approximation or bifurcation), these cannot provide an estimate of K. One needs the information in the time domain to determine both α and K simultaneously.

However, current time domain approaches, such as the aforementioned matrix measure/norm approaches and Lyapunov approaches, have inherent conservativeness, which limits their performance in obtaining optimal estimate. For example, the estimates of α from these approaches can never reach the optimal value. The estimate of K is also difficult to optimize in the Lyapunov approaches.

In (Yi et al., 2007a), a closed-form solution for the system of delay differential equations (DDEs) in (1) has been derived in terms of an infinite series based on the Lambert W function. These results have recently been extended to solve eigenvalue assignment (Yi et al., 2010a, 2010b) and stability problem (Yi et al., 2007b) for time-delay systems. Using this solution form, the trajectory of systems of DDEs can be explicitly determined in terms of system parameters and preshape functions via the Lambert W function. Following these results, an optimal estimate of the decay rate α can be obtained. The estimation of a corresponding K associated with this optimal α can be

derived analytically by numerically evaluating the infinite series, which may be more efficient than solving the optimization problems in Lyapunov approaches.

A novel approach, based on the Lambert W function, to estimate the decay function for characterizing the exponential nature of the solution of time-delay systems is presented. An optimal estimate of the decay rate, α, and an estimate of the associated factor, *K*, are derived. In Section 4.2, the problem is formulated. In Section 4.3, the method based on the Lambert W function is presented, followed by numerical examples in Section 4.4. A summary and concluding remarks are provided in Section 4.5.

4.2 Problem Formulation

Consider the continuous linear time invariant (LTI) homogeneous time-delay system (TDS):

$$\begin{aligned} &\dot{\mathbf{x}}(t) + \mathbf{A}\mathbf{x}(t) + \mathbf{A_d}\mathbf{x}(t-h) = 0, \quad t > 0 \\ &\mathbf{x}(0) = \mathbf{x}_0, \quad \mathbf{x}(t) = \mathbf{g}(t) \quad \text{for } t \in [-h, 0) \end{aligned} \tag{4.1}$$

where $\mathbf{A}$ and $\mathbf{A_d}$ are $n \times n$ coefficient matrices, $\mathbf{x}(t)$ is an $n \times 1$ state vector, $\mathbf{g}(t)$ is an $n \times 1$ preshape function, *t* is time, and *h* is a constant scalar time delay. A discontinuity is permitted at $t = 0$ when $\mathbf{g}(0^-) \neq \mathbf{x}(0) = \mathbf{x}_0$. The goal is to find an upper bound for the decay rate, which is referred to as α -stability, as well as an upper bound for the factor K, such that the norm of the states is bounded:

$$\left\|\mathbf{x}(t)\right\| \leq Ke^{\alpha t}\Phi(h) \tag{4.2}$$

where $\Phi(h) = \sup_{-h \leq t \leq 0} \{\left\|\mathbf{x}(t)\right\|\}$ and $\|\cdot\|$ denotes the 2-norm. The conditions for the existence of *K* and α have been discussed in (Hale et al., 1993).

It is important to point out that K and α are paired and cannot be estimated separately. Although there exist some frequency domain approaches to approximate the optimal α, an estimate of the corresponding K is not provided in those approaches. For a given α, it is not feasible to obtain the K using simulations since the preshape function $\mathbf{g}(t)$ and the initial condition $\mathbf{x}_0$ cannot be uniquely determined knowing only the bound of $\|\mathbf{x}(t)\|$ for $t \in [-h, 0]$. The difficulty is to find an envelope function that bounds the norm of the states for any time $t>0$ and for any possible preshape functions and initial conditions.

When $h = 0$, one has $\mathbf{A_d} = 0$ and the delay differential equation (DDE) in (1) reduces to an ordinary differential equation (ODE), whose decay function is

$$\|\mathbf{x}(t)\| \le e^{\mu(\mathbf{A})t} \|\mathbf{x}(0)\| \tag{4.3}$$

where $\mu(\mathbf{A}) = \lim_{\theta \to 0^+} \dfrac{\|\mathbf{I} + \theta\mathbf{A}\| - 1}{\theta}$ is the matrix measure (Hale et al., 1993).

In the presence of time delay, the problem becomes much more complex since the trajectory of time-delay systems depends not only on the initial states $\mathbf{x}_0$, but also on the preshape function $\mathbf{g}(t)$. Existing approaches lead to an estimate of the decay function with significant conservativeness. For example, the result from the matrix norm approach (Hale et al., 1993) yields the estimates

$$K = 1 + \|\mathbf{A_d}\| h, \;\; \alpha = \|\mathbf{A}\| + \|\mathbf{A_d}\| \tag{4.4}$$

where the estimate of α can only be positive. For the matrix measure approaches (Lehman & Shujaee, 1994; Niculescu et al., 1998), K is fixed to be 1, which renders the estimation of α very conservative. For example, consider the trajectory of the system shown in Fig.4.1. If K equals 1, the decay function has a value of 1 at t=0. Then α must

be positive for the decay function to bound the peak of the normed state trajectory at t=2s. However, the optimal α is obviously a negative number.

Alternatively, one can apply Lyapunov approaches to solve the problem computationally. Using the classical Lyapunov-Krasovskii methods, the estimates of K and α can be obtained as

$$K = \sqrt{\frac{c_2}{c_1}},\ \alpha = -c_3 \tag{4.5}$$

assuming the existence of positive constant scalars c_1 , c_2 , c_3 such that

$$c_1 \left\|\mathbf{x}(t)\right\|^2 \le V(\mathbf{x}_t) \le c_2 \left\|\mathbf{x}_t\right\|^2 \tag{4.6}$$

and

$$\dot{V}(\mathbf{x}_t) \le -2c_3 \left\|\mathbf{x}(t)\right\|^2 \tag{4.7}$$

where $\mathbf{x}_t$ denotes the segment of $\{\mathbf{x}(t+\theta)\big|\theta \in [-h, 0]\}$ and $V(\cdot)$ is a Lyapunov-Krasovskii functional. Because of the inherent conservativeness of the Lyapunov approaches, the decay rate estimate, c_3, will not be able to reach the optimal value. The estimate of K, i.e., $\sqrt{\frac{c_2}{c_1}}$, is also difficult to optimize.

From the solution form in (Yi, Nelson & Ulsoy, 2007a), the relationship between the trajectory of the system in (1) and the preshape function as well as initial conditions can be analytically determined in terms of an infinite Lambert W function series. We intend to overcome, or reduce, the inherent conservativeness in matrix measure/norm approaches and Lyapunov approaches and investigate the decay function estimation

problem from a new and different point of view by applying the Lambert W function approach.

4.3 Main Results

Consider the homogenous matrix DDE in (4.1). The solution of (4.1) can be written as (Yi et al., 2006),

$$x(t) = \sum_{k=-\infty}^{\infty} e^{\mathbf{S}_k t}\mathbf{C}_k^I \tag{4.8}$$

where

$$\mathbf{S}_k = \frac{1}{h}\mathbf{W}_k(-\mathbf{A_d}h\mathbf{Q}_k) - \mathbf{A} \tag{4.9}$$

and $\mathbf{Q}_k$ is solved by the following condition

$$\mathbf{W}_k(-\mathbf{A_d}h\mathbf{Q}_k)e^{\mathbf{A}e^{\mathbf{W}_k(-\mathbf{A_d}h\mathbf{Q})-\mathbf{A}h}} = -\mathbf{A_d}h \tag{4.10}$$

Here $\mathbf{S}_k$ and $\mathbf{Q}_k$ are $n\times n$ matrices. $\mathbf{C}_k^I$ are $n\times 1$ vectors and are determined by the preshape function $\mathbf{g}(t)$ and $\mathbf{x}_0$, by using either one of two different approaches (Yi et al., 2006, 2007b). The matrix Lambert W function, $\mathbf{W}_k(\cdot)$, is a complex valued function with a complex matrix argument $\mathbf{z}$ and an infinite number of branches denoted by *k*, where $k = -\infty,...,-1,0,1,...,\infty$ and satisfies $\mathbf{W}_k(\mathbf{z})e^{\mathbf{W}_k(\mathbf{z})} = \mathbf{z}$ for all branches. Note that $\mathbf{W}_k$ can readily be evaluated using functions available in standard software packages such as Matlab or Mathematica. The conditions for the existence and uniqueness of the solution in (4.9) are discussed in (Bellman & Cooke, 1963).

The results in (Yi et al., 2006) are extended here to derive a general solution (see Appendix B) to show that the solution of (4.1) can be written as,

$$\mathbf{x}(t) = \underbrace{\sum_{k=-\infty}^{\infty} \left\{ e^{\mathbf{S}_k t} (\sum_{j=1}^{n} \mathbf{T}_{kj}^{I} \mathbf{L}_{kj}^{I}) \mathbf{x}_0 \right\}}_{P_1} - \underbrace{\sum_{k=-\infty}^{\infty} \left\{ e^{\mathbf{S}_k t} \sum_{j=1}^{n} (\mathbf{T}_{kj}^{I} \mathbf{L}_{kj}^{I} \mathbf{A}_{\mathbf{d}} \mathbf{G}(\lambda_{kj})) \right\}}_{P_2} \tag{4.11}$$

where

$$\lambda_{kj} = eig(\mathbf{S}_k), \;\; j = 1, 2, ..., n \tag{4.12}$$

$$\mathbf{G}(\lambda_{kj}) = \int_0^h e^{-\lambda_{kj}\tau} \mathbf{g}(\tau - h) d\tau \tag{4.13}$$

$$\mathbf{L}_{kj}^{I} = \lim_{s \to \lambda_{kj}} \left\{ \frac{\frac{\partial}{\partial s} \prod_{j=1}^{n} (s - \lambda_{kj})}{\frac{\partial}{\partial s} \det(s\mathbf{I} + \mathbf{A} + \mathbf{A}_{\mathbf{d}} e^{-sh})} adj(s\mathbf{I} + \mathbf{A} + \mathbf{A}_{\mathbf{d}} e^{-sh}) \right\} \tag{4.14}$$

$$\tilde{\mathbf{R}}_k^{I+} = \begin{bmatrix} \mathbf{T}_{k1}^{I} & \mathbf{T}_{k2}^{I} & ... & \mathbf{T}_{kn}^{I} \end{bmatrix} = \tilde{\mathbf{R}}_k^{I*} (\tilde{\mathbf{R}}_k^{I} \tilde{\mathbf{R}}_k^{I*})^{-1} \tag{4.15}$$

$$\mathbf{R}_{kj}^{I} = adj(\lambda_{kj}\mathbf{I} - \mathbf{S}_k), \; \tilde{\mathbf{R}}_k^{I} = \begin{bmatrix} \mathbf{R}_{k1}^{I} \\ \mathbf{R}_{k2}^{I} \\ \\ \mathbf{R}_{kn}^{I} \end{bmatrix} \tag{4.16}$$

Note that $\tilde{\mathbf{R}}_k^{I+}$ is the $n \times n^2$ Moore-Penrose Generalized Inverse, $\tilde{\mathbf{R}}_k^{I*}$ is the $n \times n^2$ conjugate transpose of $\tilde{\mathbf{R}}_k^{I}$ and $\mathbf{T}_{kj}^{I}$ is the j^{th} square block of $\tilde{\mathbf{R}}_k^{I+}$.

Theorem 4.1: If there exist scalars α, K_1, K_2, K_3 and K_4 such that

$$\alpha = \max\{\text{Re}(eig(\mathbf{S}_{-m})), ..., \text{Re}(eig(\mathbf{S}_0)), ..., \text{Re}(eig(\mathbf{S}_m))\} \tag{4.17}$$

$$K_1 = \sup_{0 \le t < h} \left\| e^{(-\mathbf{A} - \alpha\mathbf{I})t} \right\| \tag{4.18}$$

$$K_2 = \lim_{N \to \infty} \left\{ \sup_{t \ge h} \left\| \sum_{k=-N}^{N} \left\{ e^{(\mathbf{S}_k - \alpha\mathbf{I})t} \sum_{j=1}^{n} \mathbf{T}_{kj}^{I} \mathbf{L}_{kj}^{I} \right\} \right\| \right\} \tag{4.19}$$

$$K_3 = \sup_{0 \le t < h} \int_0^t \left\| e^{(-\mathbf{A} - \alpha\mathbf{I})t + \mathbf{A}\tau} \mathbf{A}_{\mathbf{d}} \right\| d\tau \tag{4.20}$$

$$K_4 = \lim_{N\to\infty}\left\{\sup_{t\geq h}\int_0^h \left\| \sum_{k=-N}^{N}\left\{ e^{(\mathbf{S}_k-\alpha\mathbf{I})t}\sum_{j=1}^{n}(\mathbf{T}_{kj}^{I}\mathbf{L}_{kj}^{I}\mathbf{A}_{\mathbf{d}}e^{\lambda_{ki}\tau})\right\}\right\| d\tau\right\} \tag{4.21}$$

where $m = \text{nullity}(\mathbf{A_d})$ and $eig(\mathbf{S}_i)$ are the eigenvalues of $\mathbf{S}_i$. Then, the trajectories of (4.1) are bounded by the exponential function $\|\mathbf{x}(t)\| \leq Ke^{\alpha t}\Phi(h)$ for any time $t>0$, where $\Phi(h) = \sup_{-h\leq t\leq 0}\{\|\mathbf{x}(t)\|\}$ and $K = \max(K_1, K_2) + \max(K_3, K_4)$.

Proof of Theorem 4.1

Estimation of Decay Rate α

For the scalar case of (4.1), the rightmost eigenvalue can be determined by the principal branch, i.e., $k = 0$, of the scalar Lambert W function. Such a proof can readily be extended to the matrix case when $\mathbf{A}$ and $\mathbf{A_d}$ in (4.1) commute (Jarlebring & Damm, 2007). No such proof is currently available for the general case of matrix DDEs. However, in all the examples considered in the literature, it has been observed that the rightmost eigenvalue is obtained using the first m branches, where m is the nullity of $\mathbf{A_d}$ (Yi et al., 2010c). We state this here as a conjecture:

$$\max\{\text{Re}(eig(\mathbf{S}_{-m})),...,\text{Re}(eig(\mathbf{S}_0)),...,\text{Re}(eig(\mathbf{S}_m))\} \geq \max\left\{\text{Re}(eig(\mathbf{S}_i))\right\},\ \forall i \tag{4.22}$$

where $m = Nullity(\mathbf{A_d})$ and $eig(\mathbf{S}_i)$ are the eigenvalues of $\mathbf{S}_i$. Thus, based on the above conjecture, the optimal decay rate for matrix DDEs can be calculated as (4.17).

Estimation of Factor K

Having determined α using (4.17), one must then determine the factor K such that $\|x(t)\| \leq Ke^{\alpha t}\Phi$, where $\Phi = \sup_{-h\leq t\leq 0}\|x(t)\|$. Taking the norm of both sides of (4.11) yields

$$\left\|\mathbf{x}(t)\right\| \le \left\|\mathbf{P}_1(t)\right\| + \left\|\mathbf{P}_2(t)\right\| \tag{4.23}$$

where $\mathbf{P}_1(t)$ and $\mathbf{P}_2(t)$ have been defined in (4.11). The use of the inequality in (4.23) will introduce conservativeness in our results. Since the envelope function should bound any possible trajectory, one must separate $\left\|\mathbf{x}_0\right\|$ and $\left\|\mathbf{g}(\cdot)\right\|$ out from the infinite series but without affecting convergence.

First, note that for $t \in [0, h)$, the state $\mathbf{x}(t-h)$ in matrix DDEs is solely determined by the preshape function. Thus, for this period, the homogeneous matrix DDE function can be treated as a matrix ODE with an input from the preshape function:

$$\dot{\mathbf{x}}(t) + \mathbf{A}\mathbf{x}(t) = -\mathbf{A}_\mathbf{d}\mathbf{g}(t-h) \tag{4.24}$$

Therefore, for $t \in (0, h)$, $\mathbf{P}_1(t)$ equals the free response of (4.24) with $\mathbf{x}(0) = \mathbf{x}_0$ and $\mathbf{P}_2(t)$ can be treated as the forced response of (4.24) with the input $\mathbf{g}(t-h)$. Thus, for this period, the bounds for $\left\|\mathbf{P}_1(t)\right\|$ and $\left\|\mathbf{P}_2(t)\right\|$ can be obtained as,

$$\left\|\mathbf{P}_1(t)\right\| \le \left\|e^{(-\mathbf{A}-\alpha\mathbf{I})t}\mathbf{x}_0\right\| e^{\alpha t} \le K_1 e^{\alpha t}\Phi,\ t \in [0, h) \tag{4.25}$$

$$\begin{aligned} \left\|\mathbf{P}_2(t)\right\| &\le \int_0^t \left\|-e^{-\mathbf{A}(t-\tau)}\mathbf{A}_\mathbf{d}\right\| \cdot \left\|\mathbf{g}(\tau-h)\right\| d\tau \\ &\le \int_0^t \left\|-e^{(-\mathbf{A}-\alpha\mathbf{I})t+\mathbf{A}\tau}\mathbf{A}_\mathbf{d}\right\| \cdot \left\|\mathbf{g}(\tau-h)\right\| e^{\alpha t} d\tau \le K_1 e^{\alpha t}\Phi,\ t \in [0, h) \end{aligned} \tag{4.26}$$

where K_1 and K_3 are defined in (4.18) and (4.20) respectively.

For $t \in [h, \infty)$, the Lambert W function method is applied. Note that,

$$\begin{aligned} \left\|\mathbf{P}_1(t)\right\| &= \lim_{N\to\infty} \left\| \sum_{k=-N}^{N} \left\{ e^{(\mathbf{S}_k-\alpha\mathbf{I})t} \sum_{j=1}^{n} \mathbf{T}_{kj}^I \mathbf{L}_{kj}^I \mathbf{x}_0 \right\} \right\| e^{\alpha t} \\ &\le \lim_{N\to\infty} \left\{ \sup_{t\ge h} \left\| \sum_{k=-N}^{N} \left\{ e^{(\mathbf{S}_k-\alpha\mathbf{I})t} \sum_{j=1}^{n} \mathbf{T}_{kj}^I \mathbf{L}_{kj}^I \right\} \right\| \right\} e^{\alpha t} \left\|\mathbf{x}_0\right\|,\ \ t \in [h, \infty) \end{aligned} \tag{4.27}$$

Thus, if K_2 in (4.19) exists, $\|\mathbf{P}_1(t)\| \le K_2 e^{\alpha t}\Phi$ for $t \in [h,\infty)$ will be satisfied since $\Phi = \sup_{-h\le t\le 0} \|\mathbf{x}(t)\| \ge \|\mathbf{x}(0)\|$. Similarly,

$$\begin{aligned}\|\mathbf{P}_2(t)\| &= \lim_{N\to\infty}\left\{\left\|\sum_{k=-N}^{N}\left\{e^{(\mathbf{S}_k-\alpha\mathbf{I})t}\sum_{j=1}^{n}(\mathbf{T}_{kj}^I\mathbf{L}_{kj}^I\mathbf{A}_{\mathbf{d}}\int_0^h e^{\lambda_{ki}\tau}\mathbf{g}(\tau-h)d\tau)\right\}\right\|\right. \\ &\le \lim_{N\to\infty}\left\|\int_0^h\left\{\sum_{k=-N}^{N}\left\{e^{(\mathbf{S}_k-\alpha\mathbf{I})t}\sum_{j=1}^{n}(\mathbf{T}_{kj}^I\mathbf{L}_{kj}^I\mathbf{A}_{\mathbf{d}}e^{\lambda_{ki}\tau})\right\}\right\}\mathbf{g}(\tau-h)d\tau\right\|e^{\alpha t},\quad t\in[h,\infty)\end{aligned} \tag{4.28}$$

Switch the sequence of integration and obtaining the norm, and move $\|\mathbf{g}(t-h)\|$ outside of the integration:

$$\|\mathbf{P}_2(t)\| \le \lim_{N\to\infty}\left\{\sup_{t\ge h}\int_0^h\left\|\sum_{k=-N}^{N}\left\{e^{(\mathbf{S}_k-\alpha\mathbf{I})t}\sum_{j=1}^{n}(\mathbf{T}_{kj}^I\mathbf{L}_{kj}^I\mathbf{A}_{\mathbf{d}}e^{\lambda_{ki}\tau})\right\}\right\|d\tau\cdot\|\mathbf{g}(\tau-h)\|\right\} \tag{4.29}$$

Thus, if K_4 in (4.21) exists, then $\|\mathbf{P}_2(t)\| \le K_4 e^{\alpha t}\Phi$ for $t \in [h,\infty)$ will hold since $\Phi = \sup_{-h\le t\le 0} \|\mathbf{x}(t)\| \ge \|\mathbf{g}(t-h)\|$ for $t \in [0,h)$.

Hence the proof.

Remark 1: The Lambert W function approach provides a solution in terms of infinite series. The feasibility of the approach depends on the convergence of the series. The proof for the convergence of such a Lambert W function series is currently not available. However, one can still evaluate the series numerically to obtain the estimate of *K*. The procedure is demonstrated in the numerical examples in Section 4.

Remark 2: It has been observed that, although the Lambert W function series may converge slowly at $t = 0^+$, the convergence speed increases quickly when *t* becomes larger. Since the DDE can be treated as an ODE for $t \in [0,h)$, the Lambert W function approach is applied for $t \ge h$ to achieve better convergence.

Remark 3: Since the envelope function needs to bound any possible trajectories, one must separate $\|\mathbf{x}_0\|$ and $\|\mathbf{g}(\cdot)\|$ out from the infinite series but without affecting convergence. Thus, in (4.29) the sequence of integration and obtaining the norm is switched before moving $\|\mathbf{g}(t-h)\|$ outside of the integration.

Remark 4: Note that the estimates of K_1, K_2, K_3 and K_4 are obtained directly based on the solution of the system and no conservativeness is introduced following the proposed procedure. However, the use of the solution form in (4.11) accommodates the discontinuity at $t = 0$ (i.e., $\mathbf{g}(0^-) \neq \mathbf{x}(0) = \mathbf{x}_0$) but introduces conservativeness when the triangle inequality (4.23) is applied. When such a discontinuity is considered, the estimate of K from our approach is the optimal.

Theorem 4.1 gives the result for general systems of DDEs. For the scalar case, the results can be further simplified. Consider the scalar version of (4.1):

$$\begin{aligned} &\dot{x}(t) + ax(t) + a_d x(t-h) = 0, \quad t > 0 \\ &x(t) = g(t), \quad t \in [-h, 0); \quad x(0) = x_0, \quad t = 0 \end{aligned} \tag{4.30}$$

where a, a_d, h are all scalar constants, t is time, and $x(t)$, $g(t)$ are scalar functions.

Corollary 4.1: If there exist scalar α, K_1, K_2, K_3 and K_4 such that

$$\alpha = \mathrm{Re}\left[\frac{W_0(-a_d h e^{ah})}{h} - a\right] \tag{4.31}$$

$$K_1 = \sup_{0 \le t < h} \left\| e^{(-a-\alpha\mathbf{I})t} \right\| = \begin{cases} e^{(-a-\alpha)h}, & -a > \alpha \\ 1, & -a \le \alpha \end{cases} \tag{4.32}$$

$$K_2 = \lim_{N \to \infty} \left\{ \sup_{t \ge h} \left\| \sum_{k=-N}^{N} \frac{e^{(S_k - \alpha)t}}{1 - a_d h e^{-S_k h}} \right\| \right\} \tag{4.33}$$

$$K_3 = \sup_{0\le t<h} \int_0^t \left\| e^{(-a-\alpha)t+a\tau} a_d \right\| d\tau = \left\| \frac{a_d(1-e^{-ah})e^{-\alpha h}}{a} \right\| \tag{4.34}$$

$$K_4 = \lim_{N\to\infty} \left\{ \sup_{t\ge h} \int_0^h \left\| \sum_{k=-N}^{N} \frac{a_d e^{-S_k\tau}}{1-a_d h e^{-S_k h}} e^{(S_k-\alpha)t} \right\| d\tau \right\} \tag{4.35}$$

Then, the trajectories of (4.30) are bounded by the exponential function $\|x(t)\| \le Ke^{\alpha t}\Phi(h)$ for any time $t>0$, where $\Phi(h) = \sup_{-h\le t\le 0} \{\|x(t)\|\}$.

Proof of Corollary 4.1

The solution of (4.30) can be written in terms of the Lambert W function, W_k (Asl & Ulsoy, 2003), as:

$$x(t) = \sum_{k=-\infty}^{\infty} C_k^I e^{S_k t},\ S_k = \frac{1}{h} W_k(-a_d h e^{ah}) - a \tag{4.36}$$

Following the Laplace transformation based method in (Yi et al., 2006) for determining C_k^I in (4.36) gives

$$C_K^I = \frac{x_0 - a_d \int_0^h e^{-S_k t} g(t) dt}{1 - a_d h e^{-S_k h}} \tag{4.37}$$

Note that the free response $x(t)$, using (4.36) and (4.37), can be separated into two parts:

$$x(t) = \underbrace{\sum_{k=-\infty}^{\infty} \frac{x_0 e^{S_k t}}{1-a_d h e^{-S_k h}}}_{P_1(t)} - \underbrace{\sum_{k=-\infty}^{\infty} \frac{a_d \int_0^h e^{-S_k\tau} g(\tau-h) d\tau}{1-a_d h e^{-S_k h}} e^{S_k t}}_{P_2(t)} \tag{4.38}$$

One can then follow a similar procedure as for the proof of Theorem 4.1 to complete the proof for the scalar case.

4.4 Numerical Examples

In this section, one scalar example and one matrix example are provided to demonstrate the effectiveness of the proposed approach.

Example 4.1 (Scalar DDE): Consider the scalar DDE in (4.30) with $a = a_d = h = 1$ (Yi et al., 2006):

$$\dot{x}(t) + x(t) + x(t-1) = 0, \quad t > 0 \tag{4.39}$$

Note that the exact value of $g(t)$ and x_0 is not needed here but their supremum is known as $\Phi(h) = \sup_{-h \le t \le 0} \{\|x(t)\|\}$. The obtained decay function applies to any $g(t)$ and x_0 for the system.

From (4.31), the rightmost pole is found to be:

$$\alpha = \mathrm{Re}\left[\frac{W_0(-a_d h e^{ah})}{h} - a \right] = -0.605 \tag{4.40}$$

Thus, the decay rate $\alpha = -0.605$ is obtained. Next, (4.32), (4.33), (4.34) and (4.35) are used to calculate K_1, K_2, K_3 and K_4 respectively. To facilitate the process, define

$$J_1(t) = e^{(-a-\alpha)t}, \ t \in [0, h) \tag{4.41}$$

$$J_2(N,t) = \left\| \sum_{k=-N}^{N} \frac{e^{(S_k - \alpha)t}}{1 - a_d h e^{-S_k h}} \right\|, \ t \in [h, \infty) \tag{4.42}$$

$$J_3(t) = \left\| \frac{a_d (1 - e^{-ah}) e^{-\alpha h}}{a} \right\|, \ t \in [0, h) \tag{4.43}$$

$$J_4(N,t) = \int_0^h \left\{ \left\| \sum_{k=-N}^{N} \frac{a_d e^{-S_k \tau}}{1 - a_d h e^{-S_k h}} e^{(S_k - \alpha)t} \right\| \right\} d\tau, \ t \in [h, \infty) \tag{4.44}$$

and note that $K_1 = \sup_{0 \le t < h} J_1(t)$, $K_2 = \lim_{N\to\infty}\left\{\sup_{t \ge h} J_2(N,t)\right\}$, $K_3 = \sup_{0 \le t < h} J_3(t)$ and $K_4 = \lim_{N\to\infty}\left\{\sup_{t \ge h} J_4(N,t)\right\}$. For this example, $K_1 = J_1(0) = 1$ and $K_3 = J_3(h) = 1.1576$ are obtained. To estimate K_2, $J_2(N,t)$ in (4.42) must be evaluated for $t \ge h$ with a sufficiently large *N*. First, note that $J_2(N,t)$ approaches a constant amplitude for large t since $\max\{\mathrm{Re}(\mathbf{S}_k - \alpha)\} \le 0$ holds for any branch. Thus, it is always sufficient to examine the first several periods (e.g., $0 \le t \le 5h$ here) to obtain its maximum value. Second, it has been observed that the convergence of $J_2(N,t)$ w.r.t. N is much faster when t becomes larger. For example, here when t>1.5, $J_2(N,t)$ is very close to the final trajectory for $N \ge 10$. It is favorable to find the location of the peak with a large *N* (e.g., *N*=10 is sufficient here) first and then evaluate of $J_2(N,t)$ at this specific location with increased *N* for a better accuracy, if necessary.

Due to limited space, only the convergence for the worst case (i.e., *t*=*h*=1) is provided here in Fig.4.2. Here, we take $N = 50$ and obtain $K_2 = 0.9$ from Fig.4.3. Also note that $J_2(N,t)$ with *N*=50, *t*=*h* is very close to $J_1(t)$ with $t = h^-$, showing good consistency of the two estimates.

The convergence of $J_4(N,t)$ at t = 1 is shown in Fig.4.4. K_4 is selected by picking the maximum value along the trajectory of $J_4(N,t)$ with a sufficiently large number of branches N (e.g., N = 50 here) in Fig.4.5. It can been seen that $J_4(N,t)$ with *N*=50, *t*=*h* also coincides with $J_3(t)$ with $t = h^-$.

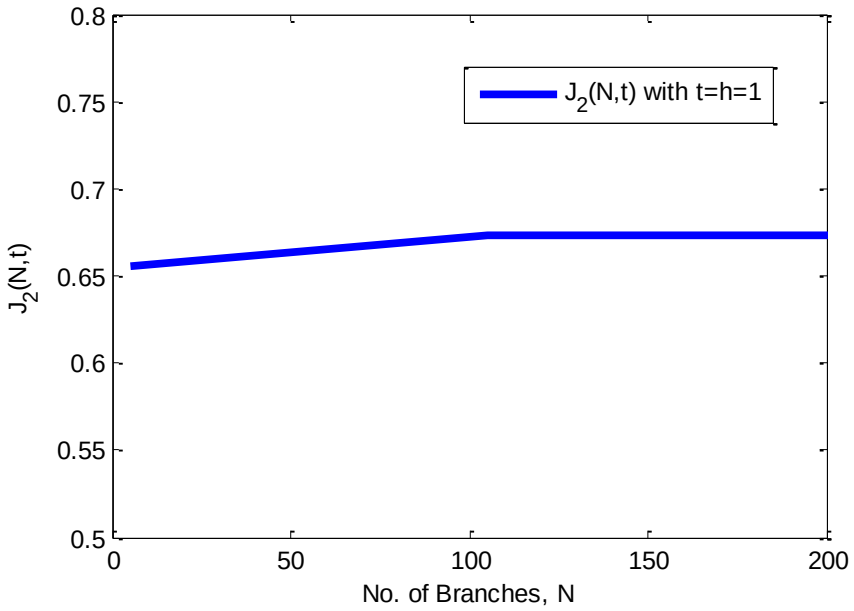

Fig. 4.2 Convergence of $J_2(N,t)$ at t=h=1 for Example 4.1

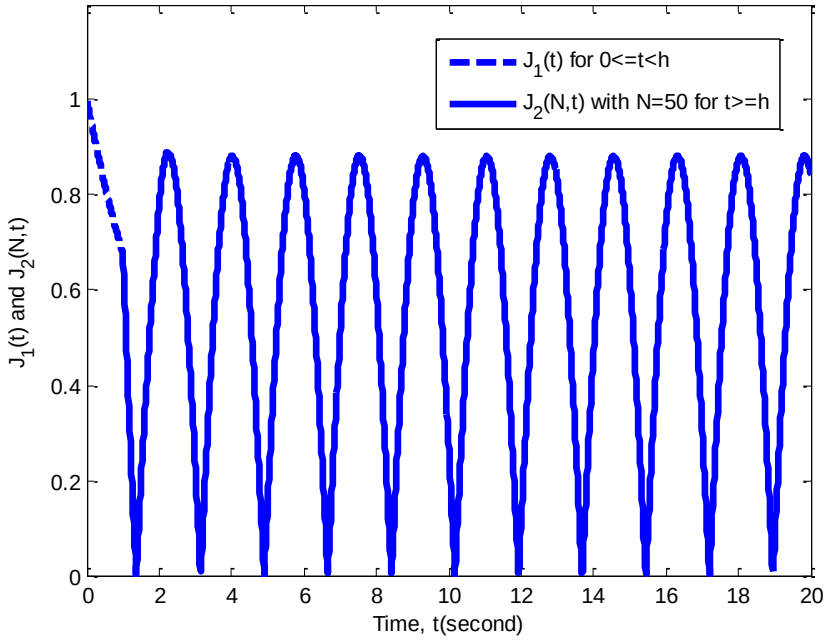

Fig. 4.3 The functions $J_1(t)$ and $J_2(N,t)$ with N=50 for Example 4.1

Consequently, one obtains

$$K_1 = 1,\ \ K_2 = 0.9,\ \ K_3 = 1.1576,\ \ K_4 = 1.16$$

and the K factor is then estimated as

$$K = \max(K_1, K_2) + \max(K_3, K_4) = 2.16$$

The decay function parameters, obtained by the methods in (Hale, 1993), in (Mondié & Kharitonov, 2005), and by using the proposed method are compared in Table 4.1. The decay rate, α, is significantly improved over the methods in (Hale et al., 1993) and (Mondié & Kharitonov, 2005). For estimating the factor, *K*, the proposed approach reaches a more conservative result in this example because we use the triangle inequality to separate P_1 and P_2 when taking the norm. Also note that the singularity at *t* = 0 (i.e., if $g(0) \neq x_0$) is considered in our approach. Such a singularity cannot be tolerated by the Lyapunov function based approaches, e.g. (Mondié & Kharitonov, 2005), since it renders the Lyapunov functions not continuously differentiable at $t = 0^+$. Although the estimate of *K* using the Lambert W function approach is larger, the exponential decay function using this new approach gives a better estimate when *t* becomes larger as the function decays exponentially.

Table 4.1 Comparison of Results for Example 4.1

	Factor, K	Decay Rate, α
Matrix Measure Approach (Hale, 1993)	2	2
Lyapunov Approach (Mondié, 2005)	1.414	-0.42
Corollary 4.1	2.16	-0.605

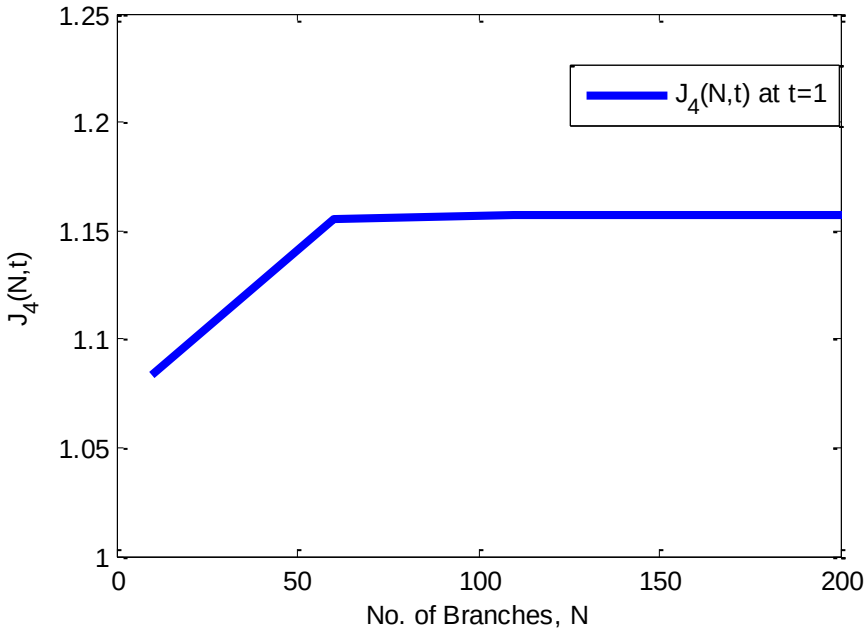

Fig. 4.4 Convergence of $J_4(N,t)$ at t=h=1 for Example 4.1

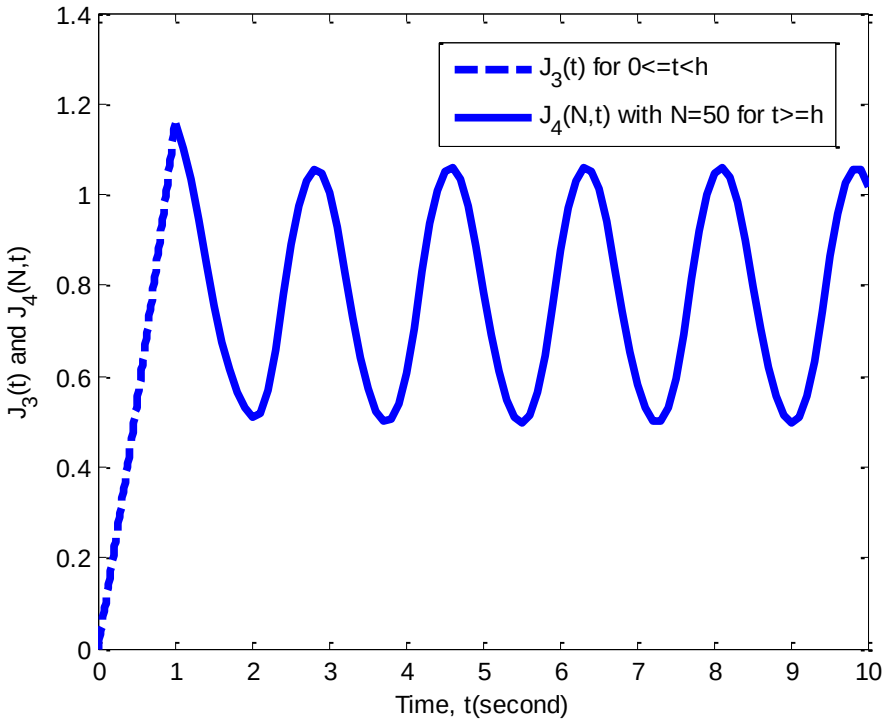

Fig. 4.5 The functions $J_3(t)$ and $J_4(N,t)$ with N = 50 for Example 4.1

Remark 5: The decay rate obtained in our proposed method is the optimal, which cannot be obtained using Lyapunov approaches and matrix measure approaches due to their conservativeness. Although only selected other approaches are compared here, the conservativeness is inherent in Lyapunov approaches and matrix measure approaches.

Example 4.2 (Matrix DDEs): Consider the example (Yi et al., 2006):

$$\begin{aligned} &\dot{\mathbf{x}}(t)+\mathbf{A}\mathbf{x}(t)+\mathbf{A}_\mathbf{d}\mathbf{x}(t-h)=0,\quad t>0 \\ &\mathbf{A}=\begin{bmatrix}1 & 3\\ -2 & 5\end{bmatrix};\ \mathbf{A}_\mathbf{d}=\begin{bmatrix}-1.66 & 0.697\\ -0.93 & 0.33\end{bmatrix};\ h=1 \end{aligned} \tag{4.45}$$

First, the Lambert W approach proposed in (Yi et al., 2006) is used to analyze the spectrum of this matrix system and locate the rightmost pole. For this example, $m=Nullity(\mathbf{A}_d)=0$ and the right most eigenvalue of the system can be obtained from the principal ($k=0$) branch. Thus,

$$\alpha=\max\left\{\mathrm{Re}(eig(\mathbf{S}_0))\right\}=\max\left\{\mathrm{Re}(eig(\frac{1}{h}\mathbf{W}_0(-\mathbf{A}_d h\mathbf{Q}_0)-\mathbf{A}))\right\}=-1.0119 \tag{4.46}$$

After the decay rate is obtained, the right-hand side of (4.18), (4.19), (4.20) and (4.21) are evaluated numerically to calculate K_1, K_2, K_3 and K_4 respectively. Similarly, define

$$J_1(t)=\left\|e^{(-\mathbf{A}-\alpha\mathbf{I})t}\right\|,\ t\in[0,h) \tag{4.47}$$

$$J_2(N,t)=\left\|\sum_{k=-N}^{N}\left\{e^{(\mathbf{S}_k-\alpha\mathbf{I})t}\sum_{j=1}^{n}\mathbf{T}_{kj}^I\mathbf{L}_{kj}^I\right\}\right\|,\ t\in[h,\infty) \tag{4.48}$$

$$J_3(t)=\int_0^t\left\|e^{(-\mathbf{A}-\alpha\mathbf{I})t+\mathbf{A}\tau}\mathbf{A}_\mathbf{d}\right\|d\tau,\ t\in[0,h) \tag{4.49}$$

$$J_4(N,t)=\int_0^h\left\|\sum_{k=-N}^{N}\left\{e^{(\mathbf{S}_k-\alpha\mathbf{I})t}\sum_{j=1}^{n}(\mathbf{T}_{kj}^I\mathbf{L}_{kj}^I\mathbf{A}_\mathbf{d}e^{\lambda_{ki}\tau})\right\}\right\|d\tau,\quad t\in[h,\infty) \tag{4.50}$$

Note that $K_1 = \sup_{0 \le t < h} J_1(t)$, $K_2 = \lim_{N \to \infty} \left\{ \sup_{t \ge h} J_2(N,t) \right\}$, $K_3 = \sup_{0 \le t < h} J_3(t)$ and $K_4 = \lim_{N \to \infty} \left\{ \sup_{t \ge h} J_4(N,t) \right\}$.

As in the scalar case, $J_2(N,t)$ in (4.48) also converges to a certain trajectory as N increases for the matrix case, as shown in Fig.4.6. Thus, K_1 is obtained by evaluating $J_1(t)$ for $0 \le t < h$ and K_2 is obtained by taking the maximum value of $J_2(N,t)$ for $t \ge h$ with a sufficiently large number of branches N (i.e., N = 50 here) as shown in Fig.4.7.

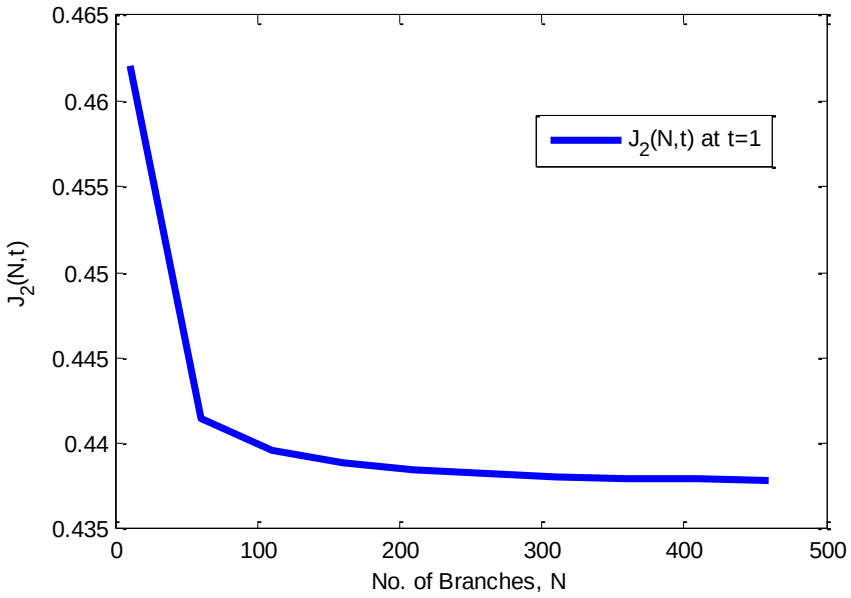

Fig. 4.6 Convergence of $J_2(N,t)$ at t=h=1 for Example 4.2

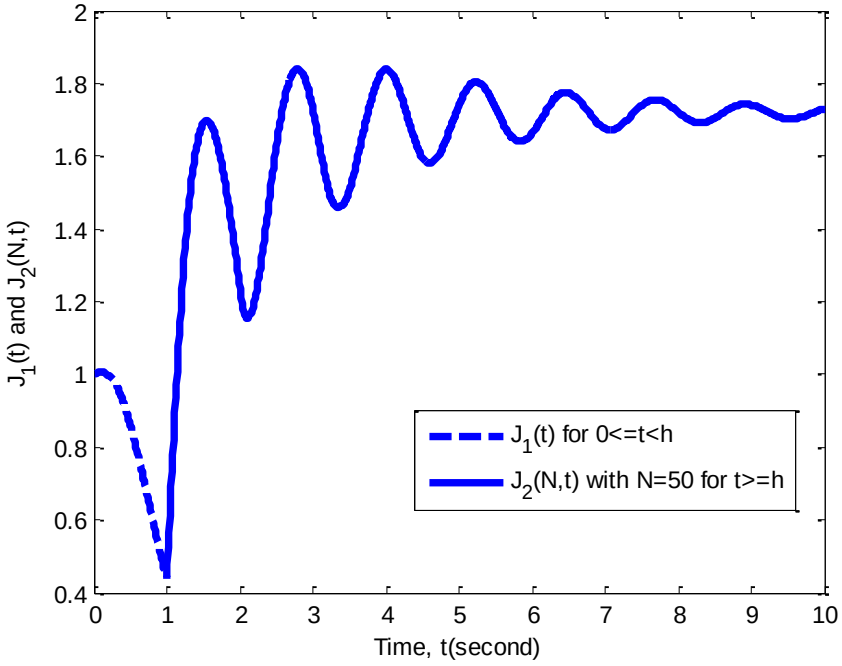

Fig. 4.7 The functions $J_1(t)$ and $J_2(N,t)$ with N=50 for Example 4.2

A similar procedure can be applied to obtain K_3 and K_4 as illustrated in Fig.4.8 and Fig.4.9. As a result, one obtains

$$K_1 = 1.076,\ \ K_2 = 1.9,\ \ K_3 = 1.89,\ \ K_4 = 1.9$$

and the factor, K, is determined as

$$K = \max(K_1, K_2) + \max(K_3, K_4) = 3.8$$

Again, the decay function estimated by the methods in (Mondié & Kharitonov, 2005) and (Hale et al., 1993) are compared to the proposed method in Table 4.2.

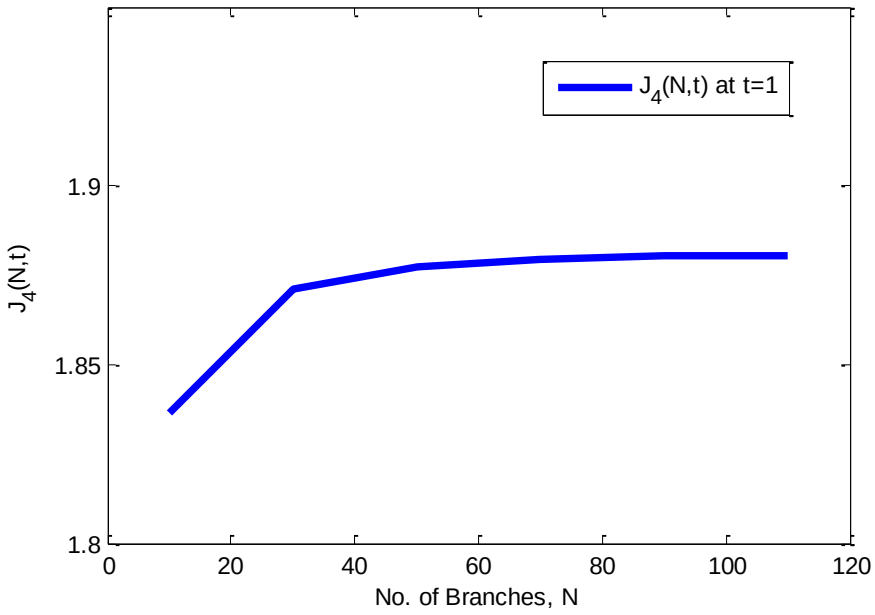

Fig. 4.8 The convergence of $J_4(N,t)$ at t=h=1 for Example 4.2

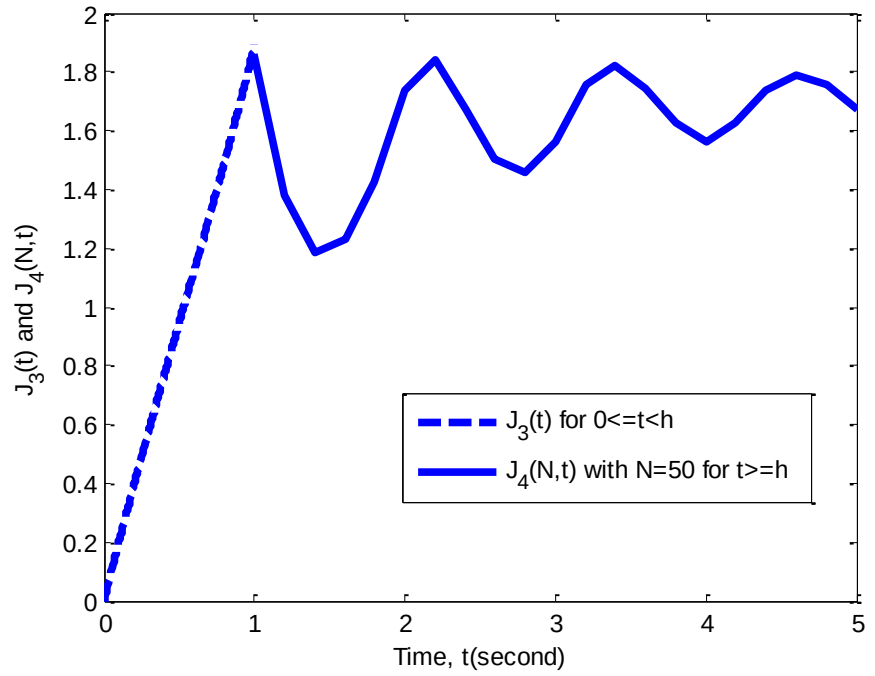

Fig. 4.9: The functions $J_3(t)$ and $J_4(N,t)$ with N = 50 for Example 4.2

Table 4.2 Comparison of Results for Example 4.2

	Factor, K	Decay Rate, α
Matrix Measure Approach (Hale, 1993)	8.0192	3.0525
Lyapunov Approach (Mondié, 2005)	9.33	-0.9071
Theorem 4.1	3.8	-1.0119

In Example 2, the decay rate obtained using the proposed method is the optimal value of α and shows significant improvement over the other time domain methods. The result for the factor *K* from our approach is also significantly less conservative than the other methods considered. For Lyapunov approaches, the increase of system order leads to a dramatic increase in the dimension of the corresponding optimization problem, which results in more conservativeness. Further, the estimate of *K* is not typically optimized in Lyapunov function approaches. For the Lambert W function approach, the problem is tackled by evaluating the explicit series, not formulating it as an optimization problem.

4.5 Concluding Remarks

A Lambert W function based approach for the estimation of the decay function for linear time-delay systems is presented. From the proposed approach, the optimal estimate of decay rate, α, can be determined analytically. The constant factor *K* is obtained using an infinite Lambert W function series and is typically less conservative compared to other approaches for matrix DDEs. Less conservative estimate of the decay function leads to not only more accurate description of the exponential behavior of time-delay systems, but also to more effective control designs based on those results. The results from our approach are explicitly expressed in terms of Lambert W function series. Convergence

properties of the Lambert W function remains an important topic for future research. A general proof for determining the rightmost poles of time-delay systems with a finite (few) number of terms from the infinite series is also of future interest. An emerging field of interest for this work is time-periodic delay systems (Insperger et al., 2002, 2010), where the delay and the time-periodic system parameter together makes the decay function estimation challenging.

CHAPTER 5
CONCLUSIONS, CONTRIBUTIONS AND FUTURE WORK

5.1 Conclusions

This doctoral research is focused on developing effective and efficient methods for the stability analysis of PWA time-delay systems with or without uncertainty. The effectiveness of the approach is demonstrated using numerical examples as well as through an application to an automotive clutch system. A method based on the Lambert W function approach is also developed to obtain a more accurate decay function estimate for time-delay systems.

First, delay-dependent stability criteria for nominal and uncertain PWA time-delay systems are derived in the form of LMIs. The proposed approach is able to achieve less conservative results compared with existing methods by including an additional triple integration term in the Lyapunov-Krasovskii functional. The computational complexity of the method is also less than the existing method for uncertain PWA time-delay systems. One of the major contributions of this approach lies in the accommodation of the switching based on delayed states as well as states of the model.

Second, the proposed method is applied to the modeling and control of a nonlinear automotive clutch system. A feed forward plus piecewise PI control is designed based on the PWA model of the open-loop system to realize reference torque tracking with consistent performance under different operating conditions and temperature state

variation. In addition, using the PWA system framework, the stability of the closed-loop system is analytically studied, with consideration of uncertainty and time delay in the model, to obtain rigorous design guarantees. A design feasibility map, illustrating the trade-off among speed of response, robustness of the system, and time delay, is also provided.

Finally, a Lambert W function based approach for the estimation of the decay function for linear time-delay systems is developed. From the proposed approach, the optimal estimate of decay rate, α, and a corresponding factor K can be obtained. The constant factor K is obtained using an infinite Lambert W function series and is typically less conservative compared to other approaches for matrix DDEs. Less conservative estimate of the decay function can lead to not only more accurate description of the exponential behavior of time-delay systems, but also to more effective control designs based on those results.

5.2 Contributions

The main contributions of this dissertation are summarized as follows:

- A method based on the Lyapunov-Krasovskii approach is presented for the stability analysis of PWA time-delay systems with structured or unstructured uncertainty. Besides the reduced conservativeness through the use of a triple integration term in the Lyapunov-Krasovskii functional, the proposed approach considers the case of switching based on delayed states (as well as states) in the model, which extends the applicability of the approach to a wider range of practical systems, especially to systems subject to controller delays. The computational load of this approach is also less than the existing method for analysis of uncertainty PWA time-delay systems.
- The application of the PWA system framework to the modeling and control of a nonlinear clutch system is presented. This application not only shows the flexibility of the framework for modeling, but also provides a rigorous stability analysis of the closed-loop system in the presence of uncertainty and time delays.
- A new Lambert W function based approach for the estimation of the decay function for linear time-delay systems is proposed. From this approach, the optimal estimate of decay rate, α, can be determined in terms of the system parameters. The constant factor K is analytically derived in the form of an infinite Lambert W function series and is typically less conservative compared to existing methods for matrix DDEs. Reduced conservativeness in these estimates can help design more efficient dwell-time control for switched time-delay systems.

5.3 Future Work

A number of future research topics are suggested following the studies in this dissertation:

- For the stability analysis of PWA time-delay systems, a common single constant time delay is assumed in each region of the model. However, for more general cases, time delay can be different from region to region and can be time-varying. An extension of the proposed method to include these cases could be valuable in practice.
- Lyapunov stability is studied for PWA time-delay systems in this work. The investigation of other types of stability, such as input-output stability with L_2 gain analysis and input-to-state stability, will also be helpful to explore the properties of PWA time-delay systems and be valuable in practice.
- PWA systems provide a flexible framework to model a variety of nonlinear systems, especially systems with saturation, dead zone, hysteresis and chaos. An application of the PWA system framework, especially the stability analysis, to systems with different types of nonlinearities would be of interest.
- In the current design procedure, the control design and stability test are conducted sequentially. Controllers are designed first, then the stability of closed-loop systems is examined using the proposed stability criterion. If no feasible solution is found, controllers will be redesigned. An extension to control synthesis (Habets, 2006), where Lypapunov function and control gains are searched for simultaneously, can

help to facilitate the procedure. However, the computational complexity will become much more challenging since the problem is usually formulated as BMIs in such synthesises.

- Convergence properties of the Lambert W function remain an important topic for future research and can be useful to evaluate those results expressed in term of the infinite Lambert W function series such as decay function estimate, controllability and observability (Yi et al., 2008b) of time-delay systems
- A general proof for determining the rightmost poles of time-delay systems with a finite (few) number of terms from the infinite Lambert W function series is also of future interest.
- Incorporating the decay function into the control design for switching time-delay systems is also an interesting topic. By tuning the control parameters, the resulting time-delay systems may smaller factor K and faster decay rate, which lead to shorter dwell time and more efficiently control.
- An emerging field of interest for this work is time-periodic delay systems, which can be found in many applications such as machine tool vibration, parametric control of robotic systems (Insperger & Stepan, 2000) and neural networks (Hagan, 1996). For time-periodic delay systems, the delay and the time-periodic system parameter together makes the decay function estimation challenging. Although the method can be readily extended to scalar time-periodic delay system, for the matrix case, the problem remains open.

APPENDICES

Appendix A: LMI stability test for clutch application

Consider the closed-loop clutch system in (3.28) represented in the form of a PWA time-delay system with structured uncertainty. Since the switching of the system solely depends on the delayed state, $\mathbf{x}(t-\tau)$, the regions are divided into the sets defined in Chapter 2. When the equilibrium point at $\tilde{i}_{ce}(t)=0$ is considered, the sets are obtained as:

$$I_0=\{\text{region 1, region 2}\},\ I_1=\{\text{region 3, region 4}\},\ I_2=null,\ I_3=null$$

Based on the partition in Table 3.1 and the procedure in (Johansson, 2003), the boundary matrices can be obtained as:

$$\mathbf{E}_1=\mathbf{E}_2=\left[\mathbf{0}_{4\times 2}\right],\ \bar{\mathbf{E}}_3=\bar{\mathbf{E}}_4=\left[\mathbf{0}_{4\times 3}\right],$$

$$\mathbf{E}_{d1}=\begin{bmatrix}0&0\\0&0\\0&0\\0&0\end{bmatrix},\ \mathbf{E}_{d2}=\begin{bmatrix}0&0\\0&0\\0&0\\0&0\end{bmatrix},\ \bar{\mathbf{E}}_{d3}=\begin{bmatrix}0&0&0\\0&0&0\\1&0&-0.8\\-1&0&3.3\end{bmatrix},\ \bar{\mathbf{E}}_{d4}=\begin{bmatrix}0&0&0\\0&0&0\\1&0&-3.3\\0&0&1\end{bmatrix}.$$

Correspondingly, the continuity matrices can be formulated as

$$\mathbf{F}_1=\mathbf{F}_2=\begin{bmatrix}\mathbf{I}_{2\times 2}\\\mathbf{0}_{5\times 2}\end{bmatrix},\ \bar{\mathbf{F}}_3=\bar{\mathbf{F}}_4=\begin{bmatrix}\mathbf{I}_{2\times 2}&\mathbf{0}_{2\times 1}\\\mathbf{0}_{5\times 2}&\mathbf{0}_{5\times 1}\end{bmatrix},$$

$$\mathbf{F}_{d1}=\begin{bmatrix}0&0\\0&0\\0&0\\0&0\\0&0\\1&0\\0&1\end{bmatrix},\ \mathbf{F}_{d2}=\begin{bmatrix}0&0\\0&0\\0&0\\0&0\\0&0\\1&0\\0&1\end{bmatrix},\ \bar{\mathbf{F}}_{d3}=\begin{bmatrix}0&0&0\\0&0&0\\1&0&0\\1&0&-0.8\\0&0&0\\1&0&0\\0&1&0\end{bmatrix},\ \bar{\mathbf{F}}_{d4}=\begin{bmatrix}0&0&0\\0&0&0\\1&0&0\\1&0&-0.8\\1&0&-3.3\\1&0&0\\0&1&0\end{bmatrix}$$

The coefficient matrices for each region are

$$\mathbf{A}_1=\begin{bmatrix}-42&0\\0&-30\end{bmatrix},\quad \mathbf{A}_{d1}=\begin{bmatrix}0&0\\0&0\end{bmatrix},\quad \mathbf{a}_1=\begin{bmatrix}0\\0\end{bmatrix},\quad \mathbf{A}_2=\begin{bmatrix}-17.2727&8.7581\\0&0\end{bmatrix},$$

$$\mathbf{A}_{d2}=\begin{bmatrix}-25.1473&0\\-102.7623&0\end{bmatrix},\ \mathbf{a}_2=\begin{bmatrix}0\\0\end{bmatrix};\ \mathbf{A}_3=\begin{bmatrix}-17.2727&3.6064\\0&0\end{bmatrix},\ \mathbf{A}_{d3}=\begin{bmatrix}-25.1473&0\\-249.5547&0\end{bmatrix},$$

$$\mathbf{a}_3=\begin{bmatrix}11.8337\\117.4340\end{bmatrix};\ \mathbf{A}_4=\begin{bmatrix}-17.2727&8.9100\\0&0\end{bmatrix},\ \mathbf{A}_{d4}=\begin{bmatrix}-25.1473&0\\-101.0097&0\end{bmatrix},\mathbf{a}_4=\begin{bmatrix}-92.8031\\-372.7647\end{bmatrix}$$

One can use the above coefficients to set the LMIs in Theorem 2.3 then utilize the Matlab LMITOOL toolbox to solve the LMI problem. An analogous procedure can be applied to check the stability for other equilibrium points.

Appendix B: Solution for matrix DDEs

Consider the linear time invariant matrix DDE in (4.1). As shown in (Yi et al., 2006), one way to determine the $\mathbf{C}_k^I$ is to Laplace transform the matrix DDE in (4.1):

$$s\mathbf{I}\mathbf{X}(s) - \mathbf{x}_0 + \mathbf{A}\mathbf{X}(s) + \mathbf{A_d}e^{-sh}\mathbf{X}(s) + \mathbf{A_d}\mathbf{G}(s) = 0 \tag{B.1}$$

Note that,

$$\begin{aligned}\int_0^\infty e^{-st}\mathbf{X}(t-h)dt &= \int_0^h e^{-st}\mathbf{X}(t-h)dt + \int_h^\infty e^{-st}\mathbf{X}(t-h)dt \\ &= \int_0^h e^{-st}\mathbf{g}(t-h)dt + \int_0^\infty e^{-s(t+h)}\mathbf{X}(t)dt = \mathbf{G}(s) + e^{-sh}\mathbf{X}(s)\end{aligned} \tag{B.2}$$

Therefore,

$$\mathbf{X}(s) = (s\mathbf{I} + \mathbf{A} + \mathbf{A_d}e^{-sh})^{-1}(\mathbf{x}_0 - \mathbf{A_d}\mathbf{G}(s)) \tag{B.3}$$

The solution in (4.8) can also be Laplace transformed to obtain

$$\mathbf{X}(s) = \sum_{k=-\infty}^{\infty} (s\mathbf{I} - \mathbf{S}_k)^{-1}\mathbf{C}_k^I \tag{B.4}$$

Equating the expressions in (B.3) and (B.4) yields

$$\frac{adj(s\mathbf{I} + \mathbf{A} + \mathbf{A_d}e^{-sh})}{\det(s\mathbf{I} + \mathbf{A} + \mathbf{A_d}e^{-sh})}(\mathbf{x}_0 - \mathbf{A_d}\mathbf{G}(s)) = \sum_{k=-\infty}^{\infty} (s\mathbf{I} - \mathbf{S}_k)^{-1}\mathbf{C}_k^I \tag{B.5}$$

where *adj*( ) denotes the adjugate matrix.

Determining the $\mathbf{C}_k^I$ in (B.5) is analogous to determining the residue in a typical partial fraction expansion. To calculate $\mathbf{C}_k^I$ for a particular branch $k = q$, i.e., to obtain

$\mathbf{C}_q^I$, both sides of (B.5) are multiplied by the expression $\prod_{i=1}^{n}(s-\lambda_{qi})$ and the resulting expression is evaluated at $s=\lambda_{qj}$, $j=1,2,...,n$, where $\lambda_{qj}=eig(\mathbf{S}_q)$. Thus,

$$\frac{adj(s\mathbf{I}+\mathbf{A}+\mathbf{A_d}e^{-sh})}{\det(s\mathbf{I}+\mathbf{A}+\mathbf{A_d}e^{-sh})}(\mathbf{x}_0-\mathbf{A_d}\mathbf{G}(s))\prod_{i=1}^{n}(s-\lambda_{qi}) = \sum_{k=-\infty}^{\infty}\left\{\frac{\prod_{i=1}^{n}(s-\lambda_{qi})}{s\mathbf{I}-\mathbf{S}_k}\mathbf{C}_k^I\right\} \qquad \text{(B.6)}$$

Therefore, substitution of λ_{qj} for s will make $\frac{\prod_{i=1}^{n}(s-\lambda_{qi})}{s\mathbf{I}-\mathbf{S}_k}=0$ except for $k=q$ since $\lambda_{qj}=eig(\mathbf{S}_q)$. However, on the left side of the equation, one obtains the indeterminate form

$$\frac{\lim_{s\to\lambda_{qj}}\prod_{i=1}^{n}(s-\lambda_{qi})}{\lim_{s\to\lambda_{qj}}\det(s\mathbf{I}+\mathbf{A}+\mathbf{A_d}e^{-sh})}=\frac{0}{0} \qquad \text{(B.7)}$$

This can be resolved by applying L' Hospital's rule. Assume, any two eigenvalues from different branches are distinct:

$$\lambda_{mj}\neq\lambda_{nj}, \quad where \quad m\neq n, \quad j=1,2,...,n \qquad \text{(B.8)}$$

On the right-hand side of (B.6),

$$\lim_{s\to\lambda_{qj}}\sum_{k=-\infty}^{\infty}\left\{\frac{\prod_{i=1}^{n}(s-\lambda_{qi})}{s\mathbf{I}-\mathbf{S}_k}\mathbf{C}_k^I\right\}=\lim_{s\to\lambda_{qj}}\frac{\det(s\mathbf{I}-\mathbf{S}_q)}{s\mathbf{I}-\mathbf{S}_q}\mathbf{C}_k^I=\lim_{s\to\lambda_{qj}}adj(s\mathbf{I}-\mathbf{S}_q)\mathbf{C}_k^I \qquad \text{(B.9)}$$

Thus, one can then rewrite (B.6) as

$$\lim_{s\to\lambda_{kj}}\left\{\frac{\frac{\partial}{\partial s}\prod_{i=1}^{n}(s-\lambda_{ki})}{\frac{\partial}{\partial s}\det(s\mathbf{I}+\mathbf{A}+\mathbf{A_d}e^{-sh})}adj(s\mathbf{I}+\mathbf{A}+\mathbf{A_d}e^{-sh})\quad(\mathbf{x}_0-\mathbf{A_d}\mathbf{G}(s))\right\}=adj(\lambda_{qj}\mathbf{I}-\mathbf{S}_q)\mathbf{C}_k^I$$

(B.10)

and define $\mathbf{L}_{qj}^I$ and $\mathbf{R}_{qj}^I$ as in (4.14) and (4.15). Then (B.10) can be simplified as,

$$\mathbf{L}_{qj}^I(\mathbf{x}_0-\mathbf{A_d}\mathbf{G}(\lambda_{qj}))=\mathbf{R}_{qj}^I\mathbf{C}_q^I,\text{for } j=1,...,n \tag{B.11}$$

When $\mathbf{S}_q$ has distinct eigenvalues, or repeated eigenvalues with geometric multiplicity of one, one can show that

$$rank(\lambda_{qj}\mathbf{I}-\mathbf{S}_q)=n-1 \text{ for } \ i=1,...,n \tag{B.12}$$

When $rank(\lambda_{qj}\mathbf{I}-\mathbf{S}_q)<n-1$, which means some states associated with the repeated eigenvalues are decoupled, one can separate these states in to independent new DDEs and solve the problems individually.

Also, one can show that (Bernstein, 2005):

$$rank(\lambda_{qj}\mathbf{I}-\mathbf{S}_q)=n-1\Leftrightarrow\ rank(\text{adj}(\lambda_{qj}\mathbf{I}-\mathbf{S}_q))=1 \tag{B.13}$$

which means that each equation in (B.11) has only one linearly independent row among *n* rows. However, *n* equations from (B.11) will provide *n* linearly independent rows, making the solution of $\mathbf{C}_q^I$ unique.

Grouping (i.e., stacking) all *n* equations in (B.11) into a single matrix equation:

$$\tilde{\mathbf{L}}_q^I=\tilde{\mathbf{R}}_q^I\mathbf{C}_q^I \tag{B.14}$$

where

$$\tilde{\mathbf{L}}_q^I = \begin{bmatrix} \mathbf{L}_{q1}^I \\ \mathbf{L}_{q2}^I \\ \vdots \\ \mathbf{L}_{qn}^I \end{bmatrix} \mathbf{x}_0 + \begin{bmatrix} -\mathbf{L}_{q1}^I \mathbf{A_d} \mathbf{G}(\lambda_{q1})) \\ -\mathbf{L}_{q2}^I \mathbf{A_d} \mathbf{G}(\lambda_{q2})) \\ \vdots \\ -\mathbf{L}_{qn}^I \mathbf{A_d} \mathbf{G}(\lambda_{qn})) \end{bmatrix}, \quad \tilde{\mathbf{R}}_q^I = \begin{bmatrix} \mathbf{R}_{q1}^I \\ \mathbf{R}_{q2}^I \\ \\ \mathbf{R}_{qn}^I \end{bmatrix} \tag{B.15}$$

The $\mathbf{C}_q^I$ can be calculated by using the Moore-Penrose Generalized Inverse:

$$\mathbf{C}_q^I = \tilde{\mathbf{R}}_q^{I+} \tilde{\mathbf{L}}_q^I = \tilde{\mathbf{R}}_q^{I+} \begin{bmatrix} \mathbf{L}_{q1}^I \\ \mathbf{L}_{q2}^I \\ \vdots \\ \mathbf{L}_{qn}^I \end{bmatrix} \mathbf{x}_0 + \tilde{\mathbf{R}}_q^{I+} \begin{bmatrix} -\mathbf{L}_{q1}^I \mathbf{A_d} \mathbf{G}(\lambda_{q1})) \\ -\mathbf{L}_{q2}^I \mathbf{A_d} \mathbf{G}(\lambda_{q2})) \\ \vdots \\ -\mathbf{L}_{qn}^I \mathbf{A_d} \mathbf{G}(\lambda_{qn})) \end{bmatrix} = \sum_{j=1}^{n} \mathbf{T}_{qj}^I \mathbf{L}_{qj}^I \mathbf{x}_0 - \sum_{j=1}^{n} (\mathbf{T}_{qj}^I \mathbf{L}_{qj}^I \mathbf{A_d} \mathbf{G}(\lambda_{qj})) \tag{B.16}$$

where $\mathbf{T}_{qj}^I$, $\tilde{\mathbf{R}}_q^{I+}$ and is defined in (4.15).

Note that $rank(\tilde{\mathbf{R}}_q^I) = n$ (full column rank), thus the $\mathbf{C}_q^I$ obtained from (B.16) using the generalized pseudo inverse will be unique. Therefore, the solution of (4.1), in (4.8), can be expressed as:

$$\mathbf{x}(t) = \sum_{k=-\infty}^{\infty} \left\{ e^{\mathbf{S}_k t} (\sum_{j=1}^{n} \mathbf{T}_{kj}^I \mathbf{L}_{kj}^I) \mathbf{x}_0 \right\} - \sum_{k=-\infty}^{\infty} \left\{ e^{\mathbf{S}_k t} \sum_{j=1}^{n} (\mathbf{T}_{kj}^I \mathbf{L}_{kj}^I \mathbf{A_d} \mathbf{G}(\lambda_{kj})) \right\} \tag{B.17}$$

BIBLIOGRAPHY

Anderson , R.J., and Spong , M.W. (1989). Bilateral control of teleoperators with time delay. *IEEE Trans. Autom. Control, 34*, 494-501.

Asl, F. M., and Ulsoy, A. G. (2003). Analysis of a system of linear delay differential equations. *ASME J. Dyn. Syst. Meas. Control, 125*, 215-223.

Azuma, S., Yanagisawa, E. and Imura, J. (2008). Controllability analysis of biosystems based on piecewise-affine systems approach. *IEEE Trans. Autom. Control*, vol.53, pp.139-152.

Baotic, M.; Vasak, M.; Morari, M.; Peric, N. (2003). Hybrid system theory based optimal control of an electronic throttle. *American Control Conference, Proceedings of the 2003*, vol.6, no., pp. 5209- 5214 vol.6, 4-6.

Barreto, G.A., and Araujo., A.F.R.(2004). Identification and control of dynamical systems using the self-organizing map. *IEEE Transactions On Neural Networks*, 15(5), 1244-1259.

Bellman, R. E., and Cooke, K. L. (1963). *Differential-Difference Equations*, New York: Academic Press.

Bemporad, A., Ferrari-Trecate, G., and Morari, M. (1999). Observability and Controllability of Piecewise Affine and Hybrid Systems. *Proceedings of the Conference on Decision and Control*.

Berstain, D. (2005). *Matrix Mathematics:Theory, Facts, and Formulas with Application to Linear Systems Theory*, Princeton University Press.

Blondel , V.D., and Tsitsiklis, J.N. (1999). Complexity of stability and controllability of elementary hybrid systems. *Automatica*, 35(3):479-490.

Bourlès, H. (1987). α-stability and robustness of large scale interconnected systems. *Int. J. Control*,*45*, 2221–2232.

Branicky, M.S.(1998). Multiple Lyapunov functions and other analysis tools for switched and hybrid systems. *IEEE Trans. Automation and Control*, 43(4):475-482.

Breda, D., Maset, S., and Vermiglio, R. (2005). Pseudospectral differencing methods for characteristic roots of delay differential equations. *SIAM J. Sci. Comput*., Vol. 27 (2), 482-495.

Chen, W. H., and Zhang, W. X. (2010). Delay-independent minimum dwell-time for exponential stability of uncertain switched delay systems, *IEEE Trans. Autom. Control*, *55*, 2406 - 2413.

Chiou, J. S. (2006). Stability analysis for a class of switched large-scale time-delay systems via time-switched method. *IEE Proc.-Control Theory Appl.*, Vol. 153, No. 6.

Cook, J. A. and Powell, B. K. (1988). Modeling of an internal combustion engine for control analysis. *IEEE Control Syst. Mag.*, pp. 20–25.

Dai, D., Hu, T., Teel, A.R., Zaccarian, L. (2009a). Piecewise-quadratic Lyapunov functions for systems with deadzones or saturations. *Systems & Control Letters*. Vol 58, pp., 365-3.

Dai, S., Lin, H., and Ge, S. (2009b). Robust stability of discrete-time switched delay systems and its application to network-based reliable control. *In Proc. 2009 conference on American Control Conference*, Piscataway, NJ, USA, 2367-2372.

Dumas, J. G., and Rondepierre, A. (2003). Modeling the Electrical Activity of a Neuron by a Continuous and Piecewise Affine Hybrid System. Hybrid Systems: Computation and Control. Vol 2623, 156-171.

Drulhe, S., Ferrari-Trecate, de Jong, G., and Viari, H. (2006). A. reconstruction of switching thresholds in piecewise-affine models of genetic regulatory networks. *Hybrid Systems: Computation and Control*. Vol 3927, 184-199.

Duan, S., Ni, J. and Ulsoy, A. G. (2010). A Lambert W function approach for decay function estimation in linear time-delay systems. *IEEE Cont. and Decision Conf.*. 4972-4977.

Duan, S., Ni, J. and Ulsoy, A. G. (2011a). Decay function estimation for linear time-delay systems via the Lambert W function**.** *Journal of Vibration and Control*, in press.

Duan, S., Ni, J. and Ulsoy, A. G. (2011b). A delay-dependant stability criterion for uncertain piecewise affine time-delay systems. *American Control Conference.* (In preparation).

Duan, S., Ni, J. and Ulsoy, A. G. (2011c). An improved LMI-based approach for stability of piecewise affine time-delay systems with uncertainty. *Int. J. Control* (Submitted).

Duan, S., Ni, J. and Ulsoy, A. G. (2011d). Control design for a nonlinear clutch thermal system via piecewise affine system framework. *American Control Conference.* (In preparation).

Duan, S., Ni, J. and Ulsoy, A. G. (2011e). Modeling and control of an automotive all-wheel drive clutch as a piecewise affine system. *ASME J. Dyn. Syst. Meas.& Cont*. (Submitted).

Engelborghs, K., Luzyanina, T., and Samaey, G. (2001). DDE-BIFTOOL v.2.00: A Matlab package for bifurcation analysis of delay differential equation. Dept. Comp. Sci., K.U. Leuven, Leuven, Belgium, T. W. Rep. 330.

Filippov, A. F. (1998). *Differential Equations with Discontinuous Right-hand Sides*, Kluwer Academic Publications.

Fofana, M. S. (2003). Delay dynamical systems and applications to nonlinear machine-tool chatter. *Chaos, Solitons and Fractals, 17*, 731-47.

Forde, J., and Nelson, P. W. (2004). Application of sturm sequences to bifurcation analysis of delay differential equation models. *J Math Anal Appl*, *300*, 273-84.

Fridman, E., and Shaked, U. (2002). An improved stabilization method for linear time-delay systems. *IEEE Trans. Autom. Control*, *47*, no.2, pp. 253-270.

Fridman, E., and Shaked, U. (2002). A descriptor system approach to H_∞ control of time-delay systems. *IEEE Trans. Autom. Control*, *47*, no.11, pp. 1931–1937.

Gu, K., and Niculescu, S. I. (2003). Survey on Recent Results in the Stability and Control of Time-Delay Systems, *J. Dyn. Sys., Meas., Control*, Vol.125, pp158, DOI:10.1115/1.1569950.

Habets, L.C.G.J.M.; Collins, P.J.; van Schuppen, J.H. (2006). Reachability and control synthesis for piecewise-affine hybrid systems on simplices. *IEEE Trans. Autom. Control*, vol.51, no.6, pp. 938- 948.

Hagan, M. T., Demuth, H. B., and Beale, M.(1996). *Neural Network Design*. PWS: Boston.

Hale, J. K., and Verduyn-Lunel, S. M. (1993). Introduction to functional differential equations. *Applied Mathematical Sciences, 99*, New York:Springer.

Hallowell, S.J. (2005). Torque distribution systems and methods for wheeled vehicles. US Patent 6, 909-959.

Hassibi, A. and Boyd, S. P. (1998). Quadratic stabilization and control of piecewise-linear systems. In *Proceedings of the American Control Conference*, pp. 3659–3664.

He**,** Y., Wang, Q.-G., Xie, L., and Lin**,** C**.(**2007). Furtherimprovement of free-weighting matrices technique for systems with time-varying delay. *IEEE Trans. Autom. Control*, Vol. 52, No. 2, pp. 293–299.

Hou, C., and Qian, J. (1998). On an estimate of the decay rate for applications of Razumikhin-type theorems. *IEEE Trans. Autom. Control, 43*, No. 7, 958-960.

Hmamed. A. (1996). Comments on 'On an estimate of the decay rate for stable linear delay systems'. *Int. J. Contro, 42,* 539–540.

Hu, B., Zhai, G., Anthony, N. M. (2002). Common quadratic Lyapunov-like functions with associated switching regions for two unstable second-order LTI systems. *Int. J. Control*, Volume 75, Issue 14, pages 1127-1135.

Insperger, T., and Stepan, G. (2000). Remote control of periodic robot motion. *Proceedings of the 13th CISM-IFTOMM Symposium*, Zakopane, Poland.

Insperger, T., and Stepan, G. (2002). Stability chart for the delayed Mathieu equation, *Proceedings of the Royal Society London A, 458,* 1989-1998

Insperger, T., Wahi, P., Colombo, A., Stepan, G., Bernardo, Di, M., and Hogan, SJ (2010). Full characterization of act-and-wait control for first-order unstable lag processes. *Journal of Vibration and Control*, *16*, 1209-1233.

Jankovic, M. (2001). Control Lyapunov–Razumikhin functions and robust stabilization of time-delay systems. *IEEE Trans. Autom. Control, 46,* 1048–1060.

Jarlebring, E., and Damm, T. (2007). The Lambert *W* function and the spectrum of some multidimensional time-delay systems. *Automatica, 43,* 2124 – 2128.

Johansson, M., and Rantzer, A. (1997). Computation of piecewise quadratic Lyapunov functions for hybrid systems. *Proc. European Control Conf*., Brussels, Belgium.

Johansson, M. (2003). *Piecewise Linear Control Systems*. Springer-Verlag, ISBN: 3540441247.

Johansen, T.A. , and Foss, B.A.(1993). Constructing narmax models using armax models. *International Journal Of Control*, 58(5):1125-53.

Kacem, W., Chaabane, M., Mehdi, D., and Kamoun, M. (2009). On α-stability criteria of linear systems with multiple time delay. *Journal of Mathematical Sciences, 161,* No. 2.

Kalmar-Nagy, T., Stepan, G., and Moon, F. C. (2001). Subcritical hopf bifurcation in the delay equation model for machine tool vibrations. *Nonlinear Dynamics*, *26*, 121-42.

Kim, D. K., Park, P. G., and Ko, J. W. (2004). Output-feedback H-infinite control of systems over communication networks using a deterministic switching system approach. *Automatica*, *40,* 1205–1212.

Kim, S., Campbell, S.A., and Liu, X. (2006). Stability of a class of linear switching

systems with time delay. *IEEE Trans. Circuits and Systems I, 53*, 384-393.

Krasovskii, N. N. (1963). *Stability of motion*. Stanford University Press, Stanford CA, USA, (translation by J. Brenner).

Kulkarni, V. (2003). Optimal mode changes for highway transportation safety. *IEEE International Conference on Systems, Man and Cybernetics.*, vol.2, pp. 1235-1240.

Kulkarni, V, Jun, M., and Hespanha, J. (2004). Piecewise quadratic Lyapunov functions for piecewise affine time-delay systems. *Proceedings of the 2004 American Control Conference,* vol.5, no.30, pp. 3885- 3889.

Lehman, B. and Shujaee, K. (1994). Delay independent stability conditions and decay estimates for time-varying functional differential equations. *IEEE Trans. Autom. Control, 39*, 1673–1676.

Li, C., Chen, G., and Liao, X. (2007). Stability of piecewise affine systems with application to chaos stabilization. *Chaos*, Volume 17, Issue 2, pp. 023123-023123-12.

Li, X., and de Souza, C. E. (1997). Criteria for robust stability and stabilization of uncertain linear systems with state-delay. *Automatica*, Vol. 33, pp.1657–1662.

Liberzon D. and Morse A. S. (1999). Basic problems in stability and design of switched systems. *IEEE Control Systems Magazine*, vol. 19 no 5.

Liberzon, D. (2003). *Switching in Systems and Control*. Spinger. ISBN:0-8176-4297-8.

Liu, P.-L. (2003). Exponential stability for linear time-delay systems with delay dependence. *J. Franklin Inst, 340*, 481–488.

Meyer, C., Schroder, S., and De Doncker, R. W. (2004). Solid-state circuit breakers and current limiters for medium-voltage systems having distributed power systems. *IEEE Trans. Power Electronics*, *19*,1333–1340.

Michiels, W., Green, K., Wagenknecht, T., and Niculescu, S.-I. (2006). Pseudospectra and stability radii for analytic matrix functions with application to time-delay systems. *Linear Algebra and its Applications*, 418, 315-335.

Moezzi, K., Rodrigues, L., and Aghdam, A. (2009). Stability of Uncertain Piecewise Affine Systems with Time Delay: Delay Dependent Lyapunov Approach. *Int. J. Control*, 82 (8), pp. 1423-1434.

Mignone, D., Ferrari-Trecate, G., Morari, M. (2000). Stability and Stabilization of Piecewise Affine and Hybrid Systems: An LMI Approach. *Proceedings of the 39th IEEE Conference on Decision and Control*, Sydney, Australia.

Mondié, S., and Kharitonov, V. L. (2005) . Exponential estimates for retarded time-delay systems: an LMI approach. *IEEE Trans. Autom. Control, 50*, No. 2.

Moon, Y. S., Park, P., Kwon, W. H., and Lee, Y. S. (2001). Delay-dependent robust stabilization of uncertain state-delayed systems. *Int. J. Control*, vol. 74, pp. 1447–1455.

Mori, T., Fukuma, N., and Kuwahara, M. (1982). On an estimate of the decay rate for stable linear delay systems. *Int. J. Control, 36*, 95–97.

Mori, T., and Kokame, H. (1989). Stability of $\dot{x}(t) = Ax(t) + Bx(t-\tau)$. *IEEE Trans. Automat. Contr, 34.*, 460-462.

Murray, R. M. (2003). *Control in an information rich world: report of the panel on future directions in control, dynamics and systems*. Philadelphia, PA: SIAM 2003.

Nayfeh, A., Chin, C., and Pratt, J. (1997). Application of perturbation methods to tool chatter dynamics. *Dynamics and Chaos in Manufacturing Processes*, F. C. Moon (ed), Wiley, New York, 193-213.

Niculescu, S. I., Souza, C. E. de, Dion, J. M., Dugard, L (1998). Robust exponential stability of uncertain systems with time varying delays. *IEEE Trans. Autom. Control, 43*, 743–748.

Niculescu, S. I. (2001). *Delay Effects on Stability: a Robust Control Approach* (Springer, New York).

Orosz, G., Wilson, E., and Stepan, G. (2010). Traffic jams: dynamics and control. *Philos. Trans. R. Soc. A, 368*, 4455-4672.

Park, P. (1999). A delay-dependent stability criterion for systems with uncertain time-invariant delays. *IEEE Trans. Autom. Control*, Vol. 44, pp. 876–877.

Pettersson, S. (1999). *Analysis and Design of Hybrid Systems*. PhD Thesis, Chalmers University, Goteborg, Sweden.

Phat, V. N., and Niamsup, P. (2006). Stability of linear time-varying delay systems and applications to control problems. *J. Comput. Appl. Math.,194*, 343–356.

Razumikin, B. S. (1956). On the stability of systems with a delay. *Prikladnava Matematika i Mekhanika*, 20, 500–512 (in Russian).

Richard, J. P. (1998). Some trends and tools for the study of time-delay systems. *Second conference IMACS-IEEE CESA'98, Computational Engineering in Systems Applications*, Tunisia, Plenary lecture (pp. 27–43).

Richard, J. P. (2003). Time-delay systems: an overview of some recent advances and open problems. *Automatica*, 39, 1667-1964.

Rodrigues, L., and How, J.P. (2003). Observer-based Control of Piecewise-affine System. *Int. J. Control*, 76, 459–477.

Rodrigues, L., and Boyd, S.P. (2005). Piecewise-affine State Feedback for Piecewise-affine Slab Systems using Convex Optimisation. *Systems & Control Letters*, 54, 835–583.

Prajna, S. and A. Papachristodoulou (2003). Analysis of switched and hybrid systems - beyond piecewise quadratic methods. In: *American Control Conference*. Denver, Colorado, USA.

Richard, J. P. (1998). Some trends and tools for the study of time-delay systems. *Second conference IMACS-IEEE CESA'98, Computational Engineering in Systems Applications*, Tunisia, Plenary lecture (pp. 27–43).

Richard, J. P. (2003). Time-delay systems: an overview of some recent advances and open problems. *Automatica*, 39, 1667-1964.

Schutter, B. D. and Moor, B. D. (1999). The extended linear complementarity problem and the modeling and analysis of hybrid systems". In Antsaklis, P., Kohn, W., Lemmon,

M., Nerode, A., and Sastry, S., editors, *Hybrid Systems Verification and Control: Lecture Notes in Computer Science*, volume 1567, pp. 70–85.Springer-Verlag.

Shinozaki, H., and Mori, T. (2006). Robust stability analysis of linear time-delay systems by Lambert W function: Some extreme point results. *Automatica, 42*, 1791-99.

Shorten, R., Wirth, F., Mason, O, Wulff, K., and King, C. (2007). Stability criteria for switched and hybrid systems. *SIAM* , Rev**.** 49, 4, 545-592.

Sipahi, R., and Olgac, N. (2003). Degenerate cases in using the Direct Method. *ASME J. Dyn. Syst. Meas. Cont., 125*, 194-201.

Sontag, E.D. (1996). Interconnected automata and linear *sy*stems: A theoretical framework in discrete-time. In R. Alur, T.A. Henzinger, and E.D. Sontag, editors, *Hybrid Systems III- Verification and Control*, number 1066 in Lecture Notes in Computer Science, pages 436-448. Springer-Verlag, 1996.

Sun, H. J., and Hsieh, J. G. (1998). On α-stability criteria of nonlinear systems with multiple delays. *J. Franklin Inst, 335*, 695–705.S. Xu, J. Lam, and M. Zhong (2006). New exponential estimates for time-delay systems. *IEEE Trans. Autom. Control, 51*, No. 9.

Takagi, T., and Sugeno, M (1985). Fuzzy identification of systems and its applications to modeling and control. *IEEE Transactions On Systems, Man And Cybernetics*, SMC,15(1):116-132.

Wu, M., He, Y., She, J.-H., and Liu, G.-P. (2004). Delay-dependent criteria for robust stability of time-varying delay systems. *Automatica*, vol. 40, pp. 1435–1439.

Xie, L. (1996). Output feedback H∞ control of systems with parameter uncertainty.

International Journal of Control, 63, 741–750.

Xu, S., and Lam, J. (2005). Improved delay-dependent stability criteria for time-delay systems. *IEEE Trans. Autom. Control,50*, 384–387.

Yi, S., Ulsoy, A. G. and Nelson, P. W. (2006). Solution of systems of linear delay differential equations via Laplace transformation. In *Proc. 45th IEEE Conf. on Decision and Control,* San Diego, CA, 2535-2540.

Yi, S., Nelson, P. W., and Ulsoy, A. G. (2007a). Survey on analysis of time delayed systems via the Lambert W function. *Dynamics of Continuous, Discrete and Impulsive Systems* (*Series A*), *14,* 296 - 301.

Yi, S., Nelson, P. W., and Ulsoy, A. G. (2007b). Delay differential equations via the matrix Lambert W function and bifurcation analysis: Application to machine tool chatter. *Mathematical Biosciences and Engineering, 14,* 355-368.

Yi, S., Nelson, P. W., and Ulsoy, A. G. (2008a). Eigenvalue and sensitivity analysis for a model of HIV-1 pathogenesis with an intracellular delay. *Proc. ASME Dynamic Systems and Control Conf.,* Ann Arbor, MI 2008, pp 573-581.

Yi, S., Nelson, P. W., and Ulsoy, A. G. (2008b). Controllability and observability of systems of linear delay differential equations via the matrix Lambert W function. *IEEE Trans. Aut. Cont.* vol. 53, pp. 854-860.

Yi, S., Nelson, P. W., and Ulsoy, A. G. (2010a). Feedback control via eigenvalue assignment for time delayed systems using the Lambert W function. *Journal of Vibration and Control,16,* 961-982..

Yi, S., Nelson, P. W., and Ulsoy, A. G. (2010b). Robust control and time-domain specifications for systems of delay differential equations via eigenvalue assignment. *ASME J. Dyn. Syst. Meas. Cont , 132*(2).

Yi, S., Ulsoy, A. G. and Nelson, P. W. (2010c). Design of observer-based feedback control for time-delay systems with application to automotive powertrain control. *Journal of the Franklin Institute, 347* (1), 358-376.

Yan, P., and Ozbay, H. (2008). Stability analysis of switched time-delay systems. *SIAM Journal on Control and Optimizations*, *47*, 936–949.

Zhang, Y., Liu, X., and Shen, X. (2007). Stability of switched systems with time delay. *Nonlinear Analysis: Hybrid Systems*, (1) pp. 44-58.